

DESCRIPTION OF ISOSCALAR GIANT DIPOLE RESONANCE IN NUCLEI

A Dissertation

by

OLEKSIY GRIGORIEVICH POCHIVALOV

Submitted to the Office of Graduate Studies of
Texas A&M University
in partial fulfillment of the requirements for the degree of

DOCTOR OF PHILOSOPHY

December 2006

Major Subject: Physics

DESCRIPTION OF ISOSCALAR GIANT DIPOLE RESONANCE IN NUCLEI

A Dissertation

by

OLEKSIY GRIGORIEVICH POCHIVALOV

Submitted to the Office of Graduate Studies of
Texas A&M University
in partial fulfillment of the requirements for the degree of

DOCTOR OF PHILOSOPHY

Approved by:

Chair of Committee,	Shalom Shlomo
Committee Members,	Dave H. Youngblood
	Joseph B. Natowitz
	Ronald A. Bryan
Head of Department,	Edward S. Fry

December 2006

Major Subject: Physics

ABSTRACT

Description of Isoscalar Giant Dipole Resonance in Nuclei.

(December 2006)

Oleksiy Grigorievich Pochivalov, B.S., Kiev State University

Chair of Advisory Committee: Dr. Shalom Shlomo

Applicability of the Hartree-Fock (HF) based random phase approximation (RPA) with several Skyrme effective interactions to the description of the isoscalar giant monopole (ISGMR) and the isoscalar giant dipole resonance (ISGDR) in ^{90}Zr , ^{116}Sn , ^{144}Sm and ^{208}Pb nuclei has been investigated. The existing Skyrme interactions SL1, SkM*, SGII, Sly4 and Sk255 were used. Hartree-Fock description of the ground state properties of all nuclei of interest was obtained using these Skyrme interactions.

Transition strength distributions for the ISGMR and the ISGDR in nuclei of interest were calculated using coordinate space representation for the RPA in the Green's function formalism with discretized continuum. A method of projecting out the spurious state contribution from the transition strength distribution and the transition density of the ISGDR was employed to eliminate spurious state mixing, due to a not fully self-consistent description of the particle-hole interaction within the RPA.

Differential cross sections of 240 MeV α -particles inelastic scattering on all nuclei of interest were calculated using the folding model within the distorted wave Born approximation (DWBA). Optical potentials were obtained by folding HF ground state densities with a α -nucleon density dependent Gaussian interaction. Parameters of the interaction were obtained by fitting experimental angular distribution of α -nucleus elastic scattering.

The inelastic differential cross sections were calculated using both collective and microscopic transition densities. Possible underestimations of the energy weighted sum rule for the case of the ISGDR are reported.

An alternative description for the ISGDR in nuclei based on the Fermi liquid drop model (FLDM) with the collisional Fermi surface distortion was investigated. The FLDM dispersion relation was obtained from the linearized Landau-Vlasov equation. Centroid energies, E_0 and E_1 , and widths, Γ_0 and Γ_1 , of the ISGMR and ISGDR, respectively, were calculated as functions of the damping parameter using appropriate boundary conditions. Comparison of the theoretical ratios of the ISGDR and ISGMR centroid energies, E_1/E_0 , to the experimental values resulted in a damping parameter equal to 0.5, however, systematic overestimation of energy of the ISGMR and ISGDR by 2.0-2.5 MeV was observed. The applicability of the HF-RPA to the description for the ISGDR in nuclei is confirmed.

ACKNOWLEDGEMENTS

I feel very fortunate to have had the opportunity to study and carry out research at the Cyclotron Institute, Texas A&M University. I would like to thank all the people at the institute for their continual help, patience and support.

Especially, I would like to thank Dr. Shalom Shlomo for suggesting the topic investigated in this dissertation. His advise, guidance and encouragement were invaluable for the completion of this work.

I also would like to thank Dr. Vladimir Kolomietz, Dr. Alexei Kolomiets, Dr. Andrey Sanzhur, Dr. Bijay Agrawal, and Dr. Tapas Sil for their kindness in helping me with the questions I encountered during my study.

My sincerest gratitude goes to my dear friend, MaryJade Pochivalova, whose support and inspiration carried me through these years.

My thanks for the great help in editing this manuscript go to John Goodwin and Natalia Samokhina.

This work was supported in part by the US National Science Foundation under grant no. PHY-0355200 and the US Department of Energy under grant no. DOE-FG03-93ER40773.

TABLE OF CONTENTS

CHAPTER	Page
I INTRODUCTION	1
II HARTREE-FOCK DESCRIPTION OF NUCLEAR GROUND STATE	10
III SELF-CONSISTENT HARTREE-FOCK BASED RANDOM PHASE APPROXIMATION DESCRIPTION OF GIANT RESONANCES	21
A. Green's Function Formalism of HF-RPA in Coordinate Representation and RPA with Skyrme Effective Interaction	21
B. Elimination of Spurious State Contribution from Strength Distribution Function of Isoscalar Giant Dipole Excitation	29
IV DISTORTED WAVE BORN APPROXIMATION	35
A. Formal Solution of Scattering Problem	35
B. Distorted Wave Approach to Inelastic Scattering	42
1. Nuclear Interaction	45
2. Coulomb Interaction	47
V FERMI LIQUID DROP MODEL (FLDM)	49
A. Time Dependent Hartree-Fock Approximation in Phase Space	49
B. Dynamic Distortion of Fermi Surface	54
C. Relaxation Process and Viscosity Effect	60
D. Boundary Conditions	65
E. Translation Invariance Condition and Isoscalar Giant Resonance Description	67
VI DESCRIPTION OF GIANT RESONANCES IN ^{90}Zr , ^{116}Sn , ^{144}Sm AND ^{208}Pb	69
A. Microscopic Analysis	69
1. Nuclear Ground State	72

CHAPTER	Page
2. Isoscalar Giant Monopole Resonance	73
3. Isoscalar Giant Dipole Resonance	77
4. Cross Section Analysis of Isoscalar Giant Dipole Resonance ...	83
B. Centroid Energies E_0 and E_1 , and Widths Γ_0 and Γ_1 , and Ratios E_1/E_0 from FLDM	89
VII SUMMARY	96
REFERENCES	100
APPENDIX A	104
APPENDIX B	109
VITA	121

LIST OF TABLES

TABLE	Page
I. Parameterizations of the Skyrme-type effective interaction used in the dissertation.	14
II. Binding energy per nucleon in ^{90}Zr , ^{116}Sn , ^{144}Sm and ^{208}Pb nuclei obtained from the HF calculations with SL1, SkM*, SGII, Sly4 and Sk255 nucleon-nucleon interactions. The experimental values are obtained from Ref. [64].	72
III. Ground state root-mean square radii obtained from the HF calculations with SL1, SkM*, SLy4, SGII, and Sk255 Skyrme interactions. $\sqrt{\langle r^2 \rangle_m}$, $\sqrt{\langle r^2 \rangle_n}$, $\sqrt{\langle r^2 \rangle_p}$, $\sqrt{\langle r^2 \rangle_c}$ denote mass, neutron, proton and charge root-mean square radii, respectively. Experimental radii are taken from Ref. [65].	73
IV. Energies E_0 of the isoscalar monopole excitation in ^{90}Zr , ^{116}Sn , ^{144}Sm and ^{208}Pb nuclei obtained using SL1, SkM*, SGII, Sly4, and Sk255 interactions.	76
V. Percentage of the energy weighted sum rules (%EWSR's) of the isoscalar monopole excitation exhausted in the excitation energy interval $5 \leq E \leq 35$ MeV in ^{90}Zr , ^{116}Sn , ^{144}Sm and ^{208}Pb nuclei. %EWSR are obtained using SL1, SKM*, SGII, Sly4, and Sk255 interactions.	76
VI. The average energies and percentages of the EWSR exhausted within the energy interval $5 < E < 35$ MeV for the low excitation energy, E_{LE} , and the high excitation energy, E_{HE} , components of the ISGDR excitations in ^{90}Zr , ^{116}Sn , ^{144}Sm , and ^{208}Pb nuclei. Experimental data is also presented.	80
VII. Parameters of the density-dependent Gaussian form of the α -nucleon effective interactions for SL1, SkM*, SGII, Sly4 and Sk255 Skyrme-type interactions.	83
VIII. Centroid energies of the ISGMR, E_0 , and the ISGDR, E_1 , obtained within fully self-consistent HF-RPA calculations [69, 70] with the SGII interaction are presented for ^{90}Zr , ^{116}Sn , ^{144}Sm , and ^{208}Pb nuclei.	88

LIST OF FIGURES

FIGURE	Page
1. Isoscalar monopole strength distributions in ^{90}Zr , ^{116}Sn , ^{144}Sm and ^{208}Pb nuclei obtained using SL1 Skyrme interaction (thin solid line). The circles with error bars show the experimentally extracted strength distribution $S(E)$ for the ISGMR in nuclei of interest [66].	74
2. Isoscalar monopole strength distributions in ^{90}Zr , ^{116}Sn , ^{144}Sm and ^{208}Pb nuclei obtained using SKM*, SGII, Sly4 and Sk255 Skyrme interactions.	75
3. Centroid energies of the ISGMR for ^{90}Zr , ^{116}Sn , ^{144}Sm , and ^{208}Pb obtained within the HF-RPA formalism with SL1 (filled circles), SKM* (filled triangles “up”), SGII (filled triangles “down”), and Sk255 (filled stars) interactions. Experimental data is presented by filled squares. The dashed line represents empirical mass dependence of the ISGMR energy $E = 79.9A^{-1/3}$	77
4. Strength distribution functions of the ISGDR in ^{90}Zr , ^{116}Sn , ^{144}Sm and ^{208}Pb nuclei obtained using SL1 Skyrme interaction (thin solid line). The experimentally extracted strength distributions $S(E)$ of the ISGDR in nuclei of interest [66] are shown by the data point with error bars.	78
5. Strength distribution functions of the ISGDR in ^{90}Zr , ^{116}Sn , ^{144}Sm and ^{208}Pb nuclei obtained using SKM*, SGII, Sly4, and Sk255 Skyrme interactions.	79
6. Centroid energies E_0 and E_1 of the ISGMR and ISGDR excitations, respectively, obtained from the HF-RPA and the FLDM calculations. The experimental data [24, 25] is presented by the solid black line. We can see that the results of the microscopic (HF-RPA) as well as macroscopic (FLDM) calculations, systematically overestimate the centroid energy of the dipole excitation. The experimental values of the monopole energy are successfully reproduced by the HF-RPA calculations; however, the FLDM results show an overestimate on the order of 2.5 MeV for E_0 as well as E_1	82
7. Elastic scattering distributions for 240 MeV α -particles, obtained from the HF calculation for the ground state density using Sly4 interaction. Experimental data is presented by black dots. Solid lines present the best fit, obtained with the parameters given in Table VI.	84

FIGURE	Page
8. Fractions of the EWSR of the ISGDR exhausted at a given excitation energy, calculated using the RPA with the SL1 Skyrme interaction (solid line) and the collective (dashed line) transition densities, are presented in the top panel. The middle panel presents the double-differential cross section calculated using the RPA transition density, obtained at the angle of maximal cross section. In the bottom panel we present the differential cross section. The solid line presents the result obtained using the RPA transition density renormalized to the 100%EWSR exhausted at a given excitation energy. The dashed line is obtained with the collective transition density.	85
9. Same as the top panel of Figure 8 with the SL1 interaction for ^{90}Zr , ^{116}Sn , and ^{144}Sm	86
10. Same as Figure 9 with the SKM* (top left), SGII (top right), SLy4 (bottom left) and Sk255 (bottom right) interactions for ^{90}Zr , ^{116}Sn , ^{144}Sm and ^{208}Pb nuclei.	87
11. Centroid energies of the ISGMR, $E0$, and the ISGDR, $E1$, in ^{90}Zr , ^{116}Sn , ^{144}Sm and ^{208}Pb nuclei presented as functions of the damping parameter β	91
12. Collisional widths $\Gamma0$ and $\Gamma1$ in ^{208}Pb of the ISGMR and ISGDR, respectively. A smooth non-monotonous dependence of the widths of collective excitation on the damping parameter β is observed.	92
13. Dependence of the energy ratio $E1/E0$ on the nuclear mass number A . The ratio $(E1/E0)_{FLDM}$ is obtained within the current model with the relaxation parameter (see Eq. 5.78) $\beta \rightarrow 0$ (dark red dashed line, LDM), $\beta \rightarrow \infty$ (dashed green line, zero sound regime), and $\beta = 0.5$ (solid blue line). The experimental ratios [24,25] for the nuclei of interest are presented by the solid black line. Also presented are ratios obtained as results of the HF-RPA calculations, performed with SGII (dash dot), SLy4 (dash dot dot), and Sk255 (short dot) Skyrme interactions.	94
14. Dependence of the ISGMR rms-width, $\sigma0$, and the ISGDR rms-width, $\sigma1$, on the nuclear mass number A . The FLDM result (dot-line) is obtained using the relaxation time of Eq. (5.78) with damping parameter $\beta = 0.5$. The experimental data is taken from Refs. [24, 25].	95

CHAPTER I

INTRODUCTION

Analyses of collective excitations in nuclei have provided important information about properties of the nuclear interaction, non-equilibrium processes in nuclei, and the properties of infinite nuclear matter. In particular, compression modes, such as isoscalar monopole and isoscalar dipole excitations, have been of great interest in nuclear research because of their relevance to the extraction of the value of the nuclear matter incompressibility coefficient. Under existing laboratory conditions, the parameters of the infinite nuclear matter cannot be measured directly. However, knowledge of such parameters, in particular, the nuclear matter incompressibility coefficient, is very important in many areas of physics research, such as astrophysics, nuclear structure and heavy ion collisions.

Collective nuclear excitations have been experimentally observed throughout the periodic table. Such excitations are identified as the occurrence of resonance peaks in the transition strength distribution obtained by a weak external field that excites the nucleus. These excitations usually exhaust a large fraction of the total transition strength for a given external field, hence the name giant resonances. It was also noted that average energies and widths of such resonances in different nuclei behave as smooth functions of the nuclear mass number A . Such a behavior is a strong indication of a coherent motion of nucleons, hence, collective nature of these excited states.

Collective nuclear excitations, and particularly, giant resonances are identified by the amount of change of total momentum J , total spin ΔS and total isospin ΔT , that are transferred to the ground state of the nucleus as a result of interaction with a weak external field. In this dissertation, the discussion is limited only to the $\Delta S = 0$ (electric), and the $\Delta T = 0$ (isoscalar) excitation modes. From a macroscopic point of view, such excitations correspond to in-phase motion of nucleons with opposite spin and isospin. From a microscopic point of view, nuclear collective excitations can be described as a

This dissertation follows the style of Physical Review C.

superposition of multiple single particle – single hole excitations (in Tamm-Dankoff or Random Phase Approximations). In the latter case, the ΔS and ΔT are the spin and isospin of each particle-hole pair, respectively. In this dissertation, for the purpose of simplicity, we limit our microscopic studies to random phase approximation (RPA).

Over the years RPA has been proven to be one of the most successful approaches of the microscopic description of nuclear excitation. This success can be attributed to the main idea of the approximation, namely, that a nuclear collective excitation can be seen as a superposition of correlated single particle – single hole excitations of the correlated nuclear ground state. The random phase approximation can be built on any of the models providing information on the single particle structure of the nuclear ground state.

Therefore, an obvious choice is to give a formulation of the RPA on the basis of Hartree-Fock single particle energies and wave functions, obtained by solving the single particle Hartree-Fock equations. This Hartree-Fock based RPA formalism have been extensively used in the description of collective excitations and has been proven to be a successful approach in describing some of the characteristic features of several giant resonances.

There are many choices of the nucleon-nucleon interaction that can be used within the Hartree-Fock method. In this dissertation we limit our choices to various parameterizations of the zero-range density-dependent Skyrme-type nucleon-nucleon interaction, due to the apparent success of the Hartree-Fock calculations with the Skyrme interactions in describing nuclear ground state properties such as binding energies, root-mean-square radii, etc. Another reason for the choice of zero-range nucleon-nucleon interaction is the simplicity of the numerical application of the Hartree-Fock method with such interactions. Further reasoning for the choice of nucleon-nucleon interaction will be explained in the following.

The zero-range effective nucleon-nucleon interaction was first formulated by Skyrme [1], [2], from an expansion of the nucleon-nucleon interaction in momentum space. Later, in order to account for the density saturation effects in nuclei, an additional zero-range density-dependent term was introduced by Vautherin and Brink [3]. Comprehensive HF calculations of the root-mean square radii and single particle energy

levels, performed for a wide range of double-closed shell nuclei showed better agreement with the available experimental data than those obtained using effective interaction derived from Brueckner's theory [4]. Over the years, various parameterizations of the Skyrme interaction have been developed [5] and multiple additional zero-range terms have been introduced in order to improve the ground state description and to account for generally known features of the nucleon-nucleon interaction, such as momentum and density dependent [6] and tensor [7] terms. One of the concerns with the Skyrme effective interaction is that different parameterizations, corresponding to different values of parameters of the nuclear matter, are known to satisfactorily reproduce properties of ground state of finite nuclei. It is especially true for such an important nuclear matter parameter as the nuclear matter incompressibility coefficient, K_{nm} . Thorough research [8] has shown that the ground state properties of a wide range of nuclei is well reproduced by the Skyrme force parameterizations, corresponding to a very wide range for the value of K_{nm} . Also, there were no indications that the nuclear matter incompressibility is correlated with any other nuclear matter parameter. The issue of the value of nuclear matter incompressibility coefficient needs to be addressed.

Additional information, obtained by studying isoscalar giant monopole resonance (ISGMR), the breathing compression mode of collective excitations of nuclei [9], narrowed the range of values of the nuclear matter incompressibility coefficient to 210 ± 20 MeV. That confirmed the value of the nuclear matter incompressibility coefficient K_{nm} , determined earlier in Ref. [10].

It was first pointed out in Ref. [11], that the HF-RPA results for the centroid energy of the isoscalar giant dipole resonance (ISGDR), $E1$, obtained with the interactions adjusted to reproduce the ISGMR data, are higher than the experimental values [12,13]. This discrepancy between theory and experiment was also reported in more recent publications [14-16]. There have been quite a few recent non-relativistic HF-RPA [17-21] and relativistic mean-field based RPA [22,23] calculations for the ISGDR, addressing issues of (i) spurious state mixing (SSM), (ii) the strength of the lower

component (at $1\hbar\omega$), and (iii) the value of K_{mm} deduced from the centroid energy $E1$ of the ISGDR compression mode (at $3\hbar\omega$). The issue of spurious state mixing in the strength distribution and transition density of the ISGDR has been successfully addressed in Refs. [17,18] by carrying out accurate microscopic calculations for the strength distribution function $S(E)$, and projecting out the SSM contribution. However, discrepancies of 1-2 MeV between centroid energies calculated within the HF-RPA method, and experimentally measured energies [24-26] of the ISGDR, are still being observed. These discrepancies in the isoscalar dipole energies indicate that the consistency in the results of the HF-RPA calculations with the Skyrme interactions for various collective excitations in nuclei must be verified. It can be achieved by careful study of the HF-RPA description for the isoscalar giant dipole resonance and the isoscalar giant monopole resonance modes, in a wide range of nuclei, using a variety of known parameterizations of the Skyrme nucleon-nucleon interaction. Reproduction of the experimentally measured energies for both the isoscalar monopole and isoscalar dipole resonances may serve as a criterion for better applicability of a given Skyrme interaction and indicate that the corresponding value of nuclear matter incompressibility coefficient is the most realistic.

The above considerations show the importance of systematic experimental and theoretical studies of ISGDR excitation in a wide range of nuclei.

The choice of the Skyrme-type effective interaction in this dissertation can be explained by two major advantages of implementation of this interaction within the HF-RPA. First, according to the Thouless theorem [27], the integrated energy weighted transition strength, corresponding to a given excitation operator, calculated within the HF-RPA, should be equal to the energy weighted sum rule obtained from the HF ground state, provided that all terms of the particle-hole interaction were consistently retained within the HF-RPA interaction. This assures the self-consistency of the method. Second, using a Skyrme-type nucleon-nucleon interaction one operates with a particle-hole interaction that has delta-dependence in coordinate space. In such a case, it is possible to formulate the RPA equations in the coordinate representation using the Green's function

formalism [28,29]. The configuration space matrix formulation of the RPA has a strong limitation on the maximal excitation energy for which the transition strength can be calculated, due to the requirement of having a large number of particle-hole configurations that should be considered for high excitation energy. The free-system particle-hole Green's function required in the RPA equation can be obtained either by directly calculating the Green's function of the Hartree-Fock mean field (see Ref. [30]) or by using the Hartree-Fock single-particle energies and wave functions within the spectral representation of the response function. The latter method of calculation of the free-system Green's function requires proper discretization of the single-particle continuum, and an artificial width can be assigned by smearing the transition strength distribution with a certain function, for example, the Lorentzian. In the case of the direct calculation of the Hartree-Fock Green's function, the particle escape width is accounted for within the continuum RPA calculations; however, smearing may still be needed in order to take into account additional width due to coupling to more complex two-particle-two-hole configurations.

The main experimental tool for studying isoscalar giant resonances is inelastic α - particle scattering. An α -particle has total spin $S = 0$ and isospin $T = 0$, therefore, only $\Delta S = 0$ and $\Delta T = 0$ modes can be excited in the target nucleus as a result of the inelastic reaction, which either eliminates or greatly reduces interference of other excitations. Also, angular distributions of inelastically scattered α -particles at small angles are characteristic of some excited multipolarities, which in the case of α -particle scattering, are determined by the amount of transferred orbital momentum, L . Observing such characteristic behavior in the experimentally determined angular distributions, at a given excitation energy, simplifies the identification of contributions from modes of different multipolarity. Another reason for the usefulness of studying inelastic α -particle reactions is that current methods of extracting the sum rule strength from differential cross sections have proven to be reliable. Such an extraction is usually done in the analysis of a particular α -particle scattering reaction, using the formalism of the distorted wave Born approximation (DWBA). According to scattering theory, the

differential cross sections of inelastically scattered α -particles are proportional to the square of the transition amplitude T_{fi} , which within the DWBA is found in terms of incoming and outgoing distorted waves, and matrix elements of a two-body α -nucleon interaction between the ground state i and the excited state f . It is known that in the Born approximation, in the case of the zero-range two-body interaction, the transition amplitude for excitation of multipolarity L satisfies the following relationship:

$$T_{fi} \propto \int r^2 dr \rho_r^L(r) j_L(qr). \quad (1.1)$$

Here $\rho_r^L(r)$ is the radial part of the transition density for the excited state with multipolarity L , $j_L(qr)$ being the spherical Bessel function, and q being the transferred momentum. It was shown in Ref. [31] that, to a good approximation, this relation also holds for a more realistic case of a finite range Gaussian type two-body interaction. Therefore, one is provided with a direct dependence of the transition amplitude on the transition strength function, corresponding to the excitation operator

$F_{LM} = \sum_{i=1}^A j_L(qr_i) Y_{LM}(\hat{r}_i)$. For first order in (qr) , the long wave-length limit, the excitation operator for multipolarity L has the same form as the isoscalar electromagnetic operator:

$$F_{LM} \propto \sum_{i=1}^A r_i^L Y_{LM}(\hat{r}_i), \quad L \geq 2, \quad \Delta T = 0. \quad (1.2)$$

Since for both the isoscalar monopole and the isoscalar dipole excitations first order terms in the expansion of Bessel function vanish, next order terms allowed by parity conservation are:

$$F_{00} \propto \sum_{i=1}^A r_i^2, \quad L = 0, \quad \Delta T = 0, \quad (1.3)$$

$$F_{1M} \propto \sum_{i=1}^A r_i^3 Y_{1M}(\hat{r}_i), \quad L = 1, \quad \Delta T = 0. \quad (1.4)$$

The theoretical and experimental descriptions of isoscalar giant monopole and isoscalar giant dipole excitations in terms of the sum rules for the simple operators (1.3) and (1.4), are common in the literature.

We have pointed out earlier that the difference between the experimentally obtained centroid energy $E1$ of the ISGDR and theoretical values calculated using the self-consistent HF-RPA with effective interactions associated with $K_{nm} = 230$ MeV (which is known to successfully reproduce the experimental values of the centroid energy $E0$ of the ISGMR, see Refs. [16], [32,33]) needs to be addressed. Moreover, the experimental value for the ratio of the isoscalar dipole to the isoscalar monopole centroid energies $(E1/E0)_{\text{exp}} = 1.56 \pm 0.09$ is close to the prediction of the hydrodynamic model [34] but lies significantly below the theoretical results for ratio $E1/E0$ obtained in both the RPA and the scaling-like calculations. To understand conflicting results for the energy ratio $E1/E0$ and to resolve the value of the nuclear matter incompressibility coefficient, K_{nm} , deduced from data on the ISGMR and the ISGDR, further analysis is needed.

In an attempt to resolve these issues we turn to the Fermi liquid drop model (FLDM) with the dynamical Fermi surface distortion (FSD). Within the FLDM the basic equation of motion for the particle density variations in the nuclear interior can be derived from the \vec{p} -moments of the collisional kinetic Landau-Vlasov equation [35].

$$\frac{\partial}{\partial t} \delta f + \vec{v} \cdot \vec{\nabla}_{\vec{r}} \delta f - \vec{\nabla}_{\vec{r}} \delta U \cdot \vec{\nabla}_{\vec{p}} \delta f = \delta \mathcal{S}t, \quad (1.5)$$

where δf , δU and $\delta \mathcal{S}t$ are small variations of the Wigner distribution function, the effective interaction and the collision integral, respectively, \vec{v} is the velocity field and $\vec{\nabla}_{\vec{r}}$ and $\vec{\nabla}_{\vec{p}}$ are gradients with respect to \vec{r} and \vec{p} phase space variables. Relations between the collisional sound relaxation time and dynamic coefficients of the dispersion relation

$$\omega^2 - c_0^2 q^2 + i\omega\gamma q^2 = 0, \quad (1.6)$$

where c_0 is the sound velocity in the nuclear interior and γ is the friction coefficient, are obtained by taking into account the FSD effect up to multipolarity $l = 2$, and assuming that the particle density variations in the nuclear interior behave as plane waves. Assuming sharp density distribution, and considering that from the macroscopic point of view, the isoscalar monopole excitation corresponds to a spherically symmetric

inflation and contraction of the nucleus and the isoscalar dipole excitation corresponds to contraction and dilatation of the nucleus along an arbitrary axis at constant volume, we write the macroscopic boundary conditions on the moving nuclear surface in the form of the appropriate secular equations:

$$qrj_0(qr) - (f_\sigma + f_\mu)j_1(qr) = 0, \quad (1.7)$$

for the ISGMR, and

$$\left[\frac{1}{9} \left(K - 6 \frac{\mu_F}{\rho_{eq}} \right) j_1(qr) - 2 \frac{\mu_F}{\rho_{eq}} j_1''(qr) \right]_{r=R_{eq}} = 0, \quad (1.8)$$

for the ISGDR, where K is the nucleus incompressibility coefficient, q is the transferred momentum, $j_i(x)$ are the spherical Bessel functions, f_σ and f_μ are the surface and dynamic amplitudes, respectively, and μ_F is the dynamic friction coefficient. Finding the lowest non-zero solution q of equation (1.7) for the ISGMR, and equation (1.8) for the ISGDR, and using the dispersion relation (1.6), allows us to calculate the centroid energies, $E0$, $E1$, and the collisional widths, $\Gamma0$, $\Gamma1$, as the real and imaginary parts of the found eigenfrequencies ω , for the ISGMR and the ISGDR, respectively. The ratios obtained, for $E1/E0$, are compared with the experimental values, to determine the best model parameters. Centroid energies of the ISGMR and the ISGDR, found at given parameters, are used for direct comparison with the experimental data and with the results of microscopic (RPA) calculations.

In this dissertation, a full microscopic description of the isoscalar monopole and the isoscalar dipole excitations in ^{90}Zr , ^{116}Sn , ^{144}Sm and ^{208}Pb nuclei is given, based on the HF-RPA calculations with a Skyrme-type effective interaction. Calculations are performed using the Green's function formalism with discretized continuum. For the purpose of comparison with the recent experimental data and systematic studies of the effects of different parameterizations of Skyrme-type interaction based on this comparison, the selection of nuclei is limited to ^{90}Zr , ^{116}Sn , ^{144}Sm , and ^{208}Pb , and calculations are performed using various parameterizations of the Skyrme interaction. The effect of spurious state mixing in the transition strength distribution and transition density due to possible not full self-consistency is eliminated by use of a method of a

projecting operator. Based on obtained results, the DWBA analysis of 240 MeV α -particle scattering reactions is performed for the nuclei considered. Optical potentials are obtained by using the folding model [36] with the microscopic HF ground state densities and a two-body α -nucleon density dependent Gaussian interaction. Transition potentials are calculated by folding the α -nucleon interaction with either microscopic or collective transition densities. The inelastic cross-section calculated using both the microscopic and the collective transition potentials are compared and possible discrepancies of determining sum rule strengths are evaluated. As an alternative way to describe the isoscalar dipole excitation in nuclei, the formalism of the Fermi liquid drop model with the dynamically distorted Fermi surface is presented. The effects of variation of the damping parameter on the position of centroid energies of the ISGDR and the ISGMR in nuclei of interest are investigated. A comparison of the FLDM results with the experimental data, and with the results of microscopic (HF-RPA) calculations, is presented.

This dissertation is organized into the following Chapters. In Chapter II we present a description of the Hartree-Fock formalism. Chapter III is dedicated to a description of the self-consistent Hartree-Fock based RPA. In Chapter IV the distorted wave Born approximation for the case of inelastic scattering of two nuclei is discussed in detail. In Chapter V the Fermi liquid drop model with collisional Fermi surface distortion is outlined. In Chapter VI the results are presented, which are then summarized in Chapter VII.

CHAPTER II

HARTREE-FOCK DESCRIPTION OF NUCLEAR GROUND STATE

The success of the phenomenologically introduced shell model in describing ground state properties of nuclei justifies the assumption that nucleons move independently in an average potential produced by all of the nucleons. To provide a more precise description of the nuclear ground state one can use the Hartree-Fock method for the microscopic calculations of the single-particle wave functions and energies. The idea of the Hartree-Fock approximation is that the ground state wave function of the system of A particles can be approximated by the fully antisymmetrized product of the single particle wave functions, i.e. the Slater-determinant, which are obtained under the assumption that each particle is moving independently in the mean field created by all other single particles of the system, and that the approximated ground state wave function minimizes the expectation value of the total Hamiltonian of the system.

In the formalism of second quantization (see Appendix A) the initial non-relativistic Hamiltonian of the system of A interacting particles is given by

$$\hat{H} = \sum_{ij} t_{ij} \hat{a}_i^+ \hat{a}_j + \frac{1}{4} \sum_{ijkl} \bar{v}_{ij,kl} \hat{a}_i^+ \hat{a}_j^+ \hat{a}_l \hat{a}_k, \quad (2.1)$$

where t_{ij} is the kinetic energy, $\bar{v}_{ij,kl} = v_{ijkl} - v_{ijlk}$ is the two-body interaction and \hat{a}_i^+ and \hat{a}_i denote the single particle creation and annihilation operators, respectively. Since the nucleus is a system of fermions, the wave function of any state of such a system must be totally antisymmetric under the interchange of the coordinates of any two nucleons. For a nucleus that consists of A nucleons, the approximated wave function Φ satisfying the required antisymmetry is a Slater-determinant

$$|\Phi\rangle = \prod_{i=1}^A a_i^+ |0\rangle, \quad (2.2)$$

built from wave functions of the lowest single-particle states, which are eigenfunctions of single-particle Hamiltonian h ,

$$h(\vec{r})\varphi_k(\vec{r}) = \varepsilon_k \varphi_k(\vec{r}). \quad (2.3)$$

In the expressions above, the sub index i and k labels the single particle state of particular nucleon.

To obtain the explicit form of the single particle Hamiltonian satisfying the requirement of the minimization of the expectation value of the total Hamiltonian the variational principle must be applied. Defining the expectation value of the total Hamiltonian of the system as

$$E = \frac{\langle \Phi | H | \Phi \rangle}{\langle \Phi | \Phi \rangle}, \quad (2.4)$$

we demand the minimization of the expectation value

$$\delta E = 0. \quad (2.5)$$

Note for the future: indices $1 \leq i, j \leq A$ and $m > A$ will describe occupied and unoccupied single-particle states, respectively.

Using properties of Thouless' variational wave function [27]

$$|\Phi'\rangle = \left[\exp \sum_{m=A+1}^{\infty} \sum_{i=1}^A (\delta C_{mi} a_m^+ a_i) \right] |\Phi\rangle, \quad (2.6)$$

where δC_{mi} is an arbitrary constant that can be taken as a small variable, it is easy to see that the variation of the Φ can be written as

$$\begin{aligned} |\delta\Phi\rangle &= |\delta\Phi'\rangle - |\Phi\rangle = \sum_{mi} \delta C_{mi} a_m^+ a_i |\Phi\rangle \\ \langle\delta\Phi| &= \langle\Phi| \sum_{mi} \delta C_{mi}^* a_i^+ a_m. \end{aligned} \quad (2.7)$$

Therefore, as the δC_{mi} and δC_{mi}^* can be considered as independent variations we can rewrite the variational principle (Eqs. (2.4) and (2.5)) in the form of

$$\langle\Phi| a_i^+ a_m \hat{H} |\Phi\rangle = 0. \quad (2.8)$$

From Eq. (2.8), using the definition of the total Hamiltonian (2.1) and properties of commutators of the operators of creation and annihilation (see Appendix A) we write the variational condition (2.5) as:

$$h_{mi} \equiv t_{mi} + \sum_{j=1}^A \bar{v}_{mj,ij} = 0. \quad (2.9)$$

Eq. (2.9) defines the single-particle Hartree-Fock Hamiltonian, applicable for all occupied and unoccupied states.

Considering the fact that Eq. (2.9) does not connect occupied states i with unoccupied states m we can conveniently choose the single-particle states so that they will diagonalize separately the sub-matrixes $h_{ii'}$ and $h_{mm'}$. Eq. (2.9) will then read

$$\varepsilon_k \delta_{kk'} = t_{kk'} + \sum_{j=1}^A \bar{v}_{kj,k'j}. \quad (2.10)$$

According to the second quantization formalism, the coordinate representation of the Eq. (2.10) can be written as

$$\begin{aligned} \varepsilon_k \varphi_k(\vec{r}) = & -\frac{\hbar^2}{2m} \nabla^2 \varphi_k(\vec{r}) + \left[\int v(\vec{r}, \vec{r}') \sum_{j=1}^A |\varphi_j(\vec{r}')|^2 d^3 r' \right] \varphi_k(\vec{r}) \\ & - \sum_{j=1}^A \varphi_j(\vec{r}) \int v(\vec{r}, \vec{r}') \varphi_j^*(\vec{r}') \varphi_k(\vec{r}') d^3 r'. \end{aligned} \quad (2.11)$$

Equation (2.11) represents a system of linked integro-differential equation and in case of general non-local nucleon-nucleon interaction, finding the solution of such a system of equations can be very challenging. However, in case of general zero range nucleon-nucleon interaction, $v(\vec{r}, \vec{r}') = f(\vec{r}) \delta(\vec{r} - \vec{r}')$, where $f(\vec{r})$ represents, for example, density or momentum dependence, Eq. (2.11) can be greatly simplified:

Therefore, solving by iteration Eq. (2.11) we obtain single-particle energies and single-particle wave functions. Knowing the single-particle energies and single-particle wave functions the total ground-state wave function and ground-state energy of the system of A nucleons are obtained as follows:

$$\Phi = \frac{1}{\sqrt{A!}} \det \begin{pmatrix} \varphi_1(\vec{r}_1) & \varphi_2(\vec{r}_1) & \dots & \varphi_A(\vec{r}_1) \\ \varphi_1(\vec{r}_2) & \varphi_2(\vec{r}_2) & \dots & \varphi_A(\vec{r}_2) \\ \vdots & \vdots & \vdots & \vdots \\ \varphi_1(\vec{r}_A) & \varphi_2(\vec{r}_A) & \dots & \varphi_A(\vec{r}_A) \end{pmatrix}, \quad (2.12)$$

and

$$\begin{aligned}
E_{HF} &= \langle \Phi | \hat{H} | \Phi \rangle = \sum_{m=1}^A t_{mm} + \frac{1}{2} \sum_{m,n=1}^A \bar{v}_{mnmn} \\
&= \sum_{m=1}^A \mathcal{E}_m - \frac{1}{2} \sum_{m,n=1}^A \bar{v}_{mnmn} .
\end{aligned} \tag{2.13}$$

Choosing a zero-range Skyrme-type interaction greatly simplifies the calculations by conforming the exchange term of the interaction in Eq. (2.11) to the form of the direct term. In the following we present method of resolving of the single-particle Hartree-Fock equations with the extended Skyrme-type effective interaction in the coordinate representation:

In coordinate space the extended Skyrme-type effective interaction can be written in coordinate space in terms of a two-body central V_{ij}^C , a spin-orbit $V_{ij}^{S.O.}$, a density dependent $V_{ij}^{D.D.}$, a tensor V_{ij}^T , and a three-body velocity and density dependent $V_{ijk}^{D.D.}$ zero-range interactions in the form [3, 5, 7]:

$$V_{Skyrme} = \frac{1}{2} \sum_{ij} [V_{ij}^C + V_{ij}^{S.O.} + V_{ij}^{D.D.} + V_{ij}^T] + \frac{1}{6} \sum_{ijk} V_{ijk}^{D.D.}, \tag{2.14}$$

$$\begin{aligned}
V_{ij}^C &= t_0 (1 + x_0 P_{ij}^\sigma) \delta(\vec{r}_i - \vec{r}_j) + \\
&\frac{1}{2} t_1 (1 + x_1 P_{ij}^\sigma) [\bar{k}_{ij}^2 \delta(\vec{r}_i - \vec{r}_j) + \delta(\vec{r}_i - \vec{r}_j) \bar{k}_{ij}^2] +, \\
&t_2 (1 + x_2 P_{ij}^\sigma) \bar{k}_{ij} \delta(\vec{r}_i - \vec{r}_j) \bar{k}_{ij}
\end{aligned} \tag{2.15}$$

$$V_{ij}^{S.O.} = iW_0 \bar{k}_{ij} \delta(\vec{r}_i - \vec{r}_j) (\vec{\sigma}_i + \vec{\sigma}_j) \times \bar{k}_{ij}, \tag{2.16}$$

$$V_{ij}^{D.D.} = \frac{1}{6} t_3 (1 + x_3 P_{ij}^\sigma) \rho^\alpha \frac{(\vec{r}_i + \vec{r}_j)}{2} \delta(\vec{r}_i - \vec{r}_j), \tag{2.17}$$

$$\begin{aligned}
V_{ij}^T &= \frac{1}{2} T \delta(\vec{r}_i - \vec{r}_j) \left[(\vec{\sigma}_i \bar{k}_{ij}) (\vec{\sigma}_j \bar{k}_{ij}) - \frac{1}{3} (\vec{\sigma}_i \vec{\sigma}_j) \bar{k}_{ij}^2 + c.c. \right] (\vec{\tau}_i \vec{\tau}_j) + \\
&\frac{1}{2} U \left[(\vec{\sigma}_i \bar{k}_{ij}) \delta(\vec{r}_i - \vec{r}_j) (\vec{\sigma}_j \bar{k}_{ij}) - \frac{1}{3} (\vec{\sigma}_i \vec{\sigma}_j) \bar{k}_{ij} \delta(\vec{r}_i - \vec{r}_j) \bar{k}_{ij} + c.c. \right] (\vec{\tau}_i \vec{\tau}_j) ,
\end{aligned} \tag{2.18}$$

$$\begin{aligned}
V_{ijk}^{D.D.} &= \frac{1}{2} t_{13} (1 + x_{13} P_{ij}^\sigma) [\bar{k}_{ij}^2 \delta(\vec{r}_i - \vec{r}_j) \delta(\vec{r}_j - \vec{r}_k) + \delta(\vec{r}_i - \vec{r}_j) \delta(\vec{r}_j - \vec{r}_k) \bar{k}_{ij}^2] +, \\
&t_{23} (1 + x_{23} P_{ij}^\sigma) \bar{k}_{ij} \delta(\vec{r}_i - \vec{r}_j) \delta(\vec{r}_j - \vec{r}_k) \bar{k}_{ij}
\end{aligned} \tag{2.19}$$

where P_{ij}^σ is the spin exchange operator, $\vec{\sigma}_k$ is the Pauli spin operator, $\vec{\tau}_k$ is the isospin operator, and $\vec{k}_{ij} = \frac{\vec{\nabla}_i - \vec{\nabla}_j}{2}$ and $\vec{k}_{ij} = \frac{\vec{\nabla}_i - \vec{\nabla}_j}{2}$ are the momentum operators acting on the right and on the left, respectively. The parameterizations of the Skyrme interaction used in this dissertation are presented in Table I.

TABLE I. Parameterizations of the Skyrme-type effective interaction used in the dissertation.

	SL1 ^a	SkM* ^b	SGII ^c	SLy4 ^d	Sk255 ^e
t_0	-1326.28	-2645.0	-2645.0	-2488.91	-1689.35
t_1	943.90	410.0	340.0	486.82	389.30
t_2	-235.66	-135.0	-41.9	-546.39	-126.07
t_3	14658.60	15595.0	15595.0	13777.0	10989.60
x_0	0.310	0.090	0.090	0.834	-0.1461
x_1	0.700	0	-0.0588	-0.344	0.1160
x_2	-1.120	0	1.425	-1.000	0.0012
x_3	0	0	0.06044	1.354	-0.7449
W_0	130.0	130.0	105.0	123.0	95.39
α	1	1/6	1/6	1/6	0.3563
T	-80.0	0	0	0	0
U	-200.0	0	0	0	0
t_{13}	-16690.2	0	0	0	0
t_{23}	8478.83	0	0	0	0
x_{13}	2.99	0	0	0	0
x_{23}	-1.0	0	0	0	0

^a Ref. [7]

^b Ref. [5]

^c Ref. [33]

^d Ref. [37]

^e Ref. [38]

One also needs to take into account that in the interaction part of the total Hamiltonian there is the contribution of the Coulomb interaction between each pair of protons

$$v_{ij}^{Coulomb} = \frac{e^2}{|\vec{r}_i - \vec{r}_j|} \delta_{\tau_i, \frac{1}{2}} \delta_{\tau_j, \frac{1}{2}}, \quad (2.20)$$

Therefore, in the single particle Hartree-Fock equations there are two contributions:

$$v_{Coulomb}^{Dir.} \varphi_j = \delta_{\tau, \frac{1}{2}} \frac{e^2}{2} \int d\vec{r}' \frac{\sum \varphi_i^*(\vec{r}', \sigma, 1/2) \varphi_i(\vec{r}', \sigma, 1/2)}{|\vec{r} - \vec{r}'|} \varphi_j(\vec{r}, \sigma_j, 1/2), \quad (2.21)$$

$$v_{Coulomb}^{Exch.} \varphi_j = \delta_{\tau, \frac{1}{2}} \frac{e^2}{2} \int d\vec{r}' \frac{\sum \varphi_i^*(\vec{r}', \sigma_i, 1/2) \varphi_i(\vec{r}, \sigma_i, 1/2) \varphi_j(\vec{r}', \sigma_j, 1/2)}{|\vec{r} - \vec{r}'|}, \quad (2.22)$$

direct Coulomb term (for the case of point-particle protons), and exchange Coulomb term, respectively. The exchange term is small compared to the direct term, and, in order to simplify numerical calculations, it is neglected, or approximated with an expression that depends only upon the local proton density.

Now defining the nucleon, $\rho_\tau(\vec{r})$, the kinetic energy, $\tau_\tau(\vec{r})$, and the spin current, $\vec{J}_\tau(\vec{r})$ densities (τ denotes isospin), obtained from the single-particle wave functions, as follows:

$$\rho_\tau(\vec{r}) = \sum_{i=1}^A \sum_{\sigma} \varphi_i^*(\vec{r}, \sigma, \tau) \varphi_i(\vec{r}, \sigma, \tau), \quad \rho(\vec{r}) = \sum_{\tau} \rho_\tau(\vec{r}), \quad (2.23)$$

$$\tau_\tau(\vec{r}) = \sum_{i=1}^A \sum_{\sigma} |\vec{\nabla} \varphi_i(\vec{r}, \sigma, \tau)|^2, \quad \tau(\vec{r}) = \sum_{\tau} \tau_\tau(\vec{r}), \quad (2.24)$$

$$\vec{J}_\tau(\vec{r}) = -i \sum_{i=1}^A \sum_{\sigma, \sigma'} \varphi_i^*(\vec{r}, \sigma, \tau) [\vec{\nabla} \varphi_i(\vec{r}, \sigma', \tau) \times \langle \sigma | \vec{\sigma} | \sigma' \rangle], \quad \vec{J}(\vec{r}) = \sum_{\tau} \vec{J}_\tau(\vec{r}), \quad (2.25)$$

and collecting coefficients at the appropriate terms we can rewrite Eq. (2.11) with the Skyrme nucleon-nucleon interaction (defined in Eqs. (2.14-2.19) in simple form:

$$\left[-\vec{\nabla} \frac{\hbar^2}{2m_\tau^*(\vec{r})} \vec{\nabla} + U_\tau(\vec{r}) - i \vec{W}_\tau(\vec{r}) (\vec{\nabla} \times \vec{\sigma}) \right] \varphi_i(\vec{r}, \sigma, \tau) = \varepsilon_i \varphi_i(\vec{r}, \sigma, \tau), \quad (2.26)$$

Where $m_\tau^*(\vec{r})$, $U_\tau(\vec{r})$, and $\vec{W}_\tau(\vec{r})$ are the effective mass, effective central and effective spin-orbit interaction potentials, respectively, and are given by:

$$\begin{aligned}
\frac{\hbar^2}{2m_\tau^*(\vec{r})} &= \frac{\hbar^2}{2m_\tau} + \frac{1}{4} \left[t_1 \left(1 + \frac{1}{2} x_1 \right) + t_2 \left(1 + \frac{1}{2} x_2 \right) \right] \rho(\vec{r}) \\
&- \frac{1}{4} \left[t_1 \left(\frac{1}{2} + x_1 \right) - t_2 \left(\frac{1}{2} + x_2 \right) \right] \rho_\tau(\vec{r}) \\
&+ \frac{1}{24} \left[t_{23} (5 + 4x_{23}) + \frac{1}{2} t_{13} (4 - x_{13}) \right] \rho_\tau(\vec{r}) \rho_{-\tau}(\vec{r}) \\
&+ \frac{1}{16} t_{23} (1 + x_{23}) \rho_\tau^2(\vec{r})
\end{aligned} \tag{2.27}$$

$$\begin{aligned}
U_\tau(\vec{r}) &= t_0 \left(1 + \frac{1}{2} x_0 \right) \rho(\vec{r}) - t_0 \left(1 + \frac{1}{2} x_0 \right) \rho_\tau(\vec{r}) \\
&+ \frac{1}{4} \left[t_1 \left(1 + \frac{1}{2} x_1 \right) + t_2 \left(1 + \frac{1}{2} x_2 \right) \right] \tau(\vec{r}) - \frac{1}{4} \left[t_1 \left(\frac{1}{2} + x_1 \right) - t_2 \left(\frac{1}{2} + x_2 \right) \right] \tau_\tau(\vec{r}) \\
&+ \frac{\alpha + 2}{12} t_3 \left(1 + \frac{1}{2} x_3 \right) \rho^{\alpha+1}(\vec{r}) - \frac{\alpha}{12} t_3 \left(\frac{1}{2} + x_3 \right) \rho^{\alpha-1}(\vec{r}) (\rho_\tau^2(\vec{r}) + \rho_{-\tau}^2(\vec{r})) \\
&- \frac{1}{6} t_3 \left(\frac{1}{2} + x_3 \right) \rho^\alpha(\vec{r}) \rho_\tau(\vec{r}) + \frac{1}{24} \left[t_{23} (5 + 4x_{23}) + \frac{1}{2} t_{13} (4 - x_{13}) \right] \rho_{-\tau}(\vec{r}) \tau(\vec{r}) \\
&+ \frac{1}{24} [t_{23} (2 + x_{23}) + t_{13} (2 + x_{13})] \rho_\tau(\vec{r}) \tau_{-\tau}(\vec{r}) + \frac{1}{8} t_{23} (1 + x_{23}) \rho_\tau(\vec{r}) \tau_\tau(\vec{r}) \\
&- \frac{1}{8} \left[3t_1 \left(1 + \frac{1}{2} x_1 \right) - t_2 \left(1 + \frac{1}{2} x_2 \right) \right] \nabla^2 \rho(\vec{r}) \\
&+ \frac{1}{8} \left[3t_1 \left(\frac{1}{2} + x_1 \right) + t_2 \left(\frac{1}{2} + x_2 \right) \right] \nabla^2 \rho_\tau(\vec{r}) \\
&- \frac{1}{96} \left[t_{13} (5 - 2x_{13}) - \frac{1}{2} t_{23} (8 + 7x_{23}) \right] (\rho_{-\tau}(\vec{r}) \nabla^2 \rho(\vec{r}) + \nabla^2 (\rho_\tau(\vec{r}) \rho_{-\tau}(\vec{r}))) \\
&+ \frac{1}{64} t_{23} (1 + x_{23}) \left[2\rho_\tau(\vec{r}) \nabla^2 \rho_\tau(\vec{r}) + (\vec{\nabla} \rho_\tau(\vec{r}))^2 \right] \\
&- \frac{1}{96} \left[t_{13} (5 + 4x_{13}) + \frac{1}{2} t_{23} (4 + 5x_{23}) \right] (\rho(\vec{r}) \nabla^2 \rho_{-\tau}(\vec{r}) + (\vec{\nabla} \rho_{-\tau}(\vec{r}))^2)
\end{aligned} \tag{2.28}$$

$$\begin{aligned}
\bar{W}_\tau(\vec{r}) = & \frac{1}{2} W_0 [\bar{\nabla} \rho(\vec{r}) + \bar{\nabla} \rho_\tau(\vec{r})] + \frac{1}{8} [t_1 - t_2] \bar{J}_\tau(\vec{r}) \\
& - \frac{1}{8} [t_1 x_1 + t_2 x_2] \bar{J}(\vec{r}) + \frac{5}{12} U \bar{J}_\tau(\vec{r}) - \frac{1}{16} t_{23} (1 + x_{23}) \rho_\tau(\vec{r}) \bar{J}_\tau(\vec{r}) \\
& - \frac{1}{24} \left[t_{13} (x_{13} - 1) + \frac{1}{2} t_{23} (4 + 3x_{23}) \right] \rho_{-\tau}(\vec{r}) \bar{J}_\tau(\vec{r}) \\
& - \frac{1}{8} \left[5T - \frac{5}{3} U \right] \bar{J}_{-\tau}(\vec{r}) - \frac{1}{48} [t_{13} x_{13} + t_{23} x_{23}] \rho(\vec{r}) \bar{J}_{-\tau}(\vec{r})
\end{aligned} \tag{2.29}$$

Solving the system of equations (2.26) we can find the single-particle energy ε_i and wave function $\varphi_i(\vec{r}, \sigma, \tau)$ for each of the A single-particle states and, thus, specify the ground state wave function Φ (see Eq. (2.2)). Knowledge of Φ allows the calculation of the energy and other properties of a nucleus in its ground state.

The expectation value of the total Hamiltonian calculated for the wave function Φ contains contributions from the ground state energy of a nucleus as well as the energy of oscillations of the system around its center of mass and energy of rotation of the system as a whole. For spherical systems the rotational energy contribution vanishes. Since in this dissertation the nuclei of interest are considered to be spherically symmetric, in the following discussion only the treatment of the center of mass motion will be described. Factorization of the wave function Φ in order to separately describe the motion of the center of mass and the motion of nucleons relative to it cannot be accomplished in a simple manner. An exact calculation of the ground state energy from the expectation value of the total Hamiltonian is particularly difficult. To a good approximation, the ground state energy can be obtained by subtracting the expectation value of the center of mass energy $\langle \Phi | \frac{P_{CM}^2}{2M} | \Phi \rangle$, where M is the total mass of a nucleus and

$\vec{P}_{CM} = -i\hbar \sum_{i=1}^A \vec{\nabla}_i$, from the expectation value of the total Hamiltonian. Using the

definition of the kinetic energy density $\tau(\vec{r})$ given by Eq. (2.24), the matrix element of

$\frac{P_{CM}^2}{2M}$, can be evaluated as:

$$\langle \Phi | \frac{P_{CM}^2}{2M} | \Phi \rangle = \frac{\hbar^2}{2M} \left\{ \int d\vec{r} \tau(\vec{r}) - \sum_{i,j=1}^A \left| \sum_{\sigma,\tau} \int d\vec{r} \varphi_i^*(\vec{r}, \sigma, \tau) \vec{\nabla} \varphi_j(\vec{r}, \sigma, \tau) \right|^2 \right\}. \quad (2.30)$$

The second term in the r. h. s. of the Eq. (2.30) is difficult to calculate, and it is common in the literature to use the approximation, based on the harmonic oscillator model

$$\langle \Phi | \frac{P_{CM}^2}{2M} | \Phi \rangle = \frac{3}{4} \hbar \omega, \text{ with } (\omega \text{ is the angular frequency}) \hbar \omega = 41A^{-1/3}.$$

For spherical closed shell nuclei the Hartree-Fock equations (Eq. (2.26)) can be simplified. In such a case a single-particle state i can be specified by the following set of quantum numbers: the principal number n , the angular momentum j and its z-component m , the orbital momentum l , the spin $s = 1/2$, and the z-component of the isospin $m_\tau = \pm 1/2$. In this case of interest, the single-particle wave function can be separated onto the radial, total angular momentum and the isospin parts as:

$$\varphi_i(\vec{r}, \sigma, \tau) = \frac{R_\alpha(r)}{r} Y_{jlm}(\hat{r}, \sigma) \chi_{m_\tau}(\tau), \quad (2.31)$$

where α denotes the quantum numbers n, j, l, m_τ corresponding to a single particle state i and $\chi_{m_\tau}(\tau)$ is the eigenfunction of the z-component of the isospin operator,

$$\chi_{m_\tau}(\tau) = \delta_{\tau, m_\tau}. \quad (2.32)$$

The total angular momentum component of the single-particle wave function is given by

$$Y_{jlm}(\hat{r}, \sigma) = \sum_{m_l m_s} \left\langle l \frac{1}{2} m_l m_s \middle| jm \right\rangle Y_{lm_l}(\hat{r}) \mu_{m_s}(\sigma), \quad (2.33)$$

where $\left\langle l \frac{1}{2} m_l m_s \middle| jm \right\rangle$ is the Clebsch-Gordan coefficient and $\mu_{m_s}(\sigma)$ denotes the eigenfunction of the z-component of the spin operator,

$$\mu_{m_s}(\sigma) = \delta_{\sigma, m_s}. \quad (2.34)$$

Using the orthonormality of spherical harmonics,

$$\sum_m Y_{jlm}^*(\hat{r}, \sigma) Y_{jlm}(\hat{r}, \sigma) = \frac{(2j+1)}{4\pi},$$

and the definitions of nucleon and kinetic densities (Eqs. (2.23) and (2.24)) we obtain in a spherically symmetric nucleus:

$$\rho_\tau(\vec{r}) = \rho_\tau(r) = \frac{1}{4\pi r^2} \sum_{n, j_\alpha, l} (2j_\alpha + 1) R_\alpha^2(r), \quad (2.35)$$

$$\tau_\tau(\vec{r}) = \tau_\tau(r) = \frac{1}{4\pi} \sum_{n, j_\alpha, l_\alpha} (2j_\alpha + 1) \left[\left(\frac{dR_\alpha(r)}{dr} \right)^2 + \frac{l_\alpha(l_\alpha + 1)}{r^2} R_\alpha^2(r) \right]. \quad (2.36)$$

Due to the spherical symmetry, the spin current density $\vec{J}_\tau(\vec{r})$ is a vector in the direction

$\hat{r} = \frac{\vec{r}}{r}$: $\vec{J}_\tau \cdot \frac{\vec{r}}{r} = J_\tau$. Therefore, from Eq. (2.25) we obtain:

$$\begin{aligned} \vec{J}_\tau(\vec{r}) &= -i \sum_{i=1}^A \varphi_i^*(\vec{r}, \tau) \frac{\vec{r}}{r} (\vec{\nabla} \times \vec{\sigma}) \varphi_i(\vec{r}, \tau) \frac{\vec{r}}{r} = \\ &= \left[\frac{1}{r^2} \frac{2}{\hbar^2} \sum_{i=1}^A \varphi_i^*(\vec{r}, \tau) (\vec{l} \cdot \vec{s}) \varphi_i(\vec{r}, \tau) \right] \vec{r} = J_\tau(r) \vec{r}, \end{aligned} \quad (2.37)$$

where

$$J_\tau(r) = \frac{1}{4\pi r^2} \sum_{n, j_\alpha, l_\alpha} (2j_\alpha + 1) \left[j_\alpha(j_\alpha + 1) - l_\alpha(l_\alpha + 1) - \frac{3}{4} \right] R_\alpha^2(r). \quad (2.38)$$

After substitution of the wave function given in Eq. (2.31) into Eq. (2.26) we obtain the single-particle Hartree-Fock equations for the radial component of the wave function $R_i(r)$:

$$\begin{aligned} \varepsilon_i R_i(r) &= \frac{\hbar^2}{2m_\tau^*(r)} \left[-R_i''(r) + \frac{l_i(l_i + 1)}{r^2} R_i(r) \right] - \frac{d}{dr} \left(\frac{\hbar^2}{2m_\tau^*(r)} \right) R_i'(r) \\ &+ \left[U_\tau(r) + \frac{1}{r} \frac{d}{dr} \left(\frac{\hbar^2}{2m_\tau^*(r)} \right) + \frac{[j_i(j_i + 1) - l_i(l_i + 1) - 3/4] W_\tau(r)}{r} \right] R_i(r), \end{aligned} \quad (2.39)$$

where the terms $\frac{\hbar^2}{2m_\tau^*(r)}$, $U_\tau(r)$, and $W_\tau(r)$ are obtained from Eqs. (2.27), (2.28), and (2.29), by substitution of particle density, $\rho_\tau(\vec{r})$, kinetic density, $\tau_\tau(\vec{r})$, and spin current density, $\vec{J}_\tau(\vec{r})$, by the radial forms $\rho_\tau(r)$, $\tau_\tau(r)$, and $J_\tau(r)\vec{r}$, from Eqs. (2.35), (2.36),

and (2.37), respectively. The set of equations (2.39) allows us to calculate single particle energies and the radial part of the single-particle wave functions of all possible states i following an iteration procedure. By taking initial set of orthogonal single-particle wave functions one calculates the nucleon, kinetic and spin current densities. Using these calculated function, one obtains initial radial shapes of $\frac{\hbar^2}{2m_\tau^*(r)}$, $U_\tau(r)$, and $W_\tau(r)$,

which are used to calculate a new set of single particle energies and wave functions. Solution is found by repeating this procedure until a desired conversion of the Hartree-Fock ground state energy and the wave function is achieved.

In the next chapter it will be shown how the knowledge of the nuclear ground state wave function, obtained by solving the Hartree-Fock equations, allows us to investigate the excited states of a nucleus.

CHAPTER III

SELF-CONSISTENT HARTREE-FOCK BASED RANDOM PHASE APPROXIMATION DESCRIPTION OF NUCLEAR EXCITED STATES

Within the Random-Phase-Approximation (RPA), nuclear excited states are described in terms of superposition of one-particle – one-hole excitations of a system of nucleons in its ground state, which contains particle-hole correlations. Since nuclear excitations in the continuum have contributions from a large number of particle-hole states, the RPA equations formulated in particle-hole configuration space in terms of A and B matrices are hard to solve numerically. Therefore, in this study the coordinate space formulation of RPA in terms of Green's functions will be used. In the following we derive the coordinate Green's function formalism for Hartree-Fock based RPA (HF-RPA) calculations using the time-dependent Hartree-Fock approach [28]. We then describe the applications of this formalism to the HF-RPA calculations with the Skyrme-type effective nucleon-nucleon interaction, and later discuss a method of elimination of the spurious state mixing from the RPA transitional strength distribution and from the corresponding transition density of the isoscalar giant dipole resonance.

A. Green's Function Formalism of HF-RPA in Coordinate Representation and RPA with Skyrme Effective Interaction

In the previous chapter we obtained the self-consistent single particle Hartree-Fock Hamiltonian for the most general type of the effective nucleon-nucleon interaction (see Eqs. (2.10)) in the form:

$$h = t + v(\rho) + v_{exch}. \quad (3.1)$$

where t is the kinetic energy operator, $v(\rho)$ is the density-dependent average field operator, and v_{exch} is the exchange interaction.

It needs to be noted, that for the case of Skyrme nucleon-nucleon interaction, both direct and exchange terms of the single particle interaction are density dependent. Due to

our expressed interest in the application of the HF-RPA with the Skyrme nucleon-nucleon interaction, this property of the single particle interaction will be considered by default.

As in the previous chapter, the nucleon density $\rho(\vec{r})$ is defined as:

$$\rho(\vec{r}) = \sum_{i=1}^A \sum_{\sigma, \tau} \varphi_i^*(\vec{r}, \sigma, \tau) \varphi_i(\vec{r}, \sigma, \tau), \quad (3.2)$$

where $\varphi_i(\vec{r}, \sigma, \tau)$ are single-particle eigenfunctions, corresponding to single particle eigenenergies ε_i of the self-consistent Hartree-Fock equation:

$$h\varphi_i(\vec{r}, \sigma, \tau) = \varepsilon_i \varphi_i(\vec{r}, \sigma, \tau). \quad (3.3)$$

In the time dependent theory, the system of nucleons in its ground state is introduced into a weak harmonic external field of the form:

$$\hat{f}(\vec{r}, t) = \hat{f}(\vec{r}) e^{-i\frac{Et}{\hbar}} + \hat{f}^+(\vec{r}) e^{i\frac{Et}{\hbar}}, \quad (3.4)$$

where E is the energy of the excitation, $E = \hbar\omega$. Considering $f(\vec{r})$ as a small perturbation, we will look for the single-particle perturbed wave functions to the first order with the same harmonic time dependence:

$$\tilde{\varphi}_i(\vec{r}, \sigma, \tau, t) = \varphi_i(\vec{r}, \sigma, \tau) + \varphi_i'(\vec{r}, \sigma, \tau) e^{-i\frac{Et}{\hbar}} + \varphi_i''(\vec{r}, \sigma, \tau) e^{i\frac{Et}{\hbar}}, \quad (3.5)$$

where we take $\varphi_i'(\vec{r}, \sigma, \tau)$, $\varphi_i''(\vec{r}, \sigma, \tau)$, the perturbed coordinate single-particle wave functions to be orthogonal to $\varphi_i(\vec{r}, \sigma, \tau)$, the Hartree-Fock single-particle wave functions. Hence, we can expect that the perturbed time-dependent nucleon density is exhibiting the same behavior as the external field and to the first order can be written as:

$$\tilde{\rho}(\vec{r}, t) = \rho(\vec{r}) + \rho'(\vec{r}) e^{-i\frac{Et}{\hbar}} + \rho^*(\vec{r}) e^{i\frac{Et}{\hbar}}, \quad (3.6)$$

where $\rho(\vec{r})$ is the unperturbed nucleon density defined in Eq. (3.2), and the perturbed coordinate-dependent nucleon density is given by:

$$\rho'(\vec{r}) = \sum_{i=1}^A \sum_{\sigma, \tau} (\varphi_i'(\vec{r}, \sigma, \tau) \varphi_i^*(\vec{r}, \sigma, \tau) - \varphi_i''^*(\vec{r}, \sigma, \tau) \varphi_i(\vec{r}, \sigma, \tau)). \quad (3.7)$$

Now, according to perturbation theory, we can formally write the new single-particle time-dependent-Hartree-Fock Hamiltonian as:

$$h_{TD}(t) = h + \left(f(\vec{r}) + \frac{\delta h}{\delta \rho} \Big|_{\rho(\vec{r})} \rho'(\vec{r}) \right) e^{-i\frac{Et}{\hbar}} + \left(f^+(\vec{r}) + \frac{\delta h^+}{\delta \rho} \Big|_{\rho(\vec{r})} \rho'^*(\vec{r}) \right) e^{i\frac{Et}{\hbar}}. \quad (3.8)$$

where h is the unperturbed single-particle HF Hamiltonian, $f(\vec{r})$ is the weak external perturbation interaction, and $\frac{\delta h}{\delta \rho}$ is the formal functional differentiation of the single-

particle Hamiltonian with respect to the density, taken at $\rho = \rho(\vec{r})$. The term $\frac{\delta h^+}{\delta \rho}$

represents all possible non-hermitian contributions in the single particle HF Hamiltonian.

Then, the time dependent HF equations take the form of:

$$i\hbar \frac{d\tilde{\varphi}_i(\vec{r}, \sigma, \tau, t)}{dt} = \left(h + \left(f(\vec{r}) + \frac{\delta h}{\delta \rho} \rho'(\vec{r}) \right) e^{-i\frac{Et}{\hbar}} + \left(f^+(\vec{r}) + \frac{\delta h^+}{\delta \rho} \rho'^*(\vec{r}) \right) e^{i\frac{Et}{\hbar}} - \varepsilon_i \right) \tilde{\varphi}_i(\vec{r}, \sigma, \tau, t). \quad (3.9)$$

In expression (3.9), the coefficients at the exponents are considered to be independent of each other and provide us with the equations for the perturbed part of the single particle wave functions. To the first order, we obtain:

$$(h - \varepsilon_i) \varphi'_i(\vec{r}, \sigma, \tau) + \left(f(\vec{r}) + \frac{\delta h}{\delta \rho} \rho'(\vec{r}) \right) \varphi_i(\vec{r}, \sigma, \tau) = E \varphi'_i(\vec{r}, \sigma, \tau), \quad (3.10)$$

$$(h - \varepsilon_i) \varphi''_i(\vec{r}, \sigma, \tau) + \left(f^+(\vec{r}) + \frac{\delta h^+}{\delta \rho} \rho'^*(\vec{r}) \right) \varphi_i(\vec{r}, \sigma, \tau) = -E \varphi''_i(\vec{r}, \sigma, \tau), \quad (3.11)$$

Formal solution of the equations (3.10) and (3.11) for the single particle wave function perturbations $\varphi'_i(\vec{r}, \sigma, \tau)$, $\varphi''_i(\vec{r}, \sigma, \tau)$ can be obtained as:

$$\varphi'_i(\vec{r}, \sigma, \tau) = \frac{-1}{h - \varepsilon_i - E} \left(f(\vec{r}) + \frac{\delta h}{\delta \rho} \rho'(\vec{r}) \right) \varphi_i(\vec{r}, \sigma, \tau), \quad (3.12)$$

$$\varphi''_i(\vec{r}, \sigma, \tau) = \frac{-1}{h - \varepsilon_i + E} \left(f^+(\vec{r}) + \frac{\delta h^+}{\delta \rho} \rho'^*(\vec{r}) \right) \varphi_i(\vec{r}, \sigma, \tau). \quad (3.13)$$

Using the definition (3.7) we obtain the following expression for the perturbed (transition) single-particle density,

$$\rho'(\vec{r}) = -\sum_{i=1}^A \sum_{\sigma, \tau} \varphi_i^*(\vec{r}, \sigma, \tau) \left(\frac{f(\vec{r}) + (\delta h / \delta \rho) \rho'(\vec{r})}{h - \varepsilon_i - E} + \frac{f(\vec{r}) + \rho'(\vec{r})(\delta h / \delta \rho)}{h - \varepsilon_i + E} \right) \varphi_i(\vec{r}, \sigma, \tau). \quad (3.14)$$

We can define a bare Green's function according to the Green's function method in spectral representation,

$$\begin{aligned} G_{\pm}^0(\vec{r}_1, \vec{r}_2, E) &= \sum_{i=1}^A \sum_{\sigma_1, \sigma_2, \tau_1, \tau_2} \varphi_i^*(\vec{r}_1, \sigma_1, \tau_1) \left[\frac{1}{h - \varepsilon_i - E} \pm \frac{1}{h - \varepsilon_i + E} \right] \varphi_i(\vec{r}_2, \sigma_2, \tau_2) \\ &= \sum_{i,m} \sum_{\sigma_1, \sigma_2, \tau_1, \tau_2} \varphi_i^*(\vec{r}_1, \sigma_1, \tau_1) \varphi_m(\vec{r}_1, \sigma_1, \tau_1) \times \\ &\quad \left[\frac{1}{\varepsilon_m - \varepsilon_i - E} \pm \frac{1}{\varepsilon_m - \varepsilon_i + E} \right] \varphi_m^*(\vec{r}_2, \sigma_2, \tau_2) \varphi_i(\vec{r}_2, \sigma_2, \tau_2). \end{aligned} \quad (3.15)$$

Then Eq. (3.14) for the transition density associated with the single-particle perturbing operator $\hat{f}(\vec{r})$ can be rewritten in form:

$$\rho'(\vec{r}, E) = -\frac{1}{2} \int d\vec{r}' \sum_{\pm} G_{\pm}^0(\vec{r}, \vec{r}', E) \left\{ (f(\vec{r}') \pm f^+(\vec{r}')) + \left(\frac{\delta h}{\delta \rho} \pm \frac{\delta h^+}{\delta \rho} \right) \rho'(\vec{r}') \right\}. \quad (3.16)$$

According to the Green's function method, the solution for $\rho'(\vec{r}, E)$ can be formally presented by the following expression:

$$\rho'(\vec{r}, E) = \rho_{tr}(\vec{r}, E) = -\int d\vec{r}' G^{RPA}(\vec{r}, \vec{r}', E) f(\vec{r}'). \quad (3.17)$$

Such a formal solution demands the RPA-Green's function to be written in the form:

$$G^{RPA} = G^0 \left(\mathbf{1} + \hat{V}_{ph} G^0 \right)^{-1}, \quad (3.18)$$

where $G^0(\vec{r}, \vec{r}', E)$ is the free particle-hole Green's function formally defined as:

$$G^0(\vec{r}, \vec{r}', E) = \sum_{i,m} \left[\frac{\varphi_m(\vec{r}) \varphi_i^*(\vec{r}) \varphi_m^*(\vec{r}') \varphi_i(\vec{r}')}{E - \varepsilon_m + \varepsilon_i + i\eta} - \frac{\varphi_i(\vec{r}) \varphi_m^*(\vec{r}) \varphi_i^*(\vec{r}') \varphi_m(\vec{r}')}{E + \varepsilon_m - \varepsilon_i + i\eta} \right], \quad (3.19)$$

and \hat{V}_{ph} is the effective particle-hole interaction obtained as a functional derivative of the energy density with respect to the ground-state density of the many-body system

obtained by solving the Hartree-Fock problem, $\hat{V}_{ph} = \delta h / \delta \rho|_{\rho=\rho(\vec{r})}$. Therefore, equation (3.18) together with Eq. (3.19) allows us to find the RPA Greens function $G^{RPA}(\vec{r}, \vec{r}', E)$ from the knowledge of single-particle energies and wave functions obtained within the Hartree-Fock approximation.

A direct way to find energies of excited states of a nucleus is by searching for poles of $G^{RPA}(\vec{r}, \vec{r}', E)$. Such a procedure should be avoided from the numerical point of view. A way to avoid numerical calculations with such singularities is to use averaging procedure on the RPA Green's function over some energy interval Γ_ν around excited state of interest, $E = E_\nu$. From the physics point of view, introduction of the interval Γ_ν can be explained by the argument that the energy of any excited state has a certain width. Following this idea we redefine the RPA Green's function as:

$$G^{RPA}(\vec{r}, \vec{r}', E) = \sum_{\nu} \int_{E_\nu - \Gamma_\nu/2}^{E_\nu + \Gamma_\nu/2} dE' K(E, E') \left[\frac{\rho_{tr}(\vec{r}, E_\nu) \rho_{tr}^*(\vec{r}', E_\nu)}{E' - E_\nu + i\eta} - \frac{\rho_{tr}(\vec{r}', E_\nu) \rho_{tr}^*(\vec{r}, E_\nu)}{E' + E_\nu - i\eta} \right], \quad (3.20)$$

where Γ_ν is the width of the excited state ν and $K(E, E')$ is an averaging function, chosen based on the model of the width of excited state ν . If $K(E, E')$ is chosen to be a Lorentzian and $E > 0$, the expression (3.18) is reduced to:

$$G^{RPA}(\vec{r}, \vec{r}', E) = \sum_{\nu} \frac{\rho_{tr}(\vec{r}, E_\nu) \rho_{tr}^*(\vec{r}', E_\nu)}{E - E_\nu + i\Gamma_\nu/2}. \quad (3.21)$$

In order to find the energies of the excited states of a nucleus, we introduce the transition strength function $S(E)$ for the one body excitation operator $\hat{f}(\vec{r})$. It is defined for $E > 0$ as:

$$S(E) = \sum_{\nu} \left| \langle 0 | \hat{f} | \nu \rangle \right|^2 \delta(E - E_\nu) = \sum_{\nu} \left[\iint (\hat{f}^+(\vec{r}') \rho_{tr}(\vec{r}', E_\nu) \rho_{tr}^*(\vec{r}, E_\nu) \hat{f}(\vec{r})) d\vec{r} d\vec{r}' \right] \delta(E - E_\nu). \quad (3.22)$$

For the case when the excited state ν has the energy width Γ_ν , we can substitute the energy delta dependence by:

$$\delta(E - E_\nu) \rightarrow -\frac{1}{\pi} \text{Im} \left[\frac{1}{E - E_\nu + i\Gamma_\nu/2} \right]. \quad (3.23)$$

Substituting expression (3.23) into Eq. (3.21) and comparing the result with Eq. (3.21) we obtain:

$$S(E) = \frac{1}{\pi} \iint \hat{f}^+(\vec{r}') \text{Im} [G^{RPA}(\vec{r}', \vec{r}, E)] \hat{f}(\vec{r}) d\vec{r} d\vec{r}' = \frac{1}{\pi} \text{Im} [Tr \{ \hat{f} \cdot \hat{G}^{RPA}(E) \cdot \hat{f} \}]. \quad (3.24)$$

This function peaks when the frequency of the external field is such that $\hbar\omega = E_\nu$ and, therefore, studying the behavior of this function allows us to specify the energies of the excited states of a nucleus.

Using Eq. (3.22) we now can redefine the transition density as:

$$\rho_{tr}(\vec{r}, E) = \frac{\Delta E}{\sqrt{S(E)\Delta E}} \int f(\vec{r}') \left[\frac{1}{\pi} \text{Im} G^{RPA}(\vec{r}', \vec{r}, E) \right] d\vec{r}'. \quad (3.25)$$

Note that $\rho_{tr}(\vec{r}, E)$, as defined in Eq. (3.25), is associated with the strength in the region $E \pm \Delta E/2$ and is consistent with

$$S(E) = \left| \int \rho_{tr}(\vec{r}, E) f(\vec{r}) d\vec{r} \right|^2 / \Delta E, \quad (3.26)$$

that can be seen as a discretized expression of Eq. (3.22).

Now, let us consider how such a useful quantity as a sum rule for one body

Hermitian excitation operator $\hat{f}(\vec{r})$ can be found in terms of the RPA Green's function.

The energy moment M_k for the operator $\hat{f}(\vec{r})$ is defined as:

$$\begin{aligned} M_k &= \sum_\nu (E_\nu)^k \left| \langle \nu | \hat{f} | 0 \rangle \right|^2 \\ &= \sum_\nu (E_\nu)^k \iint \left(\hat{f}^+(\vec{r}) \rho_{tr}(\vec{r}, E_\nu) \rho_{tr}^*(\vec{r}', E_\nu) \hat{f}(\vec{r}') \right) d\vec{r} d\vec{r}'. \end{aligned} \quad (3.27)$$

Considering Eqs. (3.25) and (3.26) we can rewrite M_k in form:

$$M_k = \int_0^\infty E^k S(E) dE. \quad (3.28)$$

By direct substitution of $S(E)$ from Eqn. (3.24) we finally obtain:

$$M_k = \frac{1}{\pi} \int_0^{\infty} E^k \text{Im} \left[\text{Tr} \left\{ \hat{f} \cdot \hat{G}^{RPA}(E) \cdot \hat{f} \right\} \right] dE. \quad (3.29)$$

For $k = 1$ we obtain the energy-weighted strength. According to the Thouless theorem [27], value of energy moment M_k of order $k = 1$ evaluated within the RPA formalism using Eq. (3.29) is equal to the value of the energy weighted sum rule obtained as an expectation value of the double commutator of the single-particle excitation operator with the total Hamiltonian of the system on the HF ground state wave function:

$$M_1 = \frac{1}{2} \langle \Phi | [\hat{f}, [H, \hat{f}]] | \Phi \rangle, \quad (3.30)$$

under the condition that particle and hole excitation energies and wave functions used in the RPA calculation were found within the HF formalism and the particle-hole interaction used in the RPA is obtained from HF Hamiltonian with all possible terms retained.

It is also important to note that the strength function $S(E)$ and the transition density $\rho_{tr}(\vec{r}, E)$ of a state at energy E_n below the particle escape threshold (or having a very small width) can be obtained from Eqs. (3.24) and (3.25), respectively, by replacing $(1/\pi)\text{Im} G^{RPA}(\vec{r}, \vec{r}', E)$ with

$$\lim_{E \rightarrow E_n} \text{Re} G^{RPA}(\vec{r}, \vec{r}', E)(E_n - E). \quad (3.31)$$

In case of a Skyrme-type nucleon-nucleon interaction, the zero-range particle-hole interaction can be obtained by functional differentiation of the energy density:

$$V_{ph}(\vec{r}, \vec{r}') = \delta(\vec{r} - \vec{r}') \sum_{s,t,s',t'} \frac{1}{16} \left[1 + (-1)^{s-s'} \vec{\sigma} \cdot \vec{\sigma}' \right] \left[1 + (-1)^{t-t'} \vec{\tau} \cdot \vec{\tau}' \right] \frac{\delta^2 H}{\delta \rho_{st} \delta \rho_{s't'}},$$

where H is the sum of the Skyrme interaction and kinetic energy densities (see APPENDIX B), and s, s' and t, t' are the third components of the spin and isospin, appropriately. Using Eqs. (B.30) and (B.31) we obtain the following:

$$V_{ph}(\vec{r}, \vec{r}') = \delta(\vec{r} - \vec{r}') \left[a + b(\bar{\nabla}^2 + \bar{\nabla}'^2 + \bar{\nabla}^2 + \bar{\nabla}'^2) + c(\bar{\nabla} - \bar{\nabla}')(\bar{\nabla}' - \bar{\nabla}') \right. \\ \left. + d(\bar{\nabla} + \bar{\nabla}')(\bar{\nabla}' + \bar{\nabla}') \right] + V'_{ph}(\vec{r}, \vec{r}'), \quad (3.32)$$

$$V_{ph}^t(\vec{r}, \vec{r}') = \delta(\vec{r} - \vec{r}') \left[b^t(\bar{\nabla}^2 + \bar{\nabla}'^2 + \bar{\nabla}^2 + \bar{\nabla}'^2) + c^t(\bar{\nabla} - \bar{\nabla}')(\bar{\nabla}' - \bar{\nabla}') \right. \\ + d^t(\bar{\nabla} + \bar{\nabla}')(\bar{\nabla}' + \bar{\nabla}') + e\bar{\sigma}(\bar{\nabla} - \bar{\nabla}')(\bar{\nabla}' - \bar{\nabla}')\bar{\sigma}' + f\bar{\sigma}(\bar{\nabla} + \bar{\nabla}')(\bar{\nabla}' + \bar{\nabla}')\bar{\sigma}' \\ + g\bar{\sigma}(\bar{\nabla} - \bar{\nabla}')\bar{\sigma}'(\bar{\nabla}' - \bar{\nabla}') + h\bar{\sigma}(\bar{\nabla} + \bar{\nabla}')\bar{\sigma}'(\bar{\nabla}' + \bar{\nabla}') \\ + p(\bar{\sigma}(\bar{\nabla} - \bar{\nabla}')(\bar{\nabla} - \bar{\nabla}')\bar{\sigma}' + \bar{\sigma}(\bar{\nabla}' - \bar{\nabla}')\bar{\sigma}'(\bar{\nabla}' - \bar{\nabla}')) \\ \left. + q(\bar{\sigma}(\bar{\nabla} + \bar{\nabla}')(\bar{\nabla} + \bar{\nabla}')\bar{\sigma}' + \bar{\sigma}(\bar{\nabla}' + \bar{\nabla}')\bar{\sigma}'(\bar{\nabla}' + \bar{\nabla}')) \right], \quad (3.33)$$

where

$$a = a_F + a_{F'}\bar{\tau} \cdot \bar{\tau}' + a_G\bar{\sigma} \cdot \bar{\sigma}' + a_{G'}(\bar{\tau} \cdot \bar{\tau}')(\bar{\sigma} \cdot \bar{\sigma}'), \\ b = b_F + b_{F'}\bar{\tau} \cdot \bar{\tau}' + b_G\bar{\sigma} \cdot \bar{\sigma}' + b_{G'}(\bar{\tau} \cdot \bar{\tau}')(\bar{\sigma} \cdot \bar{\sigma}'), \\ c = c_F + c_{F'}\bar{\tau} \cdot \bar{\tau}' + c_G\bar{\sigma} \cdot \bar{\sigma}' + c_{G'}(\bar{\tau} \cdot \bar{\tau}')(\bar{\sigma} \cdot \bar{\sigma}'), \\ d = d_F + d_{F'}\bar{\tau} \cdot \bar{\tau}' + d_G\bar{\sigma} \cdot \bar{\sigma}' + d_{G'}(\bar{\tau} \cdot \bar{\tau}')(\bar{\sigma} \cdot \bar{\sigma}'), \quad (3.34)$$

and the definitions of appropriate coefficients, given in terms of Skyrme parameters and particle and kinetic energy densities, ρ and τ , have the form:

$$a_F = \frac{3}{4}t_0 + \frac{3}{8}t_3\rho^\alpha + \frac{1}{64}t_{13}(4\tau - 3\nabla^2\rho) + \frac{1}{128}t_{23}(5 + 4x_{23})(4\tau + 3\nabla^2\rho), \\ a_{F'} = -\frac{1}{4}t_0(1 + 2x_0) - \frac{1}{8}t_3\rho^\alpha - \frac{1}{192}t_{13}(1 - x_{13})(4\tau - 3\nabla^2\rho) - \frac{1}{128}t_{23}\nabla^2\rho - \frac{1}{96}t_{23}(5 + 4x_{23})\tau, \\ a_G = -\frac{1}{4}t_0(1 - 2x_0) - \frac{1}{8}t_3\rho^\alpha - \frac{1}{192}t_{13}(1 + x_{13})(4\tau - 3\nabla^2\rho) - \frac{1}{128}t_{23}\nabla^2\rho - \frac{1}{96}t_{23}(5 + 4x_{23})\tau, \\ a_{G'} = -\frac{1}{4}t_0 - \frac{1}{8}t_3\rho^\alpha - \frac{1}{192}t_{13}(4\tau - 3\nabla^2\rho) - \frac{1}{384}t_{23}(3 + 4x_{23})\nabla^2\rho - \frac{1}{96}t_{23}(5 + 4x_{23})\tau,$$

$$b_F = -\frac{3}{32}t_1 - \frac{1}{32}t_2(5 + 4x_2) - \frac{1}{32}t_{13}\rho - \frac{1}{64}t_{23}(5 + 4x_{23})\rho, \\ b_{F'} = \frac{1}{32}t_1(1 + 2x_1) - \frac{1}{32}t_2(1 + 2x_2) + \frac{1}{192}t_{13}(2 + x_{13})\rho - \frac{1}{192}t_{23}(1 + 2x_{23})\rho, \\ b_G = \frac{1}{32}t_1(1 - 2x_1) - \frac{1}{32}t_2(1 + 2x_2) + \frac{1}{192}t_{13}(2 - x_{13})\rho - \frac{1}{192}t_{23}(1 + 2x_{23})\rho, \\ b_{G'} = \frac{1}{32}t_1 - \frac{1}{32}t_2 + \frac{1}{96}t_{13}\rho - \frac{1}{192}t_{23}\rho,$$

$$c_F = \frac{3}{32}t_1 + \frac{1}{32}t_2(5 + 4x_2) + \frac{1}{64}t_{13}\rho + \frac{1}{128}t_{23}(5 + 4x_{23})\rho, \\ c_{F'} = -\frac{1}{32}t_1(1 + 2x_1) + \frac{1}{32}t_2(1 + 2x_2) - \frac{1}{192}t_{13}(1 + 2x_{13})\rho + \frac{1}{384}t_{23}(7 + 8x_{23})\rho,$$

$$\begin{aligned}
c_G &= -\frac{1}{32}t_1(1-2x_1) + \frac{1}{32}t_2(1+2x_2) - \frac{1}{192}t_{13}(1-2x_{13})\rho + \frac{1}{384}t_{23}(7+8x_{23})\rho, \\
c_{G'} &= -\frac{1}{32}t_1 + \frac{1}{32}t_2 - \frac{1}{192}t_{13}\rho + \frac{1}{384}t_{23}(7+4x_{23})\rho, \\
d_F &= \frac{3}{32}t_1 - \frac{3}{32}t_2(5+4x_2) + \frac{1}{64}t_{13}\rho - \frac{5}{128}t_{23}(5+4x_{23})\rho, \\
d_{F'} &= -\frac{1}{32}t_1(1+2x_1) - \frac{1}{32}t_2(1+2x_2) - \frac{1}{192}t_{13}(1+2x_{13})\rho - \frac{1}{384}t_{23}(11+16x_{23})\rho, \\
d_G &= -\frac{1}{32}t_1(1-2x_1) - \frac{1}{32}t_2(1+2x_2) - \frac{1}{192}t_{13}(1-2x_{13})\rho - \frac{1}{384}t_{23}(11+16x_{23})\rho, \\
d_{G'} &= -\frac{1}{32}t_1 - \frac{1}{32}t_2 - \frac{1}{192}t_{13}\rho - \frac{1}{384}t_{23}(11+4x_{23})\rho \\
b^T &= -\frac{1}{16}(T-U)\vec{\sigma} \cdot \vec{\sigma}' + \frac{1}{48}(3T+U)(\vec{\tau} \cdot \vec{\tau}')(\vec{\sigma} \cdot \vec{\sigma}'), \\
d^T &= \frac{1}{16}(T+3U)\vec{\sigma} \cdot \vec{\sigma}' - \frac{1}{16}(T-U)(\vec{\tau} \cdot \vec{\tau}')(\vec{\sigma} \cdot \vec{\sigma}'), \\
e &= -\frac{3}{32}(T-U) + \frac{1}{32}(3T+U)(\vec{\tau} \cdot \vec{\tau}'), \\
f &= -\frac{3}{32}(T+U) + \frac{1}{32}(3T-U)(\vec{\tau} \cdot \vec{\tau}'), \\
c^T &= -b^T, \quad g = e, \quad h = f, \quad p = -e, \quad q = -f.
\end{aligned} \tag{3.35}$$

So, the free-system Green's function is obtained by substitution into the Eq. (3.19) single-particle wave functions and single-particle energies obtained as solutions of the Hartree-Fock equations (2.39). The RPA Green's function, then, is constructed using equations (3.18), (3.19) and (3.32).

B. Elimination of Spurious State Contribution from Strength Distribution Function of Isoscalar Giant Dipole Excitation

Now we will consider the analysis and elimination of the Spurious State Mixing (SSM) from the strength distribution function of the ISGDR and from the results of calculations of the inelastic cross sections.

For future references we need to mention, that within the collective model, the energy weighted sum rule M_1 (EWSR) associated with an excitation operator $f_{LM} = f(r)Y_{LM}(\hat{r})$ is given by [39]:

$$\begin{aligned}
M_1(f_{LM}) &= \int_0^{\infty} E S(E) dE \\
&= \frac{\hbar^2}{2m} \frac{A}{4\pi} \left[\langle 0 | \left(\frac{df(r)}{dr} \right)^2 + L(L+1) \left(\frac{f(r)}{r} \right)^2 | 0 \rangle \right]. \tag{3.36}
\end{aligned}$$

Assuming that there is only one collective state [3,10] with energy E_{coll} , exhausting 100% of the EWSR associated with the excitation operator $f_{LM} = f(r)Y_{LM}(\hat{r})$, the form for the corresponding transition density is found as:

$$\begin{aligned}
\rho_{ir}^{coll}(r) &= -\frac{\hbar^2}{2m} \sqrt{\frac{2L+1}{M_1(f_{LM})E_{coll}}} \left[\left(\frac{1}{r} \frac{d^2}{dr^2} (rf(r)) - \frac{L(L+1)}{r^2} f(r) \right) \rho_0 \right. \\
&\quad \left. + \frac{df(r)}{dr} \frac{d\rho_0(r)}{dr} \right]. \tag{3.37}
\end{aligned}$$

Let us consider the isoscalar dipole excitation operator

$$f = \sum_{i=1}^A f(\vec{r}_i), \tag{3.38}$$

here the single particle operators

$$f(\vec{r}) = f(r)Y_{1M}(\hat{r}), \quad f_1(\vec{r}) = rY_{1M}(\hat{r}). \tag{3.39}$$

According to the definition of the RPA Green's function (3.21), we can approximate the response function $R(\vec{r}, \vec{r}', E) = (1/\pi) \text{Im} G^{RPA}(\vec{r}, \vec{r}', E)$ in form of the sum of separable terms

$$R(\vec{r}, \vec{r}', E) = \sum_n d_n(E) \rho_n(\vec{r}) \rho_n(\vec{r}'), \tag{3.40}$$

where $d_n(E)$ accounts for the energy dependence of $R(\vec{r}, \vec{r}', E)$. In case of a discretized continuum calculation, the sum in Eq. (3.40) has only one term for each value of the discretized excitation energy E . Then, depending on the form of the coefficient $d_n(E)$, $\rho_n(\vec{r})$ is proportional to the transition density associated with the resonance and as such may contain a spurious state contribution due to approximations employed in the RPA calculations. In general, due to the finite value of the artificially introduced smearing width Γ , the sum in Eq. (3.40) may contain multiple terms.

Assuming that the density $\rho_n(\vec{r})$ has contributions of the resonance, $\rho_{n3}(\vec{r})$, and of a spurious state, $\rho_{n1}(\vec{r})$, we express it as,

$$\rho_n(\vec{r}) = a_n \rho_{n3}(\vec{r}) + b_n \rho_{n1}(\vec{r}), \quad (3.41)$$

with the amplitudes of the intrinsic resonance state and the spurious state a_n and b_n , respectively, satisfying following condition.

$$a_n^2 + b_n^2 = 1.0, \quad (3.42)$$

Note that we impose a condition on $\rho_{n3}(\vec{r})$, associated with the isoscalar giant dipole resonance (ISGDR), that it fulfills the translation invariance condition for all n :

$$\int f_1(\vec{r}) \rho_{n3}(\vec{r}) d\vec{r} = 0. \quad (3.43)$$

From Eqs. (3.40) and (3.41) we have with an obvious notation

$$\begin{aligned} R(\vec{r}, \vec{r}', E) = & \sum_n d_n(E) a_n^2 \rho_{n3}(\vec{r}) \rho_{n3}(\vec{r}') + \\ & \sum_n d_n(E) a_n b_n \rho_{n3}(\vec{r}) \rho_{n1}(\vec{r}') + \\ & \sum_n d_n(E) b_n a_n \rho_{n1}(\vec{r}) \rho_{n3}(\vec{r}') + \\ & \sum_n d_n(E) b_n^2 \rho_{n1}(\vec{r}) \rho_{n1}(\vec{r}') \end{aligned} \quad (3.44)$$

From the decomposition of the response function R , Eq. (3.44) it becomes obvious, that the required strength distribution, $S(E)$, and the transition density, $\rho_{tr}(\vec{r})$, containing no spurious contributions, can be obtained from $R_{33} = \sum_n d_n(E) a_n^2 \rho_{n3}(\vec{r}) \rho_{n3}(\vec{r}')$ using Eqs. (3.24) and (3.25) with scattering operator $f(\vec{r})$ from Eq. (3.39). However, the exact expression for R_{33} is not known. To eliminate spurious state contributions from the transition strength distribution, $S(E)$, we introduce a projection operator that projects out spurious contribution $\rho_{n1}(\vec{r})$ in the transition density,

$$f_\eta = \sum_{i=1}^A f_\eta(\vec{r}_i) = f - \eta f_1, \quad (3.45)$$

where $f_\eta(\vec{r}) = f(\vec{r}) - \eta f_1(\vec{r})$. Using Eqs. (3.24), (3.40) and (3.43) we obtain expression for the projection strength distribution, $S_\eta(E)$,

$$\begin{aligned} S_\eta(E) = & \iint d\vec{r} d\vec{r}' f_\eta(\vec{r}) R(\vec{r}, \vec{r}', E) f_\eta(\vec{r}') = \\ & \sum_n d_n(E) a_n^2 \iint d\vec{r} d\vec{r}' f(\vec{r}) \rho_{n3}(\vec{r}) \rho_{n3}(\vec{r}') + \\ & 2 \sum_n d_n(E) a_n b_n \iint d\vec{r} d\vec{r}' f_\eta(\vec{r}) \rho_{n1}(\vec{r}) f(\vec{r}') \rho_{n3}(\vec{r}') + \\ & \sum_n d_n(E) b_n^2 \iint d\vec{r} d\vec{r}' f_\eta(\vec{r}) \rho_{n1}(\vec{r}) \rho_{n1}(\vec{r}') f_\eta(\vec{r}') \end{aligned} \quad (3.46)$$

The spurious state contribution is expressed in the last two term of the equation (3.41). Therefore the condition of projecting out the spurious state contribution from the transitional strength is:

$$\int d\vec{r} (f(\vec{r}) - \eta f_1(\vec{r})) \rho_{n1}(\vec{r}) = 0, \text{ for all } n \quad (3.47)$$

We need to point out that all $\rho_{n1}(\vec{r})$, taken in form of (3.37) (see Refs. [17,40]), coincide with the coherent spurious state transition density $\rho_{ss}(\vec{r})$ (see Ref. [41]),

$$\rho_{n1}(\vec{r}) = \rho_{ss}(\vec{r}) = -\sqrt{\frac{\hbar^2}{2m} \frac{4\pi}{AE_{ss}}} \frac{\partial \rho_0}{\partial r} Y_{1M}(\hat{r}), \quad (3.48)$$

where E_{ss} is the spurious state energy and ρ_0 is the ground state density of the nucleus.

Note that $\rho_{ss}(\vec{r})$ in Eq. (3.48) is normalized to 100% of the energy weighted sum rule obtained using Eq. (3.36). Then the condition for calculating the coefficient η is:

$$\eta = \frac{\int d\vec{r} \rho_{ss}(\vec{r}) f(\vec{r})}{\int d\vec{r} \rho_{ss}(\vec{r}) f_1(\vec{r})}. \quad (3.49)$$

Under the assumption that approximation (3.40) is correct, the coefficient η , satisfying condition (3.49) for all n gives us:

$$\begin{aligned} S_\eta(E) = & \iint d\vec{r} d\vec{r}' f_\eta(\vec{r}) R(\vec{r}, \vec{r}', E) f_\eta(\vec{r}') = \\ & \sum_n d_n(E) a_n^2 \iint d\vec{r} d\vec{r}' f(\vec{r}) \rho_{n3}(\vec{r}) \rho_{n3}(\vec{r}') \end{aligned} \quad (3.50)$$

The spurious state contributions have been eliminated from the strength distribution function. To eliminate residual spurious contribution from the transition density of the ISGDR, we need to analyze the transition density associated with the strength $S_\eta(E)$.

Using Eqs. (3.25), (3.41), (3.43), (3.44) and (3.50) we calculate

$$\rho_\eta(\vec{r}, E) = \frac{\Delta E}{\sqrt{S_\eta(E)\Delta E}} \sum_n a_n d_n(E) \int d\vec{r}' f_\eta(\vec{r}') \rho_{n3}(\vec{r}) [a_n \rho_{n3}(\vec{r}) + b_n \rho_{ss}(\vec{r})]. \quad (3.51)$$

Now, let us define the intrinsic transition density of the isoscalar giant dipole resonance as:

$$\rho_{ir}(\vec{r}, E) = \rho_\eta(\vec{r}, E) - \alpha \rho_{ss}(\vec{r}, E), \quad (3.52)$$

then according to the condition that in the intrinsic resonance state there is no spurious state contribution present (see Eq. (3.43)), we can write,

$$\int d\vec{r} f_1(\vec{r}) \rho_{ir}(\vec{r}, E) = \int d\vec{r} f_1(\vec{r}) [\rho_\eta(\vec{r}, E) - \alpha \rho_{ss}(\vec{r}, E)] = 0. \quad (3.53)$$

Equation (3.53) is the condition that allows us to find value of coefficient α .

Proper normalization of the transition strength and transition density of the ISGDR requires knowledge of the mixing amplitudes a_n and b_n . Due to the fact that mixing amplitudes are not independent (see Eq. (3.42)) it is more convenient to look for the mixing amplitude of the spurious state b_n . The value of b_n can be found from the expression for the strength distribution of spurious state:

$$S_1(E) = \iint d\vec{r} d\vec{r}' f_1(\vec{r}) R(\vec{r}, \vec{r}', E) f_1(\vec{r}') = \sum_n b_n^2 d_n(E) \left(\int d\vec{r} f_1(\vec{r}) \rho_{ss}(\vec{r}) \right)^2. \quad (3.54)$$

The integral $\int d\vec{r} f_1(\vec{r}) \rho_{ss}(\vec{r})$ can be evaluated using Eqs. (3.39) and (3.48) within the collective model (when 100% of the EWSR is exhausted at any chosen excitation energy):

$$\left(\int d\vec{r} f_1(\vec{r}) \rho_{ss}(\vec{r}) \right)^2 = \frac{\hbar^2}{2m} \frac{3}{4\pi} A/E_{ss}. \quad (3.55)$$

That yields,

$$b_n^2 = \frac{S_1(E_n)}{\left(\int d\vec{r} f_1(\vec{r}) \rho_{ss}(\vec{r})\right)^2}. \quad (3.56)$$

In the present work, we take the excitation operator to be $f \equiv f_3 = \sum_{i=1}^A f_3(\vec{r}_i)$, where $f_3(\vec{r}) = r^3 Y_{1M}(\hat{r})$. For this operator, the value of η associated with the spurious transition density $\rho_{ss}(\vec{r}, E)$ is calculated analytically using the definition of the spurious transition density given by Eq. (3.48):

$$\eta = \frac{5}{3} \langle r^2 \rangle. \quad (3.57)$$

The numerical calculations of the projected out transition strength $S_\eta(E)$ involve separate calculation of the transition strength using excitation operator $f_3(\vec{r})$,

$$S_3(E) = \iint dr dr' f_3(\vec{r}) R(\vec{r}, \vec{r}', E) f_3(\vec{r}'), \quad (3.58)$$

spurious operator $f_1(\vec{r})$,

$$S_1(E) = \iint dr dr' f_1(\vec{r}) R(\vec{r}, \vec{r}', E) f_1(\vec{r}') \quad (3.59)$$

and for the non-diagonal terms of the strength function two of them together

$$S_{13}(E) = \iint dr dr' f_1(\vec{r}) R(\vec{r}, \vec{r}', E) f_3(\vec{r}'), \quad (3.60)$$

with the following correction for the spurious state contribution

$$S_\eta(E) = S_3(E) - 2\eta S_{13}(E) + \eta^2 S_1(E). \quad (3.61)$$

By following the steps described above, we obtain the transition density, $\rho_{tr}(\vec{r}, E)$, and the strength distribution function, $S_\eta(E)$, of the isoscalar giant dipole resonance.

To compare theoretical findings to the experimentally observed quantities we need to describe a particular nuclear reaction and obtain angular distributions using results of the HF-RPA calculations. In the next chapter we provide such a description within the Distorted-Wave-Born-Approximation (DWBA).

CHAPTER IV

DISTORTED WAVE BORN APPROXIMATION

A. Formal Solution of Scattering Problem

The total wave function describing a direct nuclear reaction $a + A \rightarrow b + B$ in the center of mass frame of reference can be written as a superposition of all possible scattering channels:

$$\Psi^{(+)} = \sum_{\gamma} \xi_{\gamma}(\vec{r}_{\gamma}) \psi_{\gamma} \quad (4.1)$$

where $\xi_{\gamma}(\vec{r}_{\gamma})$ is the wave function of relative motion and ψ_{γ} is the total internal wave function of the system in the reaction channel γ . The wave function $\Psi^{(+)}$ is the solution of the stationary Schrödinger equation

$$H\Psi^{(+)} = E\Psi^{(+)} \quad (4.2)$$

and satisfies the boundary condition:

$$\Psi^{(+)} \xrightarrow{\text{asymptotically}} \psi_{\alpha} e^{i\vec{k}_{\alpha}\vec{r}_{\alpha}} + \sum_{\beta} \psi_{\beta} f_{\alpha\beta}(\vec{k}_{\alpha}, \vec{k}_{\beta}) \frac{e^{i\vec{k}_{\beta}r_{\beta}}}{r_{\beta}}, \quad (4.3)$$

where $\psi_{\alpha} e^{i\vec{k}_{\alpha}\vec{r}_{\alpha}}$ is the plane wave in the incident channel α , $\psi_{\beta} \frac{e^{i\vec{k}_{\beta}r_{\beta}}}{r_{\beta}}$ is the outgoing spherical waves in a given reaction channel β and $f_{\alpha\beta}(\vec{k}_{\alpha}, \vec{k}_{\beta})$ is the scattering amplitude of the given reaction channel.

The differential cross-section $d\sigma_{\alpha\beta}$ for a transition from the channel α to a channel β is defined as the ratio between the outgoing flux per unit time through the element of area $d\vec{A} = \hat{r}_{\beta}(\theta, \phi)r_{\beta}^2 d\Omega$, and the incident flux per unit time per unit area,

$$d\sigma_{\alpha\beta} = \frac{J_r^{(\beta)} r_{\beta}^2 d\Omega}{|J_i^{(\alpha)}|}, \quad (4.4)$$

where $J_r^{(\beta)}$ is the outgoing flux in the radial direction in channel β and $\vec{J}_i^{(\alpha)}$ is the incident flux.

Assuming the asymptotic forms of the total wave function to be

$\Phi^{(\beta)} = \psi_\beta f(\vec{k}_\alpha, \vec{k}_\beta) \frac{e^{ik_\beta r_\beta}}{r_\beta}$ for the outgoing channel and $\Phi^{(\alpha)} = \psi_\alpha e^{ik_\alpha \vec{r}_\alpha}$ for the incoming

channel and using the orthonormality of ψ_α and ψ_β , which are functions of the internal coordinates of the participating nuclei, the probability flux in outgoing and incoming channels are obtained as,

$$J_r^{(\beta)} = \frac{\hbar k_\beta}{\mu_\beta} \frac{|f_{\alpha\beta}(\vec{k}_\alpha, \vec{k}_\beta)|^2}{r_\beta^2}, \quad |J_i^{(\alpha)}| = \frac{\hbar k_\alpha}{\mu_\alpha}, \quad (4.5)$$

with

$$\mu_\alpha = \frac{m_a M_A}{m_a + M_A}, \quad \text{and} \quad \mu_\beta = \frac{m_b M_B}{m_b + M_B} \quad (4.6)$$

are the reduced masses in the incoming channel α and outgoing channel β . Then, the differential cross-section in the center of mass frame of reference can be written in terms of the scattering amplitude:

$$\frac{d\sigma_{\alpha\beta}}{d\Omega} = \frac{\mu_\alpha}{\mu_\beta} \frac{k_\beta}{k_\alpha} |f_{\alpha\beta}(\vec{k}_\alpha, \vec{k}_\beta)|^2. \quad (4.7)$$

To find scattering amplitude $f_{\alpha\beta}(\vec{k}_\alpha, \vec{k}_\beta)$, we need to solve the scattering problem given by equations (4.1), (4.2) and (4.3).

For a specific scattering channel β , the total Hamiltonian of the system of projectile and target nuclei can be written as

$$H = H_\beta + T_\beta + V_\beta \quad (4.8)$$

where H_β is the sum of the internal Hamiltonians of the projectile and the target, T_β is the kinetic energy of relative motion of, and V_β is the interaction between the projectile and the target. Then Eq. (4.2) takes the form:

$$(H_\beta + \hat{T}_\beta + V_\beta - E)\Psi^{(+)} = 0. \quad (4.9)$$

Multiplying this equation by ψ_β^* from the left and integrating over the internal variables of the projectile and the target in the outgoing channel β , we obtain the equation for the wave function of the relative motion $\xi_\beta(\vec{r}_\beta)$:

$$(\hat{T}_\beta + \varepsilon_\beta - E)\xi_\beta(\vec{r}_\beta) = -(\psi_\beta, V_\beta \Psi^{(+)}), \quad (4.10)$$

where $\varepsilon_\beta = \varepsilon_b + \varepsilon_B$ is the sum of the excitation energies of the projectile and the target. The right hand side of the Eq. (4.10) is the usual scalar product integrated over the internal coordinates $\{\zeta\}$ in the scattering channel β :

$$(\psi_\beta, V_\beta \Psi^{(+)}) \equiv \int d\{\zeta\} \psi_\beta(\{\zeta\}) V_\beta(\vec{r}, \{\zeta\}) \Psi^{(+)}(\vec{r}, \{\zeta\})$$

To find a solution of Eq. (4.10) we introduce an arbitrary spherically symmetric distorting potential $U_\beta(r_\beta)$ by adding $U_\beta(r_\beta)\xi_\beta(r_\beta)$ both to the left and to the right hand side of the equation. The expression $U_\beta(r_\beta)\xi_\beta(r_\beta)$ depends only on the relative distance between the projectile and the target, r_β . Therefore, by taking into account orthonormality of the total internal wave functions ψ_γ of different scattering channels, the additional distorting term can be expressed as $U_\beta(r_\beta)\xi_\beta(r_\beta) = (\psi_\beta, U_\beta \Psi^{(+)})$.

Therefore, equation (4.10) reduces to:

$$\left(-\frac{\hbar^2}{2\mu_\beta} \nabla_{\vec{r}_\beta}^2 - \frac{\hbar^2 k_\beta^2}{2\mu_\beta} + U_\beta(r_\beta) \right) \xi_\beta(r_\beta) = -(\psi_\beta, [V_\beta - U_\beta] \Psi^{(+)}), \quad (4.11)$$

where

$$k_\beta = \sqrt{\frac{2\mu_\beta}{\hbar^2} (E - \varepsilon_\beta)}. \quad (4.12)$$

Eq. (4.11) is an inhomogeneous differential equation, provided that the r.h.s. is a known function of r_β . Therefore the general solution of equation (4.11), $\xi_\beta(r_\beta)$, is the sum of a particular solution of Eq. (4.11) and the general solution of the homogeneous equation:

$$\left(-\frac{\hbar^2}{2\mu_\beta} \nabla_{\vec{r}_\beta}^2 - \frac{\hbar^2 k_\beta^2}{2\mu_\beta} + U_\beta(r_\beta) \right) \chi_\beta^{(+)}(\vec{k}_\beta, \vec{r}_\beta) = 0. \quad (4.13)$$

The general solution of the Eq.(4.11), $\xi_\beta(r_\beta) = \chi_\beta^{(+)}(\vec{k}_\beta, \vec{r}_\beta) + \xi_\beta^{(part.)}(\vec{r}_\beta)$, must satisfy the following boundary conditions:

- i) $\chi_\beta^{(+)}(\vec{k}_\beta, \vec{r}_\beta) \xrightarrow{\text{asymptotically}} e^{i\vec{k}_\beta \vec{r}_\beta} + \text{outgoing spherical wave};$
 - ii) $\chi_\beta^{(+)}(\vec{k}_\beta, \vec{r}_\beta)$ is regular at $\vec{r}_\beta = 0$;
 - iii) $\xi_\beta^{(part.)}(r_\beta) \xrightarrow{\text{asymptotically}} \text{outgoing spherical wave};$
 - iv) $\xi_\beta^{(part.)}(r_\beta)$ is regular at $\vec{r}_\beta = 0$.
- (4.14)

The solution of the homogeneous equation (4.13) that satisfies the given boundary conditions i) and ii) is:

$$\chi_\beta^{(+)}(\vec{k}_\beta, \vec{r}_\beta) = \frac{1}{k_\beta r_\beta} \sum_{l=0}^{\infty} (2l+1) i^l e^{i\delta_l} f_l(k_\beta, r_\beta) P_l(\cos \theta), \quad (4.15)$$

where δ_l is a phase shift, $P_l(\cos \theta)$ is Legendre polynomial, θ is the angle between the direction of the incident wave vector and \vec{r}_β , and $f_l(k_\beta, r_\beta)$ is the regular solution of homogeneous equation:

$$\left(\frac{d^2}{dr^2} + k_\beta^2 - \frac{l(l+1)}{r_\beta^2} - \frac{2\mu_\beta}{\hbar^2} U_\beta(r_\beta) \right) f_l(k_\beta, r_\beta) = 0, \quad (4.16)$$

with the asymptotic form: $f_l(k_\beta, r_\beta) \xrightarrow{r_\beta \rightarrow \infty} \sin\left(k_\beta r_\beta - \frac{\pi l}{2} + \delta_l\right)$. For reason of

convenience, we express $f_l(k_\beta, r_\beta)$ in terms of functions $h_l(k_\beta, r_\beta)$,

$$f_l(k_\beta, r_\beta) = \frac{i}{2} (h_l^*(k_\beta, r_\beta) - h_l(k_\beta, r_\beta)). \quad (4.17)$$

The functions $h_l(k_\beta, r_\beta)$ are defined as a combination of the regular and irregular solutions of Eq. (4.16) $h_l(k_\beta, r_\beta) = i f_l(k_\beta, r_\beta) + g_l(k_\beta, r_\beta)$, hence, they also are solutions of Eq. (4.16). The asymptotic form of the functions $h_l(k_\beta, r_\beta)$ is:

$$h_l(k_\beta, r_\beta) \xrightarrow{r_\beta \rightarrow \infty} \exp i \left(k_\beta r_\beta - \frac{\pi l}{2} + \delta_l \right). \quad (4.18)$$

For the case of nuclear scattering reaction, the distorting potential U_β is the sum of the nuclear and Coulomb potentials i.e., $U_\beta(r_\beta) = U_\beta^{(nucl.)}(r_\beta) + Z_B Z_b e^2 / r_\beta$. Therefore, the total phase shift is given as: $\delta_l = \delta_l^{(n)} + \sigma_l$, where $\delta_l^{(n)}$ and σ_l are the nuclear and the Coulomb phase shift, respectively. The Coulomb phase shift is well known:

$$\sigma_l = \arg \Gamma(l + 1 + i n_\beta). \quad (4.19)$$

Here $\Gamma(z)$ is the gamma function and $n_\beta = Z_B Z_b e^2 \mu_\beta / (\hbar^2 k_\beta)$ is the Sommerfeld parameter. For the relative distance r_β greater than some chosen value r_a , the contribution of the nuclear term of the distorting potential can be neglected. Then, the solution $\chi_\beta^{(+)}(\vec{k}_\beta, \vec{r}_\beta)$ is dominated by Coulomb contribution, and for $r_\beta > r_a$, $f_l(k_\beta, r_\beta)$ can be written in terms of analytically known outgoing Coulomb functions $H_l(k_\beta, r_\beta)$:

$$e^{i\delta_l^{(nucl.)}} f_l(k_\beta, r_\beta) \Big|_{r_\beta > r_a} = \frac{i}{2} \left(H_l^*(k_\beta, r_\beta) - e^{i2\delta_l^{(n)}} H_l(k_\beta, r_\beta) \right). \quad (4.20)$$

In the region $r_\beta < r_a$, $f_l(k_\beta, r_\beta)$ can be found only numerically.

The nuclear phase shift $\delta_l^{(n)}$ can be found by matching $f_l(k_\beta, r_\beta) \Big|_{r_\beta < r_a}$ and it's derivative with $f_l(k_\beta, r_\beta) \Big|_{r_\beta > r_a}$ and it's derivative at the point $r_\beta = r_a$. Setting $r_\beta \rightarrow \infty$ in Eq. (4.15) and using Eq. (4.20) and the asymptotic form for the Coulomb functions:

$H_l(k_\beta, r_\beta) \xrightarrow{r_\beta \rightarrow \infty} \exp i \left(k_\beta r_\beta - n_\beta \ln 2k_\beta r_\beta - \frac{\pi l}{2} + \sigma_l \right)$, we obtain the scattering amplitude $f_{\beta\beta}^{(0)}(\theta)$:

$$f_{\beta\beta}^{(0)}(\theta) = \frac{1}{2ik_\beta} \sum_l (2l+1) \left(e^{2i(\sigma_l + \delta_l^{(n)})} - 1 \right) P_l(\cos \theta), \quad (4.21)$$

where θ is the angle between the incident and outgoing wave vector.

To complete the general solution for the wave function of relative motion $\xi_\beta(r_\beta)$, we need to find a particular solution of Eq. (4.11). This can be done within the Green's function formalism. In terms of the Green's function the particular solution is given by:

$$\xi_\beta^{part.}(\vec{r}_\beta) = -\int d\vec{r}'_\beta G(\vec{r}_\beta, \vec{r}'_\beta) (\psi_\beta, [V_\beta - U_\beta] \Psi^{(+)}). \quad (4.22)$$

Here the Green's function $G(\vec{r}_\beta, \vec{r}'_\beta)$ must satisfy the following equation:

$$\left(-\frac{\hbar^2}{2\mu_\beta} \nabla_{\vec{r}_\beta}^2 - \frac{\hbar^2 k_\beta^2}{2\mu_\beta} + U_\beta(r_\beta) \right) G(\vec{r}_\beta, \vec{r}'_\beta) = \delta(\vec{r}_\beta - \vec{r}'_\beta), \quad (4.23)$$

and the boundary conditions iii) and iv) of Eq. (4.14). Performing a multipole expansion of $G(\vec{r}_\beta, \vec{r}'_\beta)$ we obtain:

$$G(\vec{r}_\beta, \vec{r}'_\beta) = \sum_{l,m} \frac{g_l(r_\beta, r'_\beta)}{r_\beta r'_\beta} Y_{lm}^*(\hat{r}'_\beta) Y_{lm}(\hat{r}_\beta), \quad (4.24)$$

where $g_l(r_\beta, r'_\beta)$ satisfies equation

$$\left(-\frac{\hbar^2}{2\mu_\beta} \frac{d^2}{dr^2} - \frac{\hbar^2}{2\mu_\beta} k_\beta^2 + \frac{\hbar^2}{2\mu_\beta} \frac{l(l+1)}{r_\beta^2} + U_\beta(r_\beta) \right) g_l(r_\beta, r'_\beta) = \delta(r_\beta - r'_\beta). \quad (4.25)$$

According to the Green's function formalism, the radial part of the Green's function, $g_l(r_\beta, r'_\beta)$, can be written in form:

$$g_l(r_\beta, r'_\beta) = -\frac{2\mu_\beta}{\hbar^2 W} f_l(k_\beta, r_{\beta<}) h_l(k_\beta, r_{\beta>}), \quad (4.26)$$

where functions $f_l(k_\beta, r_\beta)$ and $h_l(k_\beta, r_\beta)$ are defined by Eqs. (4.16) and (4.17),

$r_{\beta<} (r_{\beta>})$ is smaller (greater) of r_β and r'_β , and W is the Wronskian:

$$W = f_l(k_\beta, r_\beta) \frac{\partial h_l(k_\beta, r_\beta)}{\partial r_\beta} - h_l(k_\beta, r_\beta) \frac{\partial f_l(k_\beta, r_\beta)}{\partial r_\beta} = const. \quad (4.27)$$

The Wronskian W in Eq. (4.26) is a constant, hence, it can be evaluated at an arbitrary r_β , for example, at $r_\beta \rightarrow \infty$. Utilizing the asymptotic forms for $f_l(k_\beta, r_\beta)$ and $h_l(k_\beta, r_\beta)$, and setting $r_\beta \rightarrow \infty$, the value of the Wronskian is obtained:

$$W = -k_\beta. \quad (4.28)$$

Now, utilizing Eqs. (4.26) and (4.28) we can write expression for the Green's function as:

$$G(\vec{r}_\beta, \vec{r}'_\beta) = \frac{2\mu_\beta}{\hbar^2 k_\beta} \sum_{l,m} \frac{f_l(k_\beta, r_{\beta<}) h_l(k_\beta, r_{\beta>})}{r_\beta r'_\beta} Y_{lm}^*(\hat{r}'_\beta) Y_{lm}(\hat{r}_\beta). \quad (4.29)$$

Before writing down the complete solution of Eq. (4.11), we need to take into account that the asymptotic form (4.3) of the total outgoing wave function $\Psi^{(+)}$ limits presence of the incoming flux only to the incident channel α . Therefore, the wave function of relative motion $\xi_\beta(\vec{r}_\beta)$ becomes:

$$\begin{aligned} \xi_\beta^p(\vec{r}_\beta) &= \chi_\beta^{(+)}(\vec{k}_\beta, \vec{r}_\beta) \delta_{\alpha\beta} - \\ &\frac{2\mu_\beta}{\hbar^2 k_\beta} \sum_{l,m} \int d\vec{r}'_\beta \frac{f_l(k_\beta, r_{\beta<}) h_l(k_\beta, r_{\beta>})}{r_\beta r'_\beta} Y_{lm}^*(\hat{r}'_\beta) Y_{lm}(\hat{r}_\beta) \cdot (\psi_\beta, [V_\beta - U_\beta] \Psi^{(+)}). \end{aligned} \quad (4.30)$$

Asymptotically, when $r_\beta \rightarrow \infty$, $\hat{r}_\beta \rightarrow \hat{k}_\beta$, behavior of the function $h_l(k_\beta, r_{\beta>})$ is described as: $h_l(k_\beta, r_{\beta>}) \rightarrow \exp(k_\beta r_\beta - n_\beta \ln 2k_\beta r_\beta - \pi l/2 + \sigma_l + \delta_l^{(nucl.)})$. Therefore, the asymptotic form of the complete solution of the Eq. (4.11) can be written as:

$$\begin{aligned} \xi_\beta(\vec{r}_\beta) &\rightarrow \left(e^{i\vec{k}_\alpha \vec{r}_\alpha} + f_{\alpha\alpha}^{(0)}(\theta) \frac{e^{i(k_\alpha r_\alpha - n_\alpha \ln 2k_\alpha r_\alpha)}}{r_\alpha} \right) \delta_{\alpha\beta} - \\ &\frac{\mu_\beta}{2\pi\hbar^2} \frac{e^{i(k_\beta r_\beta - n_\beta \ln 2k_\beta r_\beta)}}{r_\beta} \int d\vec{r}'_\beta \chi_\beta^{(-)*}(\vec{k}_\beta, \vec{r}'_\beta) (\psi_\beta, [V_\beta - U_\beta] \Psi^{(+)}), \end{aligned} \quad (4.31)$$

where $f_{\alpha\alpha}^{(0)}(\theta)$ is defined by Eq. (4.21), and the function $\chi_\beta^{(-)}(k_\beta, r_\beta)$ is the time reversed of the function $\chi_\beta^{(+)}(k_\beta, r_\beta)$, defined as:

$$\chi_\beta^{(-)*}(\vec{k}_\beta, \vec{r}_\beta) = \frac{4\pi}{k_\beta r_\beta} \sum_{l,m} (-i)^l e^{i\sigma_l + i\delta_l^n} f_l(k_\beta, r_\beta) Y_{lm}(\hat{k}_\beta) Y_{lm}^*(\hat{r}_\beta). \quad (4.32)$$

From the asymptotic form for the wave function of relative motion $\xi_\beta(\vec{r}_\beta)$, Eq. (4.31), we write the scattering as:

$$f_{\alpha\beta}(\vec{k}_\alpha, \vec{k}_\beta) = f_{\alpha\alpha}^{(0)}(\theta) \delta_{\alpha\beta} - \frac{\mu_\beta}{2\pi\hbar^2} \int d\vec{r}'_\beta \chi_\beta^{(-)*}(\vec{k}_\beta, \vec{r}'_\beta) (\psi_\beta, [V_\beta - U_\beta] \Psi^{(+)}). \quad (4.33)$$

B. Distorted Wave Approach to Inelastic Scattering

The Distorted Wave Born Approximation (DWBA) is based on the following two approximations:

- 1) We can assume, that in the expression (4.33) the term $[V_\beta - U_\beta]$ is small, hence, it can be treated as a perturbation to the Hamiltonian $H' = H_\beta + T_\beta + U_\beta$. Under such assumption, terms $\xi_\beta(\vec{r}_\beta)\psi_\beta$, corresponding to inelastic scattering channels in the expression (4.1), are also considered to be small. Therefore, the r. h. s. of the Eq. (4.33) the total outgoing wave function $\Psi^{(+)}$ can be approximated by the elastic term only:

$$\Psi^{(+)} \rightarrow \xi_\alpha(\vec{r}_\alpha)\psi_\alpha. \quad (4.34)$$

- 2) By choosing perturbed potential U_α in a way that the elastic cross-section calculated with the scattering amplitude $f_{\alpha\alpha}^{(0)}(\theta)$ from Eq. (4.21), fit the experimentally measured elastic cross-section at the given energy E , which implies

$$(\psi_\alpha, [V_\alpha - U_\alpha] \psi_\alpha) \approx 0, \quad (4.35)$$

we can approximate the wave function of the relative motion by distorted outgoing spherical wave:

$$\xi_\alpha(\vec{r}_\alpha) \approx \chi_\alpha^{(+)}(\vec{k}_\alpha, \vec{r}_\alpha), \quad (4.36)$$

where $\chi_\alpha^{(+)}(\vec{k}_\alpha, \vec{r}_\alpha)$ can be found using Eq. (4.15) and following the procedure discussed after it.

Using the approximated form for the total outgoing wave function (4.34) and the outgoing wave function of relative motion (4.36), with the appropriate form of the distorted potential, we obtain the following approximate expression for the scattering amplitude:

$$f_{\alpha\beta}(\vec{k}_\alpha, \vec{k}_\beta) = f_{\alpha\alpha}^{(0)}(\theta)\delta_{\alpha\beta} - \frac{\mu_\beta}{2\pi\hbar^2} \int d\vec{r}' \chi_\beta^{(-)*}(\vec{k}_\beta, \vec{r}') (\psi_\beta, [V_\beta - U_\beta] \psi_\alpha \chi_\alpha^{(+)}(\vec{k}_\alpha, \vec{r}')). \quad (4.37)$$

It should be noted, that the wave function $\Psi^{(+)}$, as it is given by Eq. (4.1) does not include terms which describe the formation of a compound nucleus and cannot be written as products of the intrinsic and the relative motion wave functions. In order to take into account absorption processes we can introduce an imaginary part to the nuclear part of the interaction V_α . The imaginary part of the potential, introduces imaginary phase shifts, hence reduces the incident flux in the outgoing channel (absorption).

During the typical inelastic scattering experiment a projectile nucleus remains in its ground state and a target nucleus is in the ground state before, and is excited by the interaction with the projectile, during the scattering, $a + A \rightarrow a + A^*$. For such a reaction, following the DWBA, we can write expression for the inelastic scattering amplitude as:

$$f_{\alpha\beta}(\vec{k}_\alpha, \vec{k}_\beta) = -\frac{\mu}{2\pi\hbar^2} \int d\vec{r}' \chi_\beta^{(-)*}(\vec{k}_\beta, \vec{r}') (\psi_\beta, [V - U_\alpha(r)] \psi_\alpha) \chi_\alpha^{(+)}(\vec{k}_\alpha, \vec{r}'), \quad (4.38)$$

where μ denotes the reduced mass,

$$\mu = \frac{m_a M_A}{m_a + M_A}, \quad (4.39)$$

and V is the projectile-target interaction. The distorted potential $U_\alpha(r)$ is chosen according the DWBA and the residual interaction $[V - U_\alpha(r)]$ can be treated as a small perturbation. We demand that the elastic cross-section obtained with such distorted potential $U_\alpha(r)$ fit the experimentally measured elastic cross-sections, thus, satisfying the condition:

$$(\psi_\alpha, [V - U_\alpha(r)] \psi_\alpha) \approx 0. \quad (4.40)$$

For $\alpha \neq \beta$, contribution from the distorted potential $U_\alpha(r)$ in the scalar product $(\psi_\beta, [V - U_\alpha(r)] \psi_\alpha)$ is equal zero, due to orthonormality of ψ_α and ψ_β .

For the case of a spinless projectile, that the matrix element $(\psi_\beta, [V - U_\alpha(r)] \psi_\alpha)$ describing transition between the ground state and an excited state with multipolarity l of the target nucleus can be written as a multipole expansion in spherical harmonics:

$$(\psi_\beta, [V - U_\alpha] \psi_\alpha) = T_{lm}(r')(-i)^l Y_{lm}^*(\hat{r}'), \quad (4.41)$$

where $T_{lm}(r')$ is the radial form factor.

Using the expressions for the incoming and outgoing distorted wave functions, $\chi_\beta^{(+)}(k_\beta, r_\beta)$ and $\chi_\beta^{(-)}(k_\beta, r_\beta)$, respectively, and Eq. (4.40), we rewrite scattering amplitude (4.38) in the form:

$$f_{\alpha\beta}(\vec{k}_\alpha, \vec{k}_\beta) = -\frac{8\pi\mu}{\hbar^2 k_\alpha k_\beta} \sum_{l_1, l_2, m_1, m_2} i^{l_2 - l_1 - l} e^{i(\sigma_{l_1} + \sigma_{l_2})} Y_{l_1 m_1}(\hat{k}_\beta) Y_{l_2 m_2}^*(\hat{k}_\alpha) I_{lm}^{l_1 l_2} \times \int d\hat{r} Y_{l_1 m_1}^*(\hat{r}) Y_{lm}^*(\hat{r}) Y_{l_2 m_2}(\hat{r}), \quad (4.42)$$

where

$$I_{lm}^{l_1 l_2} = \int f_{l_1}(k_\beta, r) T_{lm}(r) f_{l_2}(k_\alpha, r) dr. \quad (4.43)$$

Expanding the product $Y_{l_1 m_1}^*(\hat{r}) Y_{lm}^*(\hat{r})$ in terms of the Clebsch-Gordan coefficients,

$$Y_{l_1 m_1}^*(\hat{r}) Y_{lm}^*(\hat{r}) = \sum_{l' = |l - l_1|}^{l + l_1} \sqrt{\frac{(2l + 1)(2l_1 + 1)}{4\pi(2l' + 1)}} \langle l m_1 m_1 | l' m' \rangle \langle l_0 l_1 0 | l' 0 \rangle Y_{l' m'}^*(\hat{r}), \quad (4.44)$$

and performing the integration over the angle \hat{r} we reduce expression (4.42) to the form:

$$f_{\alpha\beta}(\theta) = -\frac{2\mu}{\hbar^2 k_\alpha k_\beta} \sqrt{2l + 1} \sum_{l_1, l_2} i^{l_2 - l_1 - l} \sqrt{\frac{2l_1 + 1}{4\pi(2l_2 + 1)}} \cdot I_{lm}^{l_1 l_2} e^{i(\sigma_{l_1} + \sigma_{l_2})} \times \langle l m_1 m_1 | l_2 m_2 \rangle \langle l_0 l_1 0 | l_2 0 \rangle Y_{l_1 m_1}(\hat{k}_\beta) Y_{l_2 m_2}^*(\hat{k}_\alpha). \quad (4.45)$$

Choosing the z-axis to be along the direction of the incident wave vector \hat{k}_α and the y-axis to be perpendicular to the plane of scattering (along the direction of $\vec{k}_\alpha \times \vec{k}_\beta$), we

can further simplify expression (4.45). The form of the spherical harmonics $Y_{l_2 m_2}^*(\hat{k}_\alpha)$ in the new coordinate system is:

$$Y_{l_2 m_2}^*(\hat{k}_\alpha) = \sqrt{\frac{2l_2 + 1}{4\pi}} \delta_{m_2, 0},$$

and the expression (4.45) can be written as:

$$f_{\alpha\beta}(\theta) = -\frac{2\mu}{\hbar^2 k_\alpha k_\beta} \sqrt{2l+1} \sum_{l_1, l_2} i^{l_2 - l_1 - l} \sqrt{2l_1 + 1} \cdot I_{lm}^{l_1 l_2} \exp[i(\sigma_{l_1} + \sigma_{l_2})] \times \langle l m l_1 - m | l_2 0 \rangle \langle l 0 l_1 0 | l_2 0 \rangle Y_{l_1 - m}(\theta), \quad (4.46)$$

Here the radial form factor $I_{lm}^{l_1 l_2}$ is defined in Eq. (4.43) and $Y_{l_1 - m}(\theta)$ depends only on the angle between the incoming and outgoing momentums, k_α and k_β .

To complete the description of the scattering reaction within the DWBA we need to find the radial form factor in the expansion (4.46). In the following we will obtain expressions for the radial form factor (4.43) for the nuclear and Coulomb part of interaction.

1. Nuclear Interaction

For simplicity we assume the case of point-like projectile and spherically symmetric target nuclei. In this case we can assume that the projectile interacts with each nucleon of the target nucleus via a two-body effective interaction. Then, the density dependent nuclear effective interaction between the projectile and the target can written in form:

$$V = \sum_i V(|\vec{r} - \vec{r}_i|, \rho(\vec{r}_i)), \quad (4.47)$$

where \vec{r}_i and $\rho(\vec{r}_i)$ are the nucleon coordinates with respect to the center of mass of the target and target density at \vec{r}_i , respectively.

The nuclear part of the distorted potential U_α can be found as:

$$U_\alpha^{nucl.}(r) = (\psi_0, V \psi_0) = \int d\vec{r}' V(|\vec{r} - \vec{r}'|, \rho_0(r')) \rho_0(r'), \quad (4.48)$$

where $\rho_0(r')$ is the ground state density in spherically symmetric target. Because the projectile is assumed to be a point-like particle the intrinsic wave functions of the system are replaced by the ground state and excited state wave functions of the target nucleus.

By expanding V in spherical harmonics,

$$V(|\vec{r} - \vec{r}'|, \rho_0(r')) = \sum_{l,m} \frac{4\pi}{2l+1} v_l(r, r', \rho_0(r')) Y_{lm}^*(\hat{r}) Y_{lm}(\hat{r}'), \quad (4.49)$$

and introducing this expansion in Eq. (4.48), we obtain:

$$U_{\alpha}^{nucl.}(r) = (\psi_0, V \psi_0) = \int_0^{\infty} dr' r'^2 v_0(r, r', \rho_0(r')) \rho_0(r'). \quad (4.50)$$

For a target's excitation to a state with certain multipolarity l the excitation can be considered as a small variation of the ground state density that will result in a small change of the effective interaction. To the lowest order, this effect can be accounted for by using the modified interaction,

$$V'(|\vec{r} - \vec{r}'|, \rho_0(r')) = V(|\vec{r} - \vec{r}'|, \rho_0(r')) + \rho_0(r') \frac{\partial V(|\vec{r} - \vec{r}'|, \rho_0(r'))}{\partial \rho_0(r')}. \quad (4.51)$$

Then, the matrix element of the residual interaction can be calculated as:

$$(\psi_{lm}, V' \psi_0) = \int d\vec{r}' \rho_{lm}^{tr.}(\vec{r}') \left[V(|\vec{r} - \vec{r}'|, \rho_0(r')) + \rho_0(r') \frac{\partial V(|\vec{r} - \vec{r}'|, \rho_0(r'))}{\partial \rho_0(r')} \right], \quad (4.52)$$

where $\rho_{lm}^{tr.}(\vec{r}')$ is the transition density at the point \vec{r}' in the target. We can write the transition density as:

$$\rho_{lm}^{tr.}(\vec{r}) = \rho_{lm}^{tr.}(r) Y_{lm}(\hat{r}). \quad (4.53)$$

If the density dependence in the effective interaction potential $V(|\vec{r} - \vec{r}'|, \rho_0(r'))$ can be factored, then using the expansion (4.49) and taking into consideration Eq. (4.53) we obtain:

$$(\psi_{lm}, V_{res.} \psi_0) = \frac{4\pi}{2l+1} (-i)^l Y_{lm}^*(\hat{r}) \int_0^{\infty} dr' r'^2 \rho_{lm}^{tr.}(r') \times$$

$$\left[v_l(r, r', \rho_0(r')) + \rho_0(r') \frac{\partial v_l(r, r', \rho_0(r'))}{\partial \rho_0(r')} \right], \quad (4.54)$$

Comparing Eq. (4.54) with the Eq. (4.41) we obtain the nuclear radial form factor,

$$T_{lm}^{tr.}(r) = \frac{4\pi}{2l+1} \int_0^\infty dr' r'^2 \rho_{lm}^{tr.}(r') \left[v_l(r, r', \rho_0(r')) + \rho_0(r') \frac{\partial v_l(r, r', \rho_0(r'))}{\partial \rho_0(r')} \right]. \quad (4.55)$$

The parameters of the two-body potential $V(|\vec{r} - \vec{r}'|, \rho_0(r'))$ are found by fitting the experimentally measured differential of elastic scattering with the differential cross section obtained using the distorted potential from Eq. (4.50). In the case when the effective nuclear interaction is taken to have both real and imaginary components, the distorted potential for both parts can be calculated separately, using the same method.

2. Coulomb Interaction

As before, the projectile is assumed to be a point particle, so the Coulomb part, V_C , of the projectile-target interaction potential can be written as:

$$V_C = \sum_i \frac{Z_p e^2}{|\vec{r} - \vec{r}_i|}, \quad (4.56)$$

where Z_p is the charge number of the projectile and \vec{r}_i is the proton coordinate in the target with respect to its center of mass.

The Coulomb part, $U_{\alpha C}(r)$, of the distorted potential is given by:

$$U_{\alpha C}(r) = \left(\psi_0, \sum_i \frac{Z_p e^2}{|\vec{r} - \vec{r}_i|} \psi_0 \right) = Z_p e^2 \int d\vec{r}' \frac{\rho_c(r')}{|\vec{r} - \vec{r}'|}, \quad (4.57)$$

where $\rho_c(r')$ is the ground state charge density of the spherical target at the point r' .

Let us expand $\frac{1}{|\vec{r} - \vec{r}'|}$ in spherical harmonics:

$$\frac{1}{|\vec{r} - \vec{r}'|} = \sum_{l,m} \frac{4\pi}{2l+1} \frac{r_{<}^l}{r_{>}^{l+1}} Y_{lm}^*(\hat{r}) Y_{lm}(\hat{r}'), \quad (4.58)$$

where $r_<$, $r_>$, denote, respectively, the lesser and the larger of the radial coordinates r and r' . Substituting expansion (4.58) in the Eq. (4.57) we obtain the Coulomb part of the optical potential:

$$U_{\alpha c}(r) = 4\pi Z_p e^2 \left[\frac{1}{r} \int_0^r dr' r'^2 \rho_c(r') + \int_r^\infty dr' r' \rho_c(r') \right]. \quad (4.59)$$

For the transition from the ground state to some excited state of the target nucleus with the multipolarity l , the matrix element $(\psi_{lm}, V_c \psi_0)$

$$(\psi_{\beta}, V_c \psi_{\alpha}) = \left(\psi_{lm}, \sum_i \frac{Z_p e^2}{|\vec{r} - \vec{r}'_i|} \psi_0 \right) = Z_p e^2 \int d\vec{r}' \frac{\rho_{c\ lm}^{tr}(\vec{r}')}{|\vec{r} - \vec{r}'|}, \quad (4.60)$$

where $\rho_{c\ lm}^{tr}(\vec{r}')$ is the charge transition density at the point \vec{r}' in the target.

Writing the charge transition density in the form (4.53) and using the expansion (4.58) we obtain:

$$(\psi_{lm}, V_c \psi_0) = \frac{4\pi Z_p e^2}{2l+1} Y_{lm}^*(\hat{r}') \left[\frac{1}{r^{l+1}} \int_0^r dr' r'^{l+2} \rho_{c\ lm}^{tr}(r') + r^l \int_r^\infty dr' \frac{\rho_{c\ lm}^{tr}(r')}{r'^{l-1}} \right]. \quad (4.61)$$

Therefore the Coulomb contribution to the radial form factor is given by:

$$T_{lm}^{Coulomb.}(r) = \frac{4\pi Z_p e^2}{2l+1} \left[\frac{1}{r^{l+1}} \int_0^r dr' r'^{l+2} \rho_{c\ lm}^{tr}(r') + r^l \int_r^\infty dr' \frac{\rho_{c\ lm}^{tr}(r')}{r'^{l-1}} \right]. \quad (4.62)$$

The total optical potential U_{α} is a sum of the real and the imaginary parts of the nuclear contribution (Eq.4.50), and the Coulomb contribution (Eq. 4.59). The total transition potential for the target nucleus transition from the ground state to the excited state with multipolarity l is a sum of the matrix elements obtained with both, real and imaginary parts of the residual interaction (Eqs. 4.54) and the Coulomb matrix element (4.61).

CHAPTER V

FERMI LIQUID DROP MODEL (FLDM)

In the previous chapters we have shown the microscopic description of quantum mechanical many-body system. However, quantum mechanics of many-body system can be presented in several forms. In this chapter we will derive formalism of the Fermi liquid drop model for calculations of the isoscalar compression energies and widths starting from the time-dependent Hartree-Fock approximation and implementing the Wigner function approach.

A. Time Dependent Hartree-Fock Approximation in Phase Space

For a system of A particles, the most general density matrix is given by

$$\rho_A(\vec{r}_1, \dots, \vec{r}_A; \vec{r}'_1, \dots, \vec{r}'_A) = \sum_n w_n \Psi_n(\vec{r}_1, \dots, \vec{r}_A) \Psi_n^*(\vec{r}'_1, \dots, \vec{r}'_A), \quad (5.1)$$

where $\Psi_n(\vec{r}_1, \dots, \vec{r}_A)$ are the orthonormal exact wave functions of the system and w_n is the probability that the system is in a state $\Psi_n(\vec{r}_1, \dots, \vec{r}_A)$, with the normalization

$$\sum_n w_n = \sum_n \|\Psi_n\|^2 = 1. \quad (5.2)$$

The description of the system of A particles using density matrix $\rho_A(\vec{r}_1, \dots, \vec{r}_A; \vec{r}'_1, \dots, \vec{r}'_A)$ is not very applicable for calculations of observables associated with commonly used one- and two-body operators. In such calculations description of a many body system using one body density matrixes $\rho(\vec{r}, \vec{r}')$ is more preferable:

$$\rho(\vec{r}, \vec{r}') = A \int d\vec{r}_2 \dots d\vec{r}_A \rho_A(\vec{r}, \vec{r}_2, \dots, \vec{r}_A; \vec{r}', \vec{r}_2, \dots, \vec{r}_A). \quad (5.2)$$

The equation of motion for the one-body density matrix $\rho(\vec{r}, \vec{r}')$ can be obtained directly from the basic many-body Schrödinger equation for $\Psi_n(\vec{r}_1, \dots, \vec{r}_A)$.

$$-\frac{\hbar^2}{2m}\nabla^2\rho(\vec{r},\vec{r}')+V(\vec{r})\rho(\vec{r},\vec{r}')+\sum_i V(\vec{r}_i)\rho(\vec{r},\vec{r}_i,\vec{r}',\vec{r}'')=E\rho(\vec{r},\vec{r}') \quad (5.3)$$

The equation (5.3) of motion for $\rho(\vec{r},\vec{r}')$ is coupled to a set of equations for higher order density matrices. To avoid solving system of coupled equations for density matrixes for up to A particles we can use the variational methods for the solution of the quantum many-body problem, assuming certain form for the initial function $\rho(\vec{r},\vec{r}')$. Particular examples of the variational method are the Hartree-Fock (HF) and time-dependent-HF (TDHF) approximations.

To obtain the TDHF equation of motion for a single particle matrix $\rho(\vec{r},\vec{r}')$, we start from the exact variational equation, taken in the form

$$\delta \int_{t_1}^{t_2} dt \langle \Psi(t) | i\hbar \frac{\partial}{\partial t} - \hat{H} | \Psi(t) \rangle = 0, \quad (5.4)$$

where \hat{H} is the exact Hamiltonian for the A nucleon. In the case of a trial function given by the fully antisymmetrized product of the time-dependent single particle wave functions $\varphi_i(\vec{r}_i, t)$,

$$\Psi(t) = \frac{1}{\sqrt{A}} \text{Det} \|\varphi_i(t)\|, \quad i = 1, \dots, A. \quad (5.5)$$

The TDHF equation of motion for the time-dependent one body density matrix, $\rho(\vec{r}_1, \vec{r}_2; t)$, which is defined as

$$\rho(\vec{r}_1, \vec{r}_2; t) = \sum_{i=1}^A \varphi_i(\vec{r}_1, t) \varphi_i^*(\vec{r}_2, t), \quad (5.6)$$

is given by

$$i\hbar \frac{\partial}{\partial t} \rho(\vec{r}_1, \vec{r}_2; t) = -\frac{\hbar^2}{2m} [\nabla_1^2 - \nabla_2^2] \rho(\vec{r}_1, \vec{r}_2; t) + [V(\vec{r}_1, t) - V(\vec{r}_2, t)] \rho(\vec{r}_1, \vec{r}_2; t). \quad (5.7)$$

The single-particle wave functions $\varphi_i(\vec{r}, t)$ in the definition (5.6) are determined by HF equations with a self-consistent potential

$$V(\vec{r}, t) = \int d\vec{r}' v(\vec{r}, \vec{r}') \rho(\vec{r}', t), \quad (5.8)$$

where $v(\vec{r}, \vec{r}')$ is the two-body effective interaction and $\rho(\vec{r}, t)$ is the time-dependent local density $\rho(\vec{r}, t) = \rho(\vec{r}, \vec{r}; t)$. In equations (5.7) and (5.8), the non-local exchange potential has been omitted for notational simplicity. We need to note, that for the local (Skyrme-type) nucleon-nucleon effective interaction, the exchange term of the self-consistent potential can be also expressed in form of Eq. (5.8).

The time dependent Wigner distribution function defined as [42]

$$f(\vec{r}, \vec{p}; t) = \int d\vec{s} e^{-i(\hbar)\vec{p}\cdot\vec{s}} \rho(\vec{r} - \vec{s}/2, \vec{r} + \vec{s}/2; t), \quad (5.9)$$

where $\vec{r} = (\vec{r}_1 + \vec{r}_2)/2$, $\vec{s} = \vec{r}_1 - \vec{r}_2$, and $\rho(\vec{r}_1, \vec{r}_2; t)$ is the time-dependent one body density matrix. The Wigner distribution function is interpreted as the quantum analog of the classical phase-space distribution function. The Wigner transform $A_w(\vec{r}, \vec{p})$ for an arbitrary one-body operator \hat{A} is presented as:

$$(\hat{A})_w = A_w(\vec{r}, \vec{p}) = \sum_i \int d\vec{s} \varphi_i^*(\vec{r} - \vec{s}/2) \hat{A} \varphi_i(\vec{r} + \vec{s}/2) e^{i(\hbar/2)\vec{s}\cdot\vec{p}}. \quad (5.10)$$

Using definition (5.10) we can write the composition formula for two one-body operators [43]:

$$(\hat{A}\hat{B})_w = A_w(\vec{r}, \vec{p}) e^{i(\hbar/2)\vec{\Lambda}} B_w(\vec{r}, \vec{p}), \quad (5.11)$$

where $\vec{\Lambda} = \vec{\nabla}_r \cdot \vec{\nabla}_p - \vec{\nabla}_r \cdot \vec{\nabla}_p$.

The collisionless quantum kinetic equation [44-46] is obtained by multiplying Eq. (5.7) by $\exp[-(i/\hbar)\vec{p}\cdot\vec{s}]$, performing coordinate transformation $(\vec{r}_1, \vec{r}_2) \rightarrow (\vec{r} - \vec{s}/2, \vec{r} + \vec{s}/2)$, and integrating the obtained expression over \vec{s} :

$$\frac{\partial}{\partial t} f(\vec{r}, \vec{p}; t) + \frac{1}{m} \vec{p} \cdot \vec{\nabla}_r f(\vec{r}, \vec{p}; t) - \frac{2}{\hbar} V(\vec{r}; t) \sin\left(\frac{\hbar}{2} \vec{\Lambda}\right) f(\vec{r}, \vec{p}; t) = 0. \quad (5.12)$$

Expanding $\sin\left(\frac{\hbar}{2} \vec{\Lambda}\right)$, we obtain:

$$\frac{\partial}{\partial t} f(\vec{r}, \vec{p}; t) + \frac{1}{m} \vec{p} \cdot \vec{\nabla}_r f(\vec{r}, \vec{p}; t) - V(\vec{r}; t) \left(-\vec{\Lambda} + \frac{1}{3!} \frac{\hbar^2}{4} (\vec{\Lambda})^3 - \dots \right) f(\vec{r}, \vec{p}; t) = 0 \quad (5.13)$$

Neglecting the terms containing \hbar^n , $n \geq 2$ in the expansion, Eq. (5.13) is transformed to the so-called Landau-Vlasov equation [47]

$$\frac{\partial}{\partial t} f(\vec{r}, \vec{p}; t) = \{h(\vec{r}, \vec{p}; t), f(\vec{r}, \vec{p}; t)\}, \quad (5.14)$$

where $h(\vec{r}, \vec{p}; t) = p^2 / 2m + V(\vec{r}; t)$ is the classical Hamiltonian and $\{\dots, \dots\}$ is a Poisson bracket.

To obtain the hydrodynamic equations, we need to consider zero, first and second \vec{p} -moments of the phase-space kinetic equation (5.12). The zero-moment is obtained by integrating Eq. (5.12) with $(1/2\pi\hbar)^3 \int d\vec{p}$;

$$\frac{\partial}{\partial t} \rho + \nabla_\nu (\rho \cdot u_\nu) = 0. \quad (5.15)$$

This is the equation of continuity, where the particle density $\rho(\vec{r}, t)$ and the velocity field $\vec{u}(\vec{r}, t)$ are given as:

$$\rho(\vec{r}, t) = \int \frac{g d\vec{p}}{(2\pi\hbar)^3} f(\vec{r}, \vec{p}; t), \quad (5.16)$$

$$\vec{u}(\vec{r}, t) = \frac{1}{\rho(\vec{r}, t)} \int \frac{g d\vec{p}}{(2\pi\hbar)^3} \frac{\vec{p}}{m} f(\vec{r}, \vec{p}; t), \quad (5.17)$$

were, $g = 4$ is the spin-isospin degeneracy factor.

The first moment is obtained by integrating Eq. (5.12) with $(1/2\pi\hbar)^3 \int d\vec{p} \vec{p}$,

$$\begin{aligned} \frac{\partial}{\partial t} (m\rho(\vec{r}, t)u_\nu(\vec{r}, t)) + \nabla_\mu (m\rho(\vec{r}, t)u_\nu(\vec{r}, t)u_\mu(\vec{r}, t)) = \\ - [\nabla_\mu P_{\nu\mu}(\vec{r}, t) + \delta_{\nu\mu} \rho(\vec{r}, t) \nabla_\mu V(\vec{r}, t)], \end{aligned} \quad (5.18)$$

where $P_{\nu\mu}(\vec{r}, t)$ is the pressure given as

$$P_{\nu\mu}(\vec{r}, t) = \frac{1}{m} \int \frac{g d\vec{p}}{(2\pi\hbar)^3} (p_\nu - mu_\nu(\vec{r}, t))(p_\mu - mu_\mu(\vec{r}, t)) f(\vec{r}, \vec{p}; t). \quad (5.19)$$

Eq. (5.18) is an Euler-type equation for the system of particles.

Similarly, the second moment is obtained by integration of the Eq. (5.12)

with $(1/2\pi\hbar)^3 \int d\vec{p} (p^2/2m)$:

$$\begin{aligned} \frac{\partial}{\partial t} \mathcal{E}_{kin}^{int}(\vec{r}, t) + \nabla_v \left(\mathcal{E}_{kin}^{int}(\vec{r}, t) u_v(\vec{r}, t) \right) = \\ - \frac{1}{2} P_{v\mu}(\vec{r}, t) (\nabla_\mu u_v(\vec{r}, t) + \nabla_v u_\mu(\vec{r}, t)) - \nabla_v q_v(\vec{r}, t). \end{aligned} \quad (5.20)$$

where $\mathcal{E}_{kin}^{int}(\vec{r}, t)$ denotes the internal kinetic energy density

$$\mathcal{E}_{kin}^{int}(\vec{r}, t) = \int \frac{g d\vec{p}}{(2\pi\hbar)^3} \frac{(\vec{p} - m\vec{u}(\vec{r}, t))^2}{2m} f(\vec{r}, \vec{p}; t), \quad (5.21)$$

and $q_v(\vec{r}, t)$ is the heat flux

$$q_v(\vec{r}, t) = \frac{1}{2m^2} \int \frac{g d\vec{p}}{(2\pi\hbar)^3} (p_v - m u_v(\vec{r}, t)) (\vec{p} - m\vec{u}(\vec{r}, t))^2 f(\vec{r}, \vec{p}; t). \quad (5.22)$$

The local equations (5.15), (5.18) and (5.20) have been deduced directly from the quantum equation (5.7) without any assumptions. However, these equations are not closed equations because the definitions of the quantities $P_{v\mu}$, q_v and \mathcal{E}_{kin}^{int} contain an unknown distribution function $f(\vec{r}, \vec{p}; t)$. Eqs. (5.15), (5.18) and (5.20) can be reduced to closed equations which involve only the local quantities ρ , \vec{u} , $P_{v\mu}$ and \mathcal{E}_{kin}^{int} , if a reasonable assumption for the distribution function $f(\vec{r}, \vec{p}; t)$ is made, see Refs. [48,49].

The continuity equation (5.15) leads to the energy-weighted sum rules. Let us consider the response of a system of particles to the external field [50]

$$\hat{f}(t) = \hat{f} \delta(t - t_0) = \sum_{j=1}^A f(\vec{r}_j) \delta(t - t_0) = \int d\vec{r} f(\vec{r}) \hat{\rho}(\vec{r}) \delta(t - t_0), \quad (5.23)$$

where \hat{f} is the arbitrary single-particle operator and $\rho(\vec{r})$ is the particle density operator

$$\hat{\rho}(\vec{r}) = \sum_{j=1}^A \delta(\vec{r} - \vec{r}_j).$$

The solution to Eq. (5.4) for $\delta t = t - t_0 \rightarrow +0$ with $\hat{H} = \hat{H}_0 + \hat{f} \delta(t - t_0)$ and

$\hat{H}_0 |\Psi_n\rangle = E_n |\Psi_n\rangle$ gives for the rate of change of particle density

$$\frac{\partial \rho}{\partial t} = \frac{\partial}{\partial t} \langle \Psi(t) | \hat{\rho}(\vec{r}) | \Psi(t) \rangle = -\frac{2}{\hbar^2} \sum_{n \neq 0}^{\infty} (E_n - E_0) \langle \Psi_0 | \hat{\rho}(\vec{r}) | \Psi_n \rangle \langle \Psi_n | \hat{f} | \Psi_0 \rangle. \quad (5.24)$$

On the other hand, including $V_{ext}(t)$ into the mean field V in Eq. (5.12) and integrating Eq. (5.13) over time in a small interval $[t_0, t_0 + \delta t]$ we find

$$f = f_0 + \frac{2}{\hbar} \sin\left(\frac{\hbar}{2} \vec{\nabla}_{\vec{p}} \cdot \vec{\nabla}_{\vec{r}} \hat{f}\right) f_0 \hat{f} \quad \text{at} \quad t = t_0 + \delta t, \quad \delta t \rightarrow +0, \quad (5.25)$$

where f_0 is the distribution function which corresponds to the initial ground state Ψ_0 .

From definition (5.17) and Eq. (5.25) we also obtain the velocity field as

$$u_v = -\frac{1}{m} \nabla_v \hat{f} \quad \text{at} \quad t = t_0 + \delta t, \quad \delta t \rightarrow +0. \quad (5.26)$$

Taking into account the continuity equation (5.15), along with equations (5.24) and (5.26), we obtain the local energy-weighted sum rule:

$$\sum_{n \neq 0}^{\infty} (E_n - E_0) \langle \Psi_0 | \hat{\rho}(\vec{r}) | \Psi_n \rangle \langle \Psi_n | \hat{f} | \Psi_0 \rangle = -\frac{\hbar^2}{2m} \vec{\nabla} \langle \Psi_0 | \hat{\rho} | \Psi_0 \rangle \cdot \vec{\nabla} \hat{f}. \quad (5.27)$$

Multiplying Eq. (5.27) by $\hat{f}(\vec{r})$ and integrating over the coordinate \vec{r} we obtain the energy weighted sum rule for the single particle operator \hat{f} :

$$m_1 = \sum_{n \neq 0}^{\infty} (E_n - E_0) \left| \langle \Psi_n | \hat{f} | \Psi_0 \rangle \right|^2 = \frac{\hbar^2}{2m} \int d\vec{r} \rho_{eq}(\vec{\nabla} \hat{f})^2. \quad (5.28)$$

B. Dynamic Distortion of Fermi Surface

The collective dynamics of the Fermi liquid exhibits strong dependence on the dynamical distortion of the Fermi surface in momentum space [51-55]. In this dissertation we consider the effect of small deviations of the Fermi surface from the equilibrium spherical shape on the nuclear dynamics. In terms of the single particle time-evolution operators $\hat{\chi}(t)$ the time dependent single particle matrix $\hat{\rho}(t) \equiv \hat{\rho}(\vec{r}, \vec{r}'; t)$ can be given in the form (see Ref. [56]):

$$\hat{\rho}(t) = \exp\left[\frac{i}{\hbar} m \hat{\chi}(t)\right] \hat{\rho}_0(t) \exp\left[-\frac{i}{\hbar} m \hat{\chi}(t)\right], \quad (5.29)$$

where $\hat{\rho}_0(t)$ is the time-even part of the density matrix. Considering time evolution as a small correction for the initial time even density matrix, we can write Eq. (5.29) in the form of expansion:

$$\hat{\rho}(t) = \hat{\rho}_0(t) + \sum_{n=0}^{\infty} \frac{1}{n+1} \left[\frac{i}{\hbar} m \hat{\chi}(t), \hat{\rho}_n(t) \right]. \quad (5.30)$$

The operators $\hat{\rho}_n(t)$ satisfy the recurrence relationships

$$\hat{\rho}_n(t) = \frac{1}{n} \left[\frac{i}{\hbar} m \hat{\chi}(t), \hat{\rho}_{n-1}(t) \right], \quad n = 1, 2, \dots \quad (5.31)$$

Using rules of the Wigner transformation on Eq. (5.31), we obtain for the time depending Wigner distribution function:

$$f(\vec{r}, \vec{p}; t) = f_{sph}(\vec{r}, \vec{p}; t) + \frac{2}{\hbar} \sum_{n=0}^{\infty} \frac{1}{n+1} g_{sc}(\vec{r}, \vec{p}; t) \sin\left[\frac{\hbar}{2} \vec{\Lambda}\right] f_n(\vec{r}, \vec{p}; t), \quad (5.32)$$

where $f_{sph}(\vec{r}, \vec{p}; t)$, $g_{sc}(\vec{r}, \vec{p}; t)$ and $f_n(\vec{r}, \vec{p}; t)$ are the Wigner-transforms for the time-even density $\hat{\rho}_0(t)$, $m\hat{\chi}(t)$ and $\hat{\rho}_n(t)$, respectively.

We consider the lowest order in the expansions (5.32) in powers of \hbar . The Wigner-transforms for the commutators in the expansion (5.31), can be approximated as:

$$[m\hat{\chi}(t), \hat{\rho}_n(t)]_W \approx i\hbar [g_{sc}, f_n]_P. \quad (5.33)$$

According to Eq. (5.33), in the lowest order in power of \hbar the distribution function $f(\vec{r}, \vec{p}; t)$ can be written as:

$$f(\vec{r}, \vec{p}; t) \approx f_{sph}\left(\vec{r} + \vec{\nabla}_{\vec{p}} g_{sc}, \vec{p} - \vec{\nabla}_{\vec{r}} g_{sc}; t\right). \quad (5.34)$$

We start the investigation of the Fermi surface distortion effects by assuming the one-body density matrix $\hat{\rho}_0(t)$ in Eq. (5.30) such that the corresponding distribution function $f_{sph}(\vec{r}, \vec{p}; t)$ is spherically symmetric in momentum space. The result (5.34) states that the dynamic distribution function $f(\vec{r}, \vec{p}; t)$ can be obtained from the spherical distribution function $f_{sph}(\vec{r}, \vec{p}; t)$ using a time-dependent shift in phase space:

$$\vec{r} \rightarrow \vec{r}' = \vec{r} + \vec{\nabla}_{\vec{p}} g_{sc}(\vec{r}, \vec{p}; t), \quad \vec{p} \rightarrow \vec{p}' = \vec{p} - \vec{\nabla}_{\vec{r}} g_{sc}(\vec{r}, \vec{p}; t). \quad (5.35)$$

Assuming that the function $g_{sc}(\vec{r}, \vec{p}; t)$ is a smooth function of the variables \vec{r} and \vec{p} , we can expand it into a series in \vec{p} and retain only the first two terms

$$g_{sc}(\vec{r}, \vec{p}; t) \approx \chi^{(0)}(\vec{r}, t) - p_\nu \chi_\nu^{(1)}(\vec{r}, t). \quad (5.36)$$

Eq. (5.36) allows us to rewrite the coordinate transformation in the phase space as:

$$\begin{aligned} r'_\nu &= r_\nu - \chi_\nu^{(1)}(\vec{r}, t), \\ p'_\nu &= -\nabla_\nu \chi^{(0)}(\vec{r}, t) + (\delta_{\nu\mu} + \nabla_\nu \chi_\mu^{(1)}(\vec{r}, t)) p_\mu. \end{aligned} \quad (5.37)$$

Therefore, Eq. (5.34) takes form:

$$f(\vec{r}, \vec{p}; t) \approx f_{sph}(\vec{r}', \vec{p}'; t). \quad (5.38)$$

We assumed the Fermi surface for the distribution function $f_{sph}(\vec{r}, \vec{p}; t)$ to be a sphere with radius p_F , therefore, from the form of Eqs. (5.37) and from Eq. (5.36) we can conclude that an excitation in the nucleus leads to the displacement of the Fermi sphere as a whole by the vector $\vec{\nabla} \chi^{(0)}(\vec{r}, t)$ and to its deformation into an ellipsoid. The deformation of the Fermi surface is a result of the non-local character of the time evolution operator, $\hat{\chi}$, and disappears when $\vec{\chi}^{(1)}(\vec{r}, t) = 0$. The vector $\vec{\chi}^{(1)}(\vec{r}, t)$ can be interpreted as a time-dependent local displacement of particles from their equilibrium positions.

We can describe the phase shift (5.37) using the transformation matrix:

$$a_{\nu\mu}(\vec{r}, t) = \delta_{\nu\mu} + \nabla_\nu \chi_\mu^{(1)}(\vec{r}, t), \quad (5.39)$$

and the inverse matrix $a_{\nu\mu}^{-1}(\vec{r}, t)$. Then, using equations (5.37), (5.38) and (5.39), with the definition of the local single-particle density matrix we obtain the local particle density in the form:

$$\rho(\vec{r}, t) = \text{Det} \| a_{\nu\mu}^{-1}(\vec{r}, t) \| \rho_0(\vec{r}', t), \quad (5.40)$$

where

$$\rho_0(\vec{r}, t) = \int \frac{g d\vec{p}}{(2\pi\hbar)^3} f_{sph}(\vec{r}, \vec{p}; t) \quad (5.41)$$

is the initial time even unperturbed particle density. Using the fact that the distribution function $f_{sph}(\vec{r}, \vec{p}; t)$ is an even function of the momentum, $f_{sph}(\vec{r}, \vec{p}; t) = f_{sph}(\vec{r}, -\vec{p}; t)$, along with Eqs. (5.37) and (5.39) we obtain the expression for the local velocity field:

$$u_v(\vec{r}, t) = \frac{1}{m} a_{\mu\nu}^{-1}(\vec{r}, t) \nabla_\mu \chi^{(0)}(\vec{r}, t). \quad (5.42)$$

The distribution function $f_{sph}(\vec{r}, \vec{p}; t)$ is isotropic in momentum space, therefore, we can write the equation for the kinetic energy density in the form:

$$\begin{aligned} \varepsilon_{kin}(\vec{r}, t) &= \int \frac{g d\vec{p}}{(2\pi\hbar)^3} \frac{p^2}{2m} f(\vec{r}, \vec{p}; t) = \\ &= \frac{1}{3} Det \|a_{\mu\nu}^{-1}(\vec{r}, t)\| Tr \|A_{\mu\nu}(\vec{r}, t)\| \varepsilon_{kin}^{int}(\vec{r}, t) + \frac{1}{2} m \rho(\vec{r}, t) u^2(\vec{r}, t), \end{aligned} \quad (5.43)$$

where $A_{\mu\nu}(\vec{r}, t) = a_{\mu\beta}^{-1}(\vec{r}, t) a_{\beta\nu}^{-1}(\vec{r}, t)$. The quantity $\varepsilon_{kin}^{int}(\vec{r}, t)$ in Eq. (5.43) is the internal energy density associated with the distribution function $f_{sph}(\vec{r}, \vec{p}; t)$, the Wigner-transform of the initial time-even particle density. The first term in (5.43) does not depend on the velocity field, $\vec{u}(\vec{r}, t)$, and can be identified with the internal kinetic energy density for the case with deformation of the Fermi surface, $\tilde{\varepsilon}_{kin}^{int}$. The deviation of the quantity $\tilde{\varepsilon}_{kin}^{int}$ from the kinetic energy density ε_{kin}^{int} vanishes in the local approximation, when $\vec{\chi}^{(1)}(\vec{r}, t) = 0$. The second term in (5.43) is the collective kinetic energy density of a classical fluid,

$$\varepsilon_{kin}^{(coll)} = \frac{1}{2} m \rho(\vec{r}, t) u^2(\vec{r}, t). \quad (5.44)$$

The collective kinetic energy density $\varepsilon_{kin}^{(coll)}$ depends on the velocity field $\vec{u}(\vec{r}, t)$ due to the quasi-classical approximation (5.33) and assumption (5.36). Eq. (5.44) is also valid in the local approximation. Therefore, we can conclude, that the dynamical deformation of the Fermi surface does not change (for $l \leq 2$) the hydrodynamic relation between the collective kinetic energy density and the velocity field. In the following section we will show that the contribution from FSD to the kinetic energy density ε_{kin} has a significant effect on the spectrum of the oscillations of nuclei.

Using definition (5.19) and expressions (5.34) and (5.37), we can write the expression for the pressure tensor in terms of the internal kinetic energy density and the local displacement field as:

$$P_{\nu\mu} = \frac{2}{3} \epsilon_{kin}^{int} \delta_{\nu\mu} - \frac{2}{3} \nabla_{\beta} (\epsilon_{kin}^{int} \chi_{\beta}^{(1)}) \delta_{\nu\mu} - \frac{2}{3} \epsilon_{kin}^{int} (\nabla_{\mu} \chi_{\nu}^{(1)} + \nabla_{\nu} \chi_{\mu}^{(1)}). \quad (5.45)$$

The distortion of the Fermi surface gives rise to the correction of the off-diagonal components of the pressure tensor. The heat flux, \vec{q} , defined by Eq. (5.22), is written in terms of Eqs. (5.34) and (5.37) and taken in an approximation linear in $\bar{\chi}^{(1)}$.

Let us consider the time evolution of the system as deviations of the density $\rho(\vec{r}, t)$ and velocity field $\vec{u}(\vec{r}, t)$ about the equilibrium values $\rho_{eq}(\vec{r})$ and $\vec{u}_{eq}(\vec{r}) = 0$. In this case the distribution function $f_{sph}(\vec{r}, \vec{p}; t)$ in Eq. (5.34) coincides with the static equilibrium distribution function, $f_{eq}(\vec{r}, \vec{p})$. In such approximation, the time dependent particle density can be expressed in terms of the static equilibrium particle density and to the first order in $\bar{\chi}^{(1)}$ is given as (see Eq. (5.40)):

$$\rho(\vec{r}, t) \approx \rho_{eq}(\vec{r}) - \nabla_{\nu} (\rho_{eq}(\vec{r}) \chi_{\nu}^{(1)}(\vec{r}, t)). \quad (5.46)$$

The continuity equation (5.15), taken with the time-dependent particle density from Eq. (5.46), provides us with the connection of the quantities \vec{u} and $\bar{\chi}^{(1)}$:

$$\frac{\partial}{\partial t} \bar{\chi}^{(1)}(\vec{r}, t) = \vec{u}(\vec{r}, t). \quad (5.47)$$

Eq. (5.47) confirms the interpretation of the $\bar{\chi}^{(1)}$ as the time-dependent displacement field. In the following derivations we will assume the change of the particle density to be defined according to Eq. (5.46):

$$\delta\rho(\vec{r}, t) = \rho(\vec{r}, t) - \rho_{eq}(\vec{r}) = \nabla_{\nu} (\rho_{eq}(\vec{r}) \chi_{\nu}^{(1)}(\vec{r}, t)). \quad (5.48)$$

If the Fermi surface remains spherical during the motion (first sound, $\bar{\chi}^{(1)}(\vec{r}, t) = 0$), then the pressure tensor is diagonal:

$$P_{\nu\mu} = \frac{2}{3} \epsilon_{kin}^{int} \delta_{\nu\mu}. \quad (5.49)$$

According to Ref. [10] we can define the chemical potential λ , as:

$$\lambda = \delta(\varepsilon_{kin}^{int} + \varepsilon_{pot}) / \delta\rho. \quad (5.50)$$

The chemical potential is constant in the equilibrium, therefore, we can use equilibrium condition $\vec{\nabla}[\delta(\varepsilon_{kin}^{int} + \varepsilon_{pot}) / \delta\rho]_{eq} = 0$ along with the continuity equation (5.15), and obtain the equation for the first sound in nucleus as:

$$\frac{\partial^2}{\partial t^2} \chi_{\mu}^{(1)} = \frac{1}{m} \nabla_{\mu} \kappa \nabla_{\nu} \rho_{eq} \chi_{\nu}^{(1)}. \quad (5.51)$$

Here the local incompressibility coefficient is given as (see Ref. [10]):

$$\kappa \equiv \kappa(\vec{r}) = \left(\frac{\delta^2(\varepsilon_{kin}^{int} + \varepsilon_{pot})}{\delta\rho^2} \right)_{eq}. \quad (5.52)$$

For infinite nuclear matter ($\vec{\nabla} \rho_{eq} = \vec{\nabla} \kappa = 0$) this equation goes over to the ordinary equation for compression waves:

$$\frac{\partial^2}{\partial t^2} \delta\rho = \frac{1}{9m} K \nabla^2 \delta\rho, \quad (5.53)$$

where K is the incompressibility coefficient of the nuclear matter

$$K = 9\rho_{eq} \left(\frac{\delta^2(\varepsilon_{kin}^{int} + \varepsilon_{pot})}{\delta\rho^2} \right)_{eq} = 9\rho_{eq} \kappa = 9\rho_{eq}^2 \frac{\delta^2}{\delta\rho^2} \frac{E}{A} \Big|_{eq}, \quad (5.54)$$

and E/A is the nuclear matter binding energy per particle.

We can take the dynamical FSD into account by using expression (5.45) and equations (5.46) and (5.52), and obtain a closed Euler-like equation for the zero-sound regime in the nucleus:

$$m\rho_{eq} \frac{\partial^2}{\partial t^2} \chi_{\mu}^{(1)} = \nabla_{\mu} \rho_{eq} \kappa \nabla_{\alpha} (\rho_{eq} \chi_{\alpha}^{(1)}) + \frac{2}{3} \nabla_{\beta} \tau_{eq} \Lambda_{\mu\beta}, \quad (5.55)$$

where

$$\Lambda_{\alpha\beta} = \nabla_{\beta} \chi_{\alpha}^{(1)} + \nabla_{\alpha} \chi_{\beta}^{(1)} - \frac{2}{3} \nabla_{\gamma} \chi_{\gamma}^{(1)} \delta_{\alpha\beta}. \quad (5.56)$$

In the infinite nuclear matter $\vec{\nabla} \tau_{eq} = \vec{\nabla} \rho_{eq} = \vec{\nabla} \kappa = 0$, and Eq. (5.55) can be written in the form:

$$m\rho_{eq} \frac{\partial^2}{\partial t^2} \chi_{\mu}^{(1)} = \left(\frac{1}{9} K\rho_{eq} + \frac{2}{9} \tau_{eq} \right) \nabla_{\mu} \nabla_{\alpha} \chi_{\alpha}^{(1)} + \frac{2}{3} \tau_{eq} \nabla^2 \chi_{\mu}^{(1)}. \quad (5.57)$$

Eq. (5.57) describes elastic waves propagating in an infinite non-isotropic medium with Lamé coefficients [57]

$$\lambda_{Lame} = \frac{1}{9} (K\rho_{eq} + 2\tau_{eq}), \quad \mu_{Lame} = \frac{2}{3} \tau_{eq} \quad (5.58)$$

The second term in Eq. (5.57) allows for two types of solutions: a longitudinal wave $\vec{\chi}_l^{(1)}$ ($\vec{\nabla} \times \vec{\chi}_l^{(1)} = 0$) and a transverse wave $\vec{\chi}_t^{(1)}$ ($\vec{\nabla} \cdot \vec{\chi}_t^{(1)} = 0$). It is easy to see, that due to the deformation of the Fermi surface, the nucleus incompressibility coefficient K for the longitudinal wave $\vec{\chi}_l^{(1)}$ gets renormalized, and becomes equal to $K' = K + 8\tau_{eq} / \rho_{eq}$.

C. Relaxation Process and Viscosity Effect

Incorporation of an inter-particle collision term into the equation of motion (5.7) for the one-body density matrix is needed in order to describe dissipative behavior.

Following Ref. [58] and making use of the continuity equation (5.15), along with Eqs. (5.46), (5.47) and (5.54) the Euler-like equation (5.18) can be written as

$$m\rho_{eq} \frac{\partial u_{\nu}}{\partial t} + \nabla_{\mu} P_{\nu\mu} = 0, \quad (5.59)$$

where ρ_{eq} is the equilibrium particle density, u_{ν} is the velocity field, and $P_{\nu\mu}$ is the momentum flux tensor.

The derivation of the momentum flux tensor $P_{\nu\mu}$ in the Euler-like equation (5.59) depends on the equation of state of the nuclear Fermi liquid. In the nuclear interior, the momentum flux tensor, $P_{\nu\mu}$, can be given as, see Ref. [58],

$$P_{\lambda\mu} = \delta P_{\lambda\mu} + \delta P_{\lambda\mu}^{(\nu)}, \quad (5.60)$$

where $\delta P_{\lambda\mu}$ is the dynamic part of the pressure tensor including pressure of external field

$$\delta P_{\lambda\mu} = \frac{K}{9} \delta\rho \delta_{\lambda\mu} - \mu_F \left[\frac{\partial \chi_{\lambda}^{(1)}}{\partial r_{\mu}} + \frac{\partial \chi_{\mu}^{(1)}}{\partial r_{\lambda}} - \frac{2}{3} \nabla_{\alpha} \chi_{\alpha}^{(1)} \delta_{\lambda\mu} \right], \quad (5.61)$$

and $\delta P_{\lambda\mu}^{(\nu)}$ is the viscosity tensor

$$\delta P_{\lambda\mu}^{(\nu)} = -\nu \left[\frac{\partial u_{\lambda}}{\partial r_{\mu}} + \frac{\partial u_{\mu}}{\partial r_{\lambda}} - \frac{2}{3} \nabla_{\alpha} u_{\alpha} \delta_{\lambda\mu} \right]. \quad (5.62)$$

Here, ν is the viscosity coefficient, μ_F is the FSD parameter, $\vec{\chi}$ is the displacement field, and \vec{u} is the velocity field, as defined in Eq. (5.47). In general, the kinetic coefficients μ_F and ν can be derived through the solution of the Landau's dispersion equation, [59]. To derive expressions for these coefficients we will consider the collisional Landau-Vlasov equation for a small variation of the Wigner distribution function,

$$\frac{\partial}{\partial t} \delta f + \vec{\nabla}_{\vec{p}} \varepsilon_{eq} \cdot \vec{\nabla}_{\vec{r}} \delta f - \vec{\nabla}_{\vec{r}} \delta V \cdot \vec{\nabla}_{\vec{p}} f_{eq} - \vec{\nabla}_{\vec{r}} V_{eq} \cdot \vec{\nabla}_{\vec{p}} \delta f = \delta S t. \quad (5.63)$$

Here ε_{eq} , V_{eq} , and f_{eq} are the equilibrium energy density, Wigner transform of the equilibrium particle-particle interaction and equilibrium Wigner distribution function, and δV , δf and $\delta S t$ are small variations of the particle-particle interaction, Wigner distribution function and collision integral from their equilibrium values, respectively. For simplification, we assume that the deformation of the Fermi surface is restricted by multipolarities $l \leq 2$. The first \vec{p} -moment of Eq. (5.63) reproduces the fluid dynamics equation (5.59). Now assuming that the displacement function to be harmonic,

$$\chi_{\mu}^{(1)}(\vec{r}, t) = \chi_{\mu}^{(1)}(\vec{r}) e^{-i\omega t}, \quad (5.64)$$

we can rewrite Eq. (5.59) in the form:

$$\begin{aligned} -\omega^2 \rho_{eq} \chi_{\mu,\omega}^{(1)} &= \left(\frac{\rho_{eq}}{m} \right) \nabla_{\mu} \kappa \nabla_{\nu} \rho_{eq} \chi_{\nu,\omega}^{(1)} + \frac{\omega_R^2 \tau^2}{1 + (\omega_R \tau)^2} \nabla_{\nu} P_{eq} \Lambda_{\mu\nu,\omega} \frac{1}{m} + \\ & i\omega \frac{\tau}{1 + (\omega_R \tau)^2} \nabla_{\nu} P_{eq} \Lambda_{\mu\nu,\omega} \frac{1}{m}. \end{aligned} \quad (5.65)$$

Here sub-index ω indicates the Fourier transformation of the appropriate functions. Comparing the form of Eq. (5.65) with equations (5.59), (5.60), (5.61) and (5.62) we can conclude that for the distortion of the Fermi surface of multipolarities $l \leq 2$ the coefficients μ_F and ν can be given by:

$$\mu_F = \text{Im}\left(\frac{\omega\tau}{1-i\omega\tau}\right)P_{eq}, \quad \nu = \text{Re}\left(\frac{\tau}{1-i\omega\tau}\right)P_{eq}, \quad (5.66)$$

where $P_{eq} \approx \frac{2}{5}\epsilon_F\rho_{eq}$ is the equilibrium pressure of the Fermi gas and τ is the relaxation time for sound excitations in the Fermi liquid. We need to point out, that both Eqs. (5.59) and (5.65) were obtained from the collisional Landau-Vlasov equation (5.63), under the assumption that the variation of the collision integral $\delta\mathcal{S}t$ can be written in terms of the relaxation time τ and the equilibrium forms of the total energy density and Wigner distribution function and their small variations (see Refs.[58] and [60]).

Now, using the relation between the variation of the particle density, $\delta\rho$, and the displacement field, $\vec{\chi}^{(1)}$, Eq. (5.48), and assuming that the behavior of the displacement field can be approximated by a plane-wave $\chi_\mu^{(1)}(\vec{r}, t) \sim \exp(i\vec{q} \cdot \vec{r} - i\omega t)$ we can rewrite Eq. (5.65) in the form:

$$\omega^2 - c_0^2 q^2 - i\gamma\omega q^2 = 0. \quad (5.67)$$

Here c_0 is the zero sound velocity

$$c_0^2 = \frac{1}{9m} \left[K + 12 \frac{\mu_F}{\rho_{eq}} \right], \quad (5.68)$$

and γ is the friction coefficient

$$\gamma = \frac{4\nu}{3\rho_{eq}m}. \quad (5.69)$$

From the equations (5.66) and (5.67) we can see that the eigenfrequency of the oscillation of nuclear media has both real and imaginary parts. The real part of the eigenfrequency corresponds to the centroid energy of appropriate excitation, $E = \text{Re}(\hbar\omega)$. The imaginary part of the eigenfrequency corresponds to the width of

collective excitation, $\Gamma = -\text{Im}(\hbar\omega)$, introduced due to the collisional damping effect of the dynamic Fermi surface deformation.

To complete our model we need to approximate the relaxation time in the nuclear medium. To do so, we start from the expression for the variation of collision integral [60]:

$$\begin{aligned} \delta St(\vec{r}, \vec{p}) = & \int \frac{d\vec{p}_2 d\vec{p}_3 d\vec{p}_4}{(2\pi\hbar)^6} w(\{\vec{p}_j\}) \delta(\vec{p}_3 + \vec{p}_4 - \vec{p}_1 - \vec{p}_2) \times \\ & \left[\sum_{i=1}^4 \frac{\delta Q(\{f_{eq,i}\})}{\mathcal{F}_{eq,i}} \frac{1}{2\pi\hbar} \int_{-\infty}^t dt' \cos\left(\frac{h_{eq,3}(t-t') + h_{eq,4}(t-t') - h_{eq,1}(t-t') - h_{eq,2}(t-t')}{\hbar}\right) \mathcal{F}_i(t') + \right. \\ & \left. \frac{1}{2\pi\hbar} \int_{-\infty}^t dt' (\delta V_3(t') + \delta V_4(t') - \delta V_1(t') - \delta V_2(t')) \times \right. \\ & \left. \int_{-\infty}^{t'} dt'' \sin\left(\frac{h_{eq,3}(t-t'') + h_{eq,4}(t-t'') - h_{eq,1}(t-t'') - h_{eq,2}(t-t'')}{\hbar}\right) \right]. \end{aligned} \quad (5.70)$$

Here $w(\{\vec{p}_j\})$ are the nucleon-nucleon scattering probabilities in nuclear medium,

$h_{eq,j} = p_j^2 / 2m + V(\vec{r}, \vec{p}_j, t)$ - the classical single particle Hamiltonian in phase space, and $Q(\{f_j\})$ is the Pauli blocking factor, given as:

$$Q(\{f_j\}) = (1 - f_1)(1 - f_2)f_3f_4 - f_1f_2(1 - f_3)(1 - f_4) \quad (5.71)$$

Under the assumption that the variation of the Wigner distribution function exhibits a harmonic time dependence $\mathcal{F}_j \sim \exp(-i\omega t)$, we can rewrite Eq. (5.70) in the form:

$$\begin{aligned} \delta St(\vec{r}, \vec{p}) = & \int \frac{d\vec{p}_2 d\vec{p}_3 d\vec{p}_4}{(2\pi\hbar)^6} w(\{\vec{p}_j\}) \delta(\vec{p}_3 + \vec{p}_4 - \vec{p}_1 - \vec{p}_2) \times \\ & \left[\sum_{i=1}^4 \frac{\delta Q(\{f_{eq,i}\})}{\mathcal{F}_{eq,i}} \mathcal{F}_i(t) \frac{1}{2} (\delta(h_{eq,3} + h_{eq,4} - h_{eq,1} - h_{eq,2} + \hbar\omega) + \right. \\ & \left. \delta(h_{eq,1} + h_{eq,2} - h_{eq,3} - h_{eq,4} - \hbar\omega)) + \right. \\ & \left. Q(\{f_{eq,i}\}) (\delta V_3 + \delta V_4 - \delta V_1 - \delta V_2) \frac{1}{2\hbar\omega} \{(\delta(h_{eq,3} + h_{eq,4} - h_{eq,1} - h_{eq,2} + \hbar\omega) + \right. \end{aligned}$$

$$\left. \begin{aligned} & \delta(h_{eq.1} + h_{eq.2} - h_{eq.3} - h_{eq.4} - \hbar\omega) + \\ & \delta(h_{eq.1} + h_{eq.2} - h_{eq.3} - h_{eq.4}) - \delta(h_{eq.3} + h_{eq.4} - h_{eq.1} - h_{eq.2}) \end{aligned} \right\} \quad (5.72)$$

Then the relaxation time corresponding to the collisional damping can be defined as:

$$\frac{1}{\tau(\omega)} = \frac{\int d\Omega_p Y_{l_0}^*(\hat{p}) \delta \mathcal{S} t}{\int d\Omega_p Y_{l_0}^*(\hat{p}) \delta \mathcal{f}}. \quad (5.73)$$

Now, let us consider the case of the equilibrium distribution function taken as:

$$f_{eq.}(\vec{r}, \vec{p}) = \left[1 + \exp\left(\frac{h_{eq.}(\vec{r}, \vec{p}) - \lambda}{T}\right) \right]^{-1}, \quad (5.74)$$

where T is the temperature of nuclear medium in the equilibrium, and λ is the chemical potential. Then the functional differentiation of the equilibrium distribution function with respect to classical Hamiltonian can be found as:

$$\frac{\delta f_{eq.}}{\delta h_{eq.}} = -\frac{f_{eq.}(1-f_{eq.})}{T}, \quad (5.75)$$

and the relaxation time for the collisional damping can be reformulated as:

$$\tau(\omega) = \frac{\tilde{\tau}}{1 + (\hbar\omega / 2\pi T)^2}, \quad (5.76)$$

where oscillation frequency ω is complex and $\tilde{\tau}$ is an energy independent quantity. For the isoscalar collective excitations, this quantity can be taken as a temperature dependent function of the collisional relaxation parameter β (see Refs. [58], [60]):

$$\frac{1}{\tilde{\tau}} = \frac{T^2}{\hbar\beta}. \quad (5.77)$$

Therefore considering the case of a cold nucleus ($T = 0$) we obtain the expression for the energy-dependent collisional relaxation time:

$$\tau(\omega) = \frac{4\pi^2 \hbar\beta}{(\text{Re}(\hbar\omega))^2}. \quad (5.78)$$

D. Boundary Conditions

In this dissertation, to derive the boundary conditions for the isoscalar compression excitations in finite nuclei we will assume a sharp particle density distribution

$$\rho_{total}(\vec{r}, t) = \rho(\vec{r}, t) \theta(r - R(t)), \quad \rho(\vec{r}, t) = \rho_{eq} + \delta\rho(\vec{r}, t), \quad (5.79)$$

where the vibrations of the nuclear surface for a given multipolarity L , can be written as:

$$R(t) = R_{eq}(1 + \beta_s(t)Y_{L0}(\hat{r})), \quad (5.80)$$

with the amplitude of the surface vibration $\beta_s(t) \sim \exp(-i\omega t)$. Then, considering the definition of the bulk density variation (5.48), we can write a solution of Eq. (5.65) corresponding to an isoscalar excitation of certain multipolarity L in the form:

$$\delta\rho^{vol}(\vec{r}, t) = \beta_L(t)\rho_{eq}j_L(qr)Y_{L0}(\hat{r}), \quad (5.81)$$

where $\beta_L(t)$ is the time-dependent amplitude of density oscillations $\beta_L(t) \sim \exp(-i\omega t)$. The amplitudes $\beta_L(t)$ and $\beta_s(t)$ are related to each other by the boundary condition for the velocity field on the moving nuclear surface. The macroscopic boundary conditions for the total particle density, obtained as a solution of Eq. (5.65) and satisfying continuity equation (5.15), taken on the moving nuclear surface (5.80) is given by the following (see Ref. [60]),

$$u_r(\vec{r}, t)|_{r=R_{eq}} = R_{eq}\dot{\beta}_s(t)Y_{L0}(\hat{r}), \quad (5.82)$$

$$\delta P_{rr}(\vec{r}, t)|_{r=R_{eq}} = \beta_s(t)\delta P_{\sigma}Y_{L0}(\hat{r}). \quad (5.83)$$

On the left hand side of Eqs. (5.82) and (5.83) we have the radial components of the velocity field, u_r , and the pressure tensor variation, δP_{rr} , on the nuclear surface, respectively. By inserting Eq. (5.81) in the definitions of the velocity field $\vec{u}(\vec{r}, t)$, Eq. (5.47), and the pressure tensor variation $\delta P_{rr}(\vec{r}, t)$, (5.60), we obtain expression for the boundary conditions on the nuclear surface in terms of the oscillation amplitudes $\beta_L(t)$ and $\beta_s(t)$:

$$u_r(\vec{r}, t) = \dot{\beta}_L(t) \frac{1}{q^2} \frac{\partial j_L(qr)}{\partial r} Y_{L0}(\hat{r}) = R_{eq} \dot{\beta}_S(t) Y_{L0}(\hat{r}), \quad (5.84)$$

$$\delta P_{rr}(\vec{r}, t) = \frac{1}{9} \left(K - 6 \frac{\mu_F}{\rho_{eq}} \right) \delta \rho(\vec{r}, t) - 2\mu_F \beta_L(t) j_L''(qr) Y_{L0}(\hat{r}) = \beta_S(t) \delta P_\sigma Y_{L0}(\hat{r}). \quad (5.85)$$

From Eq. (5.84) we obtain the relation between the oscillation amplitudes $\beta_S(t)$ and $\beta_L(t)$:

$$x\beta_S(t) = j_L'(x)\beta_L(t), \quad (5.86)$$

where $x = qR_{eq}$, and $j_L'(x)$ is the first derivative of the spherical Bessel function, see Ref. [61].

From the macroscopic point of view, the isoscalar dipole excitation corresponds to inflation and dilatation of the nucleus along an arbitrary direction at the constant nuclear surface. Therefore, the surface contribution to the variation of density is given by following: $\delta P_\sigma = 0$. Then, from Eq. (5.85), we obtain the boundary condition for the isoscalar dipole excitation in the form of the following secular equation for the transferred momentum q :

$$\left[\frac{1}{9} \left(K - 6 \frac{\mu_F}{\rho_{eq}} \right) j_1(qr) - 2 \frac{\mu_F}{\rho_{eq}} j_1''(qr) \right]_{r=R_{eq}} = 0. \quad (5.87)$$

In the case of the isoscalar monopole excitation, the additional contribution to the pressure tensor variation from the surface pressure can be taken in the form:

$$\delta P_\sigma = 2\sigma/R_{eq}, \quad (5.88)$$

where σ is the surface tension coefficient. Therefore, from Eqs. (5.83), (5.85), (5.86) and (5.88) we obtain:

$$\frac{j_0'(rq)}{\rho_{eq}m} = \frac{1}{9m} \left(K - 6 \frac{\mu_F}{\rho_{eq}} \right) (rq) j_0(rq) - \frac{2\mu_F}{\rho_{eq}m} (rq) j_0''(rq). \quad (5.89)$$

By defining damping amplitudes as follows:

$$f_\sigma = \frac{2\sigma}{m\rho_{eq}R_{eq}c_0^2}, \quad \text{and} \quad f_\mu = \frac{4\mu_F}{mc_0^2}, \quad (5.90)$$

where c_0 is the zero-sound velocity as it is given in Eq. (5.68), and using recurrent relations for the spherical Bessel functions

$$j'_n(x) = \frac{n}{x} j_n(x) - j_{n+1}(x) \quad \text{and} \quad \frac{d}{dx}(x^{-n} j_n(x)) = -x^{-n} j_{n+1}(x),$$

we obtain the secular equation for the transferred momentum q corresponding to the isoscalar monopole excitation:

$$\left[q r j_0(qr) - (f_\sigma + f_\mu) j_1(qr) \right]_{r=R_{eq}} = 0. \quad (5.91)$$

E. Translation Invariance Condition and Isoscalar Giant Resonance Description

A general condition of translation invariance states that any internal excitation must not affect the center of mass motion of the system. For the case of nuclear excitation this condition can be written as:

$$\int d\vec{r} \vec{r} \delta\rho_{total}(\vec{r}, t) = 0. \quad (5.92)$$

In the case of interest, the total variation of the particle density must be given in terms of the variation of bulk density and the variation of nuclear surface (see Eqs. (5.79) and (5.80)):

$$\delta\rho_{total}(\vec{r}, t) = \delta\rho(\vec{r}, t) + \rho_{eq} \delta(R_{eq} - r) \beta_S(t) R_{eq} Y_{L0}(\hat{r}), \quad (5.93)$$

Expressing the variation of bulk particle density in terms of the oscillation amplitude and using Eq. (5.86), we obtain an expression for the total particle density variations for multipolarity $L \neq 1$:

$$\delta\rho_{total}(\vec{r}, t) = \beta_L(t) \left[\theta(R_{eq} - r) j_L(qr) + \frac{1}{q} \delta(R_{eq} - r) j'_L(qR_{eq}) \right] \rho_{eq} Y_{L0}(\hat{r}). \quad (5.94)$$

Integrating Eq. (5.94) over $\iint r^3 dr d\Omega_{\hat{r}}$ and using recurrence relations for the spherical Bessel functions we will see that the condition (5.92) is readily satisfied for any $L \neq 1$. On the other hand, integration of Eq. (5.94) over $\iint r^3 dr d\Omega_{\hat{r}}$ is not equal zero.

Demanding that condition of invariance must be satisfied for any internal excitation we

can re-define the total particle density variation for the case of isoscalar dipole excitation as:

$$\delta\rho(\vec{r}, t) = \beta_1(t) \left[\theta(R_{eq} - r) j_1(qr) + \frac{1-a}{q} \delta(R_{eq} - r) j_1'(qR_{eq}) \right] \rho_{eq} Y_{10}(\hat{r}), \quad (5.95)$$

where the constant a is obtained using the condition (5.92) and is given by

$$a = j_1(x) / x j_1'(x), \quad x = qR_{eq}. \quad (5.96)$$

Note, that by re-defining the variation of total particle density for the isoscalar dipole we eliminate the spurious contribution to the isoscalar dipole excitation energy.

Based on the derivation given above, we conclude that within the Fermi liquid drop model with the collisional Fermi surface distortion centroid energies and widths of the isoscalar compression modes can be found as lowest non-zero solutions of the appropriate equations for the boundary conditions. These solutions must satisfy the dispersion relation, defined by Eqs. (5.66) - (5.69), taken with the energy-dependent collisional relaxation time given by Eq. (5.78).

CHAPTER VI

DESCRIPTION OF GIANT RESONANCES IN ^{90}Zr , ^{116}Sn , ^{144}Sm AND ^{208}Pb

In this chapter we present the results of a microscopic and macroscopic analysis of isoscalar monopole and isoscalar dipole giant resonance excitations in ^{90}Zr , ^{116}Sn , ^{144}Sm and ^{208}Pb . The microscopic analysis is based on self-consistent HF-RPA calculations with the SL1, SkM*, SGII, Sly4 and Sk255 Skyrme effective interactions. Results of microscopic calculations are used in a study of possible discrepancies in describing excitation of the isoscalar dipole mode in α – particle scattering reactions, which are introduced by the use of collective instead of microscopic transition densities. The macroscopic analysis is performed within the Fermi liquid drop model with collisional Fermi surface distortion. The results of calculations for the position and collisional widths of the isoscalar monopole and dipole excitation modes are compared to the results of microscopic calculations and to the experimentally obtained values.

A. Microscopic Analysis

In our calculations we used the SL1, SkM*, SGII, Sly4 and Sk255 Skyrme interactions, parameterizations which are given in Table I. These interactions are claimed to be successful in reproducing both the ground state properties and the average energies of the isoscalar giant monopole resonance excitations in heavy nuclei. To confirm these claims, in Section B. values for the binding energy per nucleon obtained with all interactions of interest are compared to the experimentally obtained results. Also, results for the root mean-square radii are presented. Using SL1, SkM*, SGII, Sly4 and Sk255 interactions average energies for the isoscalar giant monopole resonance are calculated and compared to experimentally obtained values in Section C. Fractions of the energy weighted sum rule exhausted within the experimentally observed region of excitation energy $5 \leq E \leq 35$ MeV are presented in the same section. Comparison of these results

proves the acceptability of these interactions in the description of isoscalar monopole resonance in heavy nuclei.

In order to obtain particle and hole wave functions and energies for both discrete and continuum states we start our calculations by finding the numerical solutions of radial Skyrme-based Hartree-Fock equations (2.39). In our calculations we discretize the single-particle continuum by placing a nucleus inside a sufficiently large sphere and imposing the boundary condition that wave functions of the continuum states vanish on the sphere's surface. Calculations with a discretized single-particle continuum were performed, for example, by Liu and Brown [62] and by Agrawal, Shlomo and Sanzhur [18]. In the mentioned works, the continuum appears to be well approximated by the set of discrete particle-hole states obtained using the bounding sphere whose radius was taken to be >2.5 times larger than the nuclear radius.

Using Hartree-Fock single-particle energies and wave functions, we obtain the radial part of the PRA Green's function defined by Eqs. (3.18), and (3.19), with the particle-hole interaction obtained as a functional double-derivative of the total energy density for the unperturbed Hartree-Fock single particle Hamiltonian with respect to the ground-state density of the many-body system, obtained by solving the Hartree-Fock problem. Using the obtained RPA Green's function, we calculate the transition strength distribution function (3.24) for the single particle excitation operators

$$\hat{f}_{L=0} = \sum_i r_i^2 Y_{00} \quad \text{and} \quad \hat{f}_{L=1} = \sum_i r_i^3 Y_{1M}(\hat{r}_i), \quad (6.1)$$

for the isoscalar giant monopole resonance and isoscalar giant dipole resonance, respectively. In the case of the monopole excitation, the transition strength distribution function is calculated directly using Eq. (3.24). The energy weighted sum rule for the isoscalar giant monopole resonance is calculated as the first energy moment of the isoscalar monopole strength distribution. In the case of the isoscalar dipole excitation, we employ the method of projecting out spurious state contribution, as described in Chapter III. By separately calculating $S_3(E)$, $S_{13}(E)$ and $S_1(E)$, and using Eq. (3.61), we obtain the isoscalar dipole strength distribution function $S_\eta(E)$, with no spurious

state contribution. The isoscalar giant dipole resonance transition density $\rho_{tr}(r, E)$ is calculated by projecting out the spurious state transition density $\rho_{ss}(r)$ from the transition density $\rho_{\eta}(r, E)$, obtained using the isoscalar giant dipole strength distribution $S_{\eta}(E)$ and the projection operator $f_{\eta} = f_3 - \eta f_1$.

The angular distributions for the inelastic scattering of 240 MeV α - particles on the nuclei of interest are calculated within the distorted-wave Born approximation. In this dissertation, attention is focused on the isoscalar dipole excitation in target nuclei. The real and imaginary parts of the optical potential are found by folding the radial part of the Hartree-Fock ground state density $\rho_0(r)$ with the real and imaginary parts of the α - nucleon effective interaction, respectively. The α -nucleon effective interaction is taken in the form of a density-dependent Gaussian potential:

$$V(|\vec{r} - \vec{r}'|, \rho_0(r')) = V(1 + \beta_V \rho_0^{2/3}(r')) e^{-\frac{|\vec{r} - \vec{r}'|^2}{\alpha_V}} + iW(1 + \beta_W \rho_0^{2/3}(r')) e^{-\frac{|\vec{r} - \vec{r}'|^2}{\alpha_W}}. \quad (6.2)$$

Parameters V , β_V , α_V and W , β_W , α_W of the α -nucleon effective interaction are determined by fitting experimentally measured angular distributions for the case of elastic scattering with the angular distributions obtained using optical potential (see Table VII). The real and imaginary parts of the radial form factor are obtained by folding HF-RPA transition density with the transition potential. The transition potential is calculated as a convolution of the transition density with the following expression:

$$V_{tr}(|\vec{r} - \vec{r}'|, \rho_0(r')) = V(|\vec{r} - \vec{r}'|, \rho_0(r')) + \rho_0(r') \frac{\partial V(|r - r'|, \rho_0(r'))}{\partial \rho_0(r')}, \quad (6.3)$$

where $V(|\vec{r} - \vec{r}'|, \rho_0(r'))$ is the α -nucleon effective interaction as defined in Eq. (6.2).

To study possible discrepancies that may arise in experimental analysis, we also perform calculations of the angular distribution using the collective form of the corresponding transition density:

$$\rho_{tr}^{coll}(r) \propto 10r\rho_0(r) + \left[3r^2 - \frac{5}{3}\langle r^2 \rangle\right] \frac{d\rho_0(r)}{dr}. \quad (6.4)$$

In our numerical DWBA calculations, the computer code PTOLEMY [63] was used.

1. Nuclear Ground State

In this section we evaluate the ability of the Hartree-Fock calculation with the Skyrme-type effective interaction to describe the nuclear ground state. Ground state root-mean square (RMS) radii and binding energies of ^{90}Zr , ^{116}Sn , ^{144}Sm and ^{208}Pb nuclei are obtained as a result of the Hartree-Fock calculations performed with SL1, SKM*, SLy4 and Sk255 Skyrme-type effective interactions. Binding energy per nucleon obtained in the nuclei of interest calculated using various effective interactions are given in Table II. In Table III we present results for the mass, neutron, proton and charge root-mean-square radii for nuclei of interest. Overall satisfactory agreement with experimentally measured charge RMS radii and binding energies can be seen.

TABLE II. Binding energy per nucleon in ^{90}Zr , ^{116}Sn , ^{144}Sm and ^{208}Pb nuclei obtained from the HF calculations with SL1, SkM*, SGII, Sly4 and Sk255 nucleon-nucleon interactions. The experimental values are obtained from Ref. [64].

	Interaction	^{90}Zr	^{116}Sn	^{144}Sm	^{208}Pb
E/A , (MeV)	SL1	-8.85	-8.56	-8.39	-7.96
	SkM*	-8.70	-8.45	-8.24	-7.87
	SLy4	-8.73	-8.48	-8.28	-7.86
	SGII	-8.91	-8.65	-8.42	-8.01
	Sk255	-8.99	-8.75	-8.55	-8.09
E/A , (MeV)	Exp.	-8.71	-8.52	-8.30	-7.87

TABLE III. Ground state root-mean square radii obtained from the HF calculations with SL1, SkM*, SLy4, SGII, and Sk255 Skyrme interactions. $\sqrt{\langle r^2 \rangle_m}$, $\sqrt{\langle r^2 \rangle_n}$, $\sqrt{\langle r^2 \rangle_p}$, $\sqrt{\langle r^2 \rangle_c}$ denote mass, neutron, proton and charge root-mean square radii, respectively. Experimental radii are taken from Ref. [65].

Nucleus	Interaction	^{90}Zr	^{116}Sn	^{144}Sm	^{208}Pb
$\sqrt{\langle r^2 \rangle_m}$, (fm)	SL1	4.24	4.62	4.95	5.59
	SkM*	4.26	4.62	4.95	5.55
	SLy4	4.27	4.63	4.95	5.56
	SGII	4.23	4.60	4.92	5.54
	Sk255	4.26	4.63	4.95	5.59
$\sqrt{\langle r^2 \rangle_n}$, (fm)	SL1	4.27	4.67	4.98	5.66
	SkM*	4.29	4.66	4.98	5.62
	SLy4	4.30	4.67	4.98	5.62
	SGII	4.26	4.63	4.95	5.59
	Sk255	4.31	4.69	5.01	5.69
$\sqrt{\langle r^2 \rangle_p}$, (fm)	SL1	4.20	4.56	4.90	5.49
	SkM*	4.22	4.56	4.90	5.45
	SLy4	4.23	4.57	4.90	5.46
	SGII	4.20	4.55	4.89	5.46
	Sk255	4.20	4.54	4.88	5.44
$\sqrt{\langle r^2 \rangle_c}$, (fm)	SL1	4.28	4.63	4.97	5.54
	SkM*	4.30	4.63	4.97	5.51
	SLy4	4.30	4.64	4.97	5.52
	SGII	4.28	4.62	4.96	5.52
	Sk255	4.28	4.61	4.94	5.50
$\sqrt{\langle r^2 \rangle_c}$, (fm)	Exp.	4.27	4.63	4.94	5.50

2. Isoscalar Monopole Resonance

Calculated isoscalar monopole ($L = 0$) transition strength distributions for ^{90}Zr , ^{116}Sn , ^{144}Sm and ^{208}Pb nuclei obtained using SL1, SkM*, SGII, Sly4 and Sk255 effective interactions are presented in Figure 1. The thin solid line represents the results of the microscopic (HF-RPA) calculations. Also shown are the isoscalar monopole strength distributions extracted from the experimental data on the inelastic α -particle scattering on the nuclei of interest [66].

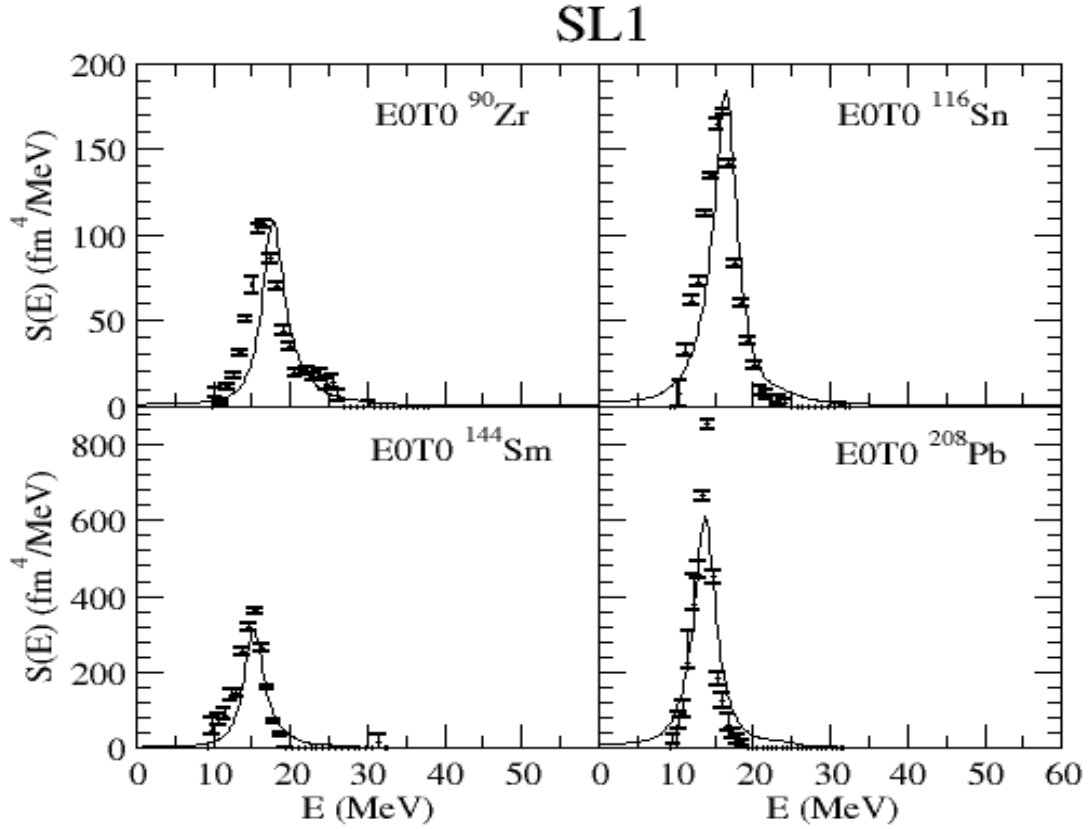


FIG. 1. Isoscalar monopole strength distributions in ^{90}Zr , ^{116}Sn , ^{144}Sm and ^{208}Pb nuclei obtained using SL1 Skyrme interaction (thin solid line). The circles with the error bars show the experimentally extracted strength distribution $S(E)$ for the ISGMR in nuclei of interest [66].

The HF-RPA strength distributions for ^{144}Sm and ^{208}Pb appear to be in good agreement with the experimental data. The HF-RPA isoscalar monopole resonance appear to be shifted with respect to the experimentally observed peak in both ^{90}Zr and ^{116}Sn . We need to point out that a small fraction of strength is predicted to be present at higher excitation energies. The isoscalar monopole strength distributions obtained in the HF-RPA calculations with SkM*, SGII, SLy4 and Sk255 Skyrme interactions are presented in Figure 2.

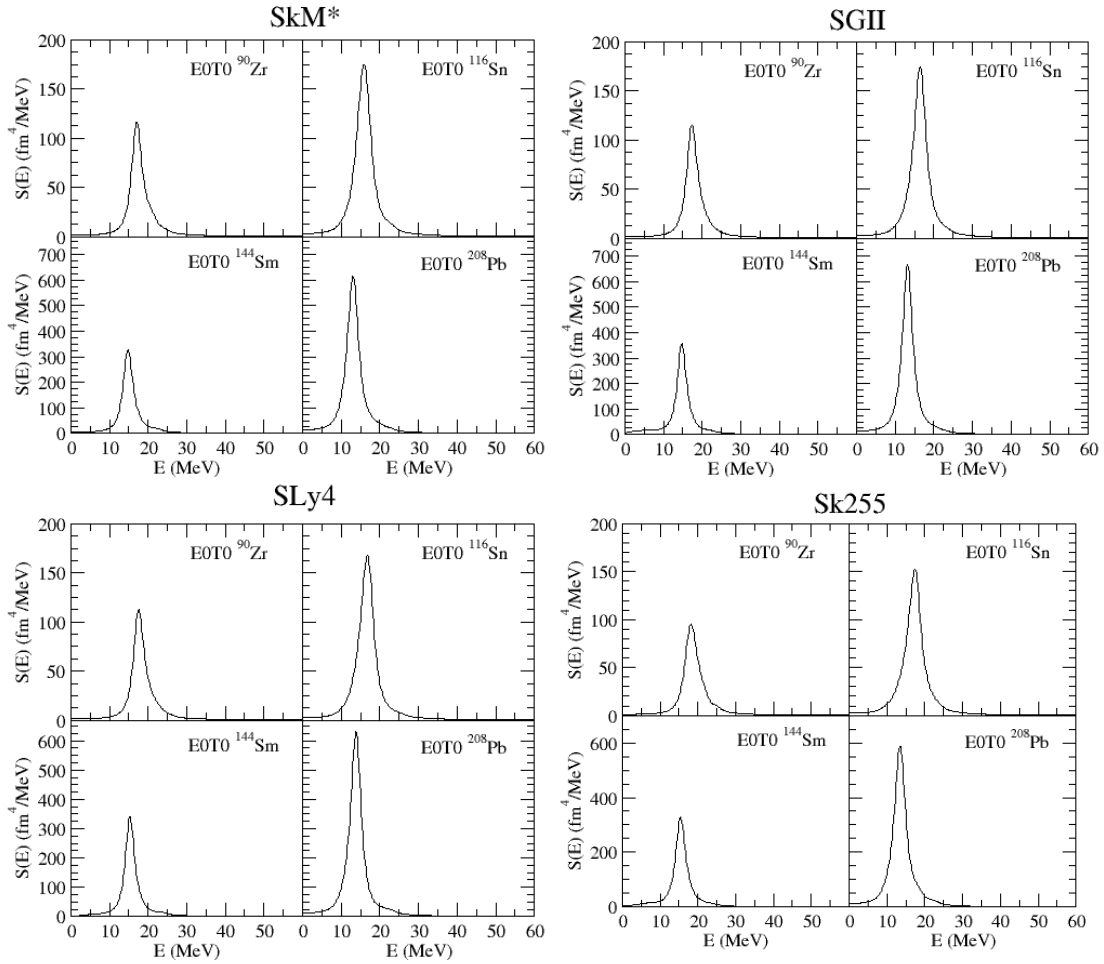


FIG. 2. Isoscalar monopole strength distributions in ^{90}Zr , ^{116}Sn , ^{144}Sm and ^{208}Pb nuclei obtained using SkM*, SGII, Sly4 and Sk255 Skyrme interactions.

The average energy of the isoscalar giant monopole resonance is calculated as the ratio of the first and the zeroth energy-moments of the presented transition strength distributions, $E_{ave.} = M_1/M_0$. In Table IV we present the average energies for the isoscalar giant monopole resonance states, $E0_{ave.}$. The results of HF-RPA calculations appear to be in a good agreement with the experimental data.

TABLE IV. Energies of the isoscalar monopole excitation $E0$ in ^{90}Zr , ^{116}Sn , ^{144}Sm and ^{208}Pb nuclei obtained using SL1, SKM*, SGII, Sly4, and Sk255 interactions.

Nucleus	Interaction	^{90}Zr	^{116}Sn	^{144}Sm	^{208}Pb
$E0_{ave.}$ (MeV)	SL1	18.53	16.57	15.98	14.3
	SKM*	17.97	16.26	15.57	14.3
	SGII	18.09	16.65	15.27	13.78
	Sly4	18.45	16.90	15.95	14.3
	Sk255	19.06	17.37	15.88	14.08
$E0_{exp}$ (MeV)		$17.81^{+0.32\text{ a}}_{-0.20}$	$15.85 \pm 0.20^{\text{b}}$	$15.40 \pm 0.40^{\text{b}}$	$13.96 \pm 0.20^{\text{b}}$

^a Ref. [25]

^b Ref. [24]

In the region of excitation energy $5 \leq E_x \leq 35$ MeV available for experimental observation we find that the isoscalar giant monopole resonance almost entirely exhausts the energy weighted sum rule M_1 (see Table V). Therefore, we can conclude that most of the isoscalar monopole strength in the nuclei of interest is located below 35 MeV excitation energy.

TABLE V. Percentage of the energy weighted sums rule ($\%EWSR$'s) of the isoscalar monopole excitation exhausted in the excitation energy interval $5 \leq E \leq 35$ MeV in ^{90}Zr , ^{116}Sn , ^{144}Sm and ^{208}Pb nuclei. $\%EWSR$'s are obtained using SL1, SkM*, SGII, Sly4, and Sk255 interactions.

Nucleus	Interaction	^{90}Zr	^{116}Sn	^{144}Sm	^{208}Pb
$\%EWSR$	SL1	96.3	96.6	96.6	96.3
	SkM*	96.2	96.5	96.5	96.4
	SGII	96.3	96.5	94.1	96.4
	Sly4	96.0	96.3	95.9	96.3
	Sk255	96.3	96.4	94.0	96.3
$\%EWSR$	Exp.	$100 \pm 12^{\text{a}}$	$112 \pm 15^{\text{b}}$	$92 \pm 12^{\text{b}}$	$99 \pm 15^{\text{b}}$

^a Ref. [25]

^b Ref. [24]

In Figure 3 we plot the calculated ISGMR average energies, obtained using the HF-RPA method with a variety of Skyrme-type interaction parameterizations, as a function of

nuclear mass number, and compare them with experimentally obtained data. Also shown in Figure 3 is the empirical mass dependence of the ISGMR excitation energy given by $E = 79.9A^{-1/3}$ MeV [67].

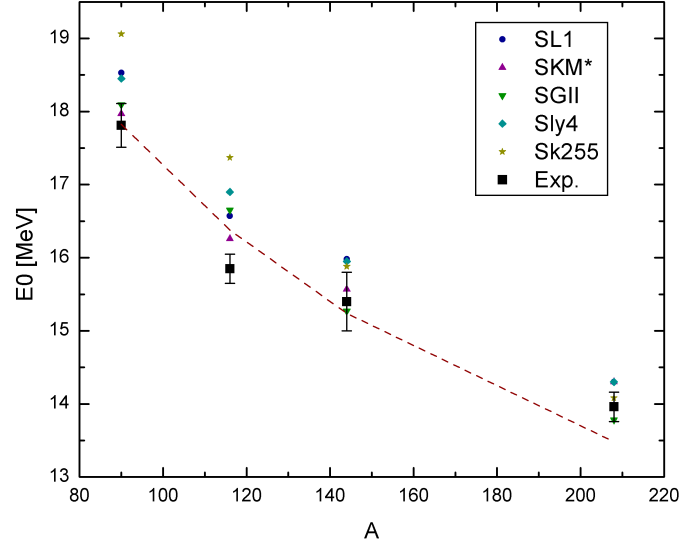


FIG. 3. Centroid energies of the ISGMR for ^{90}Zr , ^{116}Sn , ^{144}Sm , and ^{208}Pb obtained within the HF-RPA formalism with SL1 (filled circles), SKM* (filled triangles “up”), SGII (filled triangles “down”), and Sk255 (filled stars). Experimental data is presented by filled squares. The dashed line represents the empirical mass dependence of the ISGMR energy $E = 79.9A^{-1/3}$.

3. Isoscalar Giant Dipole Resonance

The isoscalar dipole transition strength distribution functions are obtained from self-consistent HF-RPA calculations with different Skyrme-type effective interactions, using a method of projecting out the spurious state contribution. The results of the calculations performed with SL1 Skyrme interaction are presented in Figure 4.

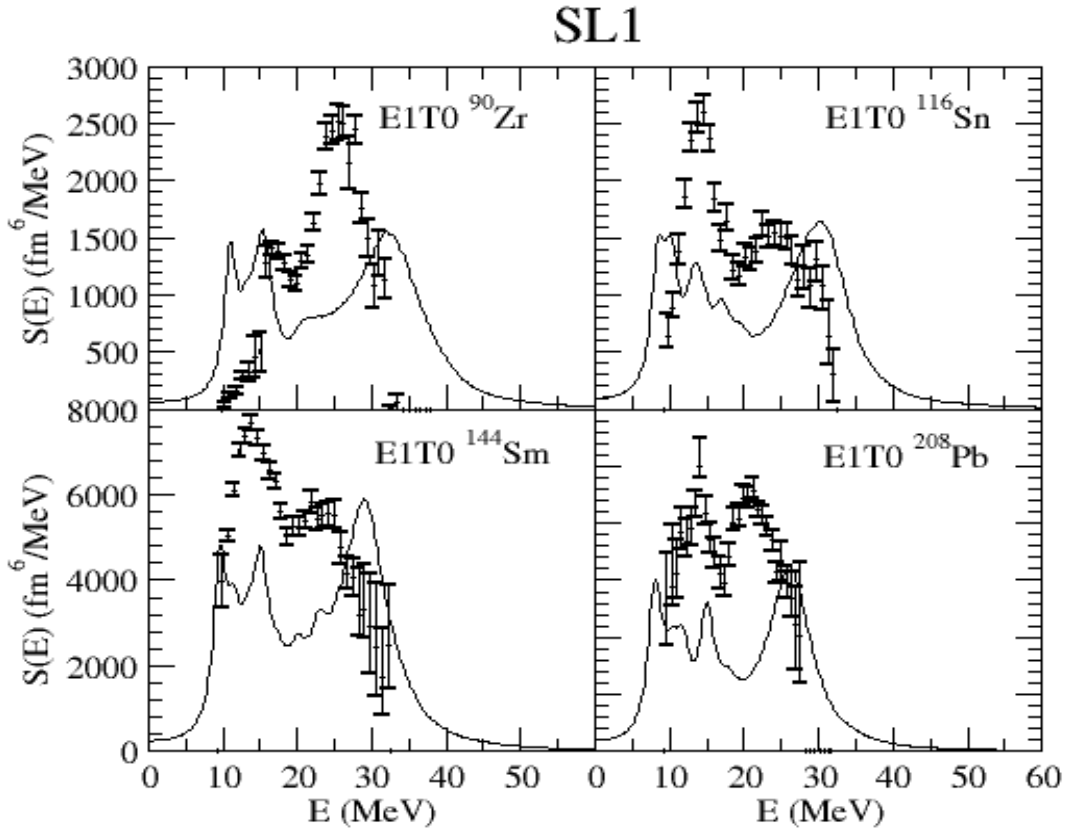


FIG. 4. Strength distribution functions of the ISGDR in ^{90}Zr , ^{116}Sn , ^{144}Sm and ^{208}Pb nuclei obtained using SL1 Skyrme interaction (thin solid line). The experimentally extracted strength distributions $S(E)$ of the ISGDR in nuclei of interest [66] are shown by the data point with error bars.

The obtained strength distributions clearly exhibit two characteristic peaks of the ISGDR in all nuclei considered. However, the position of the calculated low excitation energy and the high excitation energy components of the ISGDR strengths do not represent experimental data. The HF-RPA calculations for both of the components of the isoscalar dipole excitation predict presence of the ISGDR strength beyond the excitation energy region where the ISGDR strength was experimentally observed. The results of the HF-RPA calculations for the strength distribution functions of the ISGDR in ^{90}Zr , ^{116}Sn , ^{144}Sm and ^{208}Pb nuclei obtained using SkM*, SGII, Sly4, and Sk255 Skyrme interactions are presented in Figure 5.

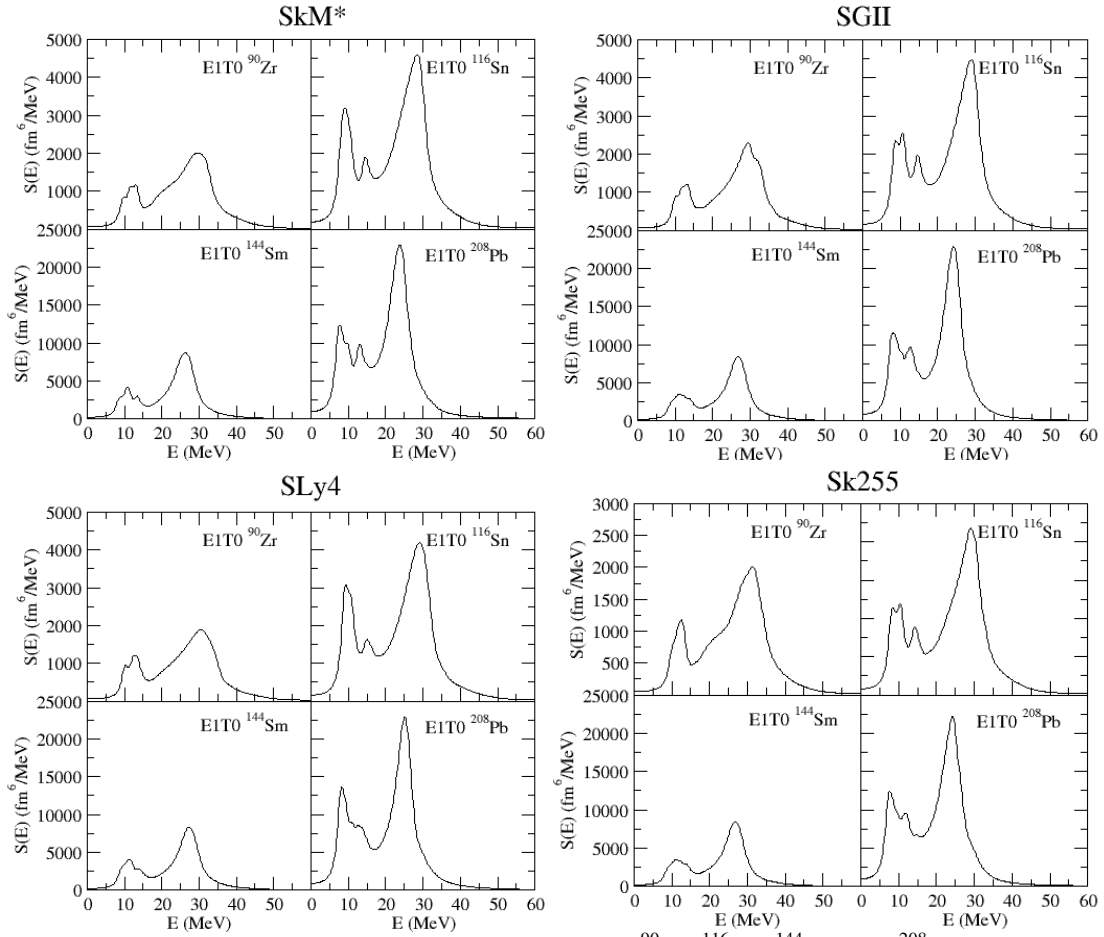


FIG. 5. Strength distribution functions of the ISGDR in ^{90}Zr , ^{116}Sn , ^{144}Sm and ^{208}Pb nuclei obtained using SkM*, SGII, Sly4, and Sk255 Skyrme interactions.

In Table VI we summarize the calculated energies of the lower (at $1\hbar\omega$) and higher (at $3\hbar\omega$) components of the isoscalar dipole resonance peaks and compare them with experimentally obtained values. Our results for the percentages of the energy weighted sum rule for the dipole excitation operator, calculated as the ratio of the energy-moment M_1 from Eqs. (3.28) and the exact energy weighted sum rule calculated using Eq.(3.30), that was exhausted within the experimentally measured region of the excitation energy ($5 \leq E_x \leq 35$ MeV) in the considered nuclei, are also presented in Table VI.

TABLE VI. The average energies and percentages of the EWSR exhausted within the energy interval of $5.0 < E < 35.0$ MeV for the low excitation energy, E_{LE} , and the high excitation energy, E_{HE} , of the ISGDR excitation in ^{90}Zr , ^{116}Sn , ^{144}Sm , and ^{208}Pb nuclei. Experimental data is also presented.

		$E_{LE\ ISGDR}$ (MeV)	EWSR (%)	$E_{HE\ ISGDR}$ (MeV)	EWSR (%)
^{90}Zr	SL1	13.45	16.9	29.69	71.8
	SkM*	11.67	8.84	27.44	82.6
	SGII	12.30	10.4	28.09	81.5
	Sly4	12.22	10.2	28.35	79.9
	Sk255	11.72	7.92	28.16	83.1
	Exp. ^{a)}	17.1 ± 0.4	13 ± 3	26.7 ± 0.5	70 ± 10
^{116}Sn	SL1	13.65	17.2	28.56	68.2
	SkM*	11.73	17.1	26.65	71.8
	SGII	11.71	15.2	26.76	73.2
	Sly4	11.77	15.5	27.21	70.5
	Sk255	11.29	13.2	26.95	73.0
	Exp.	14.38 ± 0.25	25 ± 15	25.50 ± 0.60	61 ± 15
^{144}Sm	SL1	12.68	20.6	26.93	66.6
	SkM*	11.46	12.9	25.50	78.5
	SGII	11.85	13.5	25.87	77.3
	Sly4	11.85	13.6	26.32	75.7
	Sk255	11.73	12.0	26.19	78.1
	Exp. ^{b)}	14.00 ± 0.30	32 ± 15	24.51 ± 0.40	64 ± 12
^{208}Pb	SL1	12.42	30.7	26.27	61.3
	SkM*	10.97	19.4	23.77	74.7
	SGII	10.84	18.5	23.94	75.6
	Sly4	10.92	18.9	24.68	73.6
	Sk255	10.26	16.4	23.65	77.5
	Exp. ^{b)}	13.26 ± 0.30	24 ± 15	22.20 ± 0.30	88 ± 15

^a Ref. [25]

^b Ref. [24]

Due to the fact that most of the isoscalar dipole energy weighted sum rule has been observed within the region of experimentally measured excitation energies for all nuclei of interest, it is possible to make a meaningful comparison between the ISGDR and the ISGMR average energies obtained theoretically, both by using the HF-RPA and Fermi-liquid drop model (see Chapter VI), and experimentally observed values. Figure 6 shows such a comparison.

The values for the high lying component of the ISGDR obtained within the HF-RPA formalism are higher than the respective experimental values by 1.5 to 3.0 MeV. One of the possible explanations for this phenomenon is the overestimation of the energy weighted sum rules in experimental analysis of the measured inelastic scattering cross sections. Such overestimations, first studied in Ref. [68] for the case of the ISGMR, might result in reported experimental energies lower than actual, since locating, in the experimental analysis, nearly 100% of the energy weighted sum rule within a certain excitation energy region might not guarantee that the energy weighted sum rule was actually exhausted and it can be seen in Fig. 4. that there is considerable strength predicted above the 35 MeV limit of the data.

We also need to point out that the use of different Skyrme force parameterizations, corresponding to the different values of the nuclear matter incompressibility coefficient, results in different values of the high lying component of isoscalar dipole excitation in ^{90}Zr , ^{116}Sn , ^{144}Sm and ^{208}Pb nuclei. In general, the values of the low-lying component of the ISGDR within the HF-RPA method are underestimated with respect to the experimental values by 1.5-3.5 MeV for heavy nuclei. It has to be noted, that for ^{90}Zr the low energy component of the ISGDR is also underestimated; however, the value of underestimation is much greater, 3.5 to 5.0 MeV. As our results show, the HF-RPA calculations with the Skyrme-type effective interaction do not provide correct descriptions of the low-energy features of the ISGDR. To verify the obtained results for the high-energy component of the strength function of the ISGDR, we also completed fully self-consistent HF-RPA calculations of the ISGDR excitation, with accurately introduced the spin-orbit, momentum and Coulomb terms [69, 70]. The results of these calculations will be presented in following section.

Also in Figure 6 we present data regarding the centroid energies of the ISGMR, E_0 , and ISGDR, E_1 , obtained using microscopic (HF-RPA) and collective (FLDM) methods, and its comparison to the experimentally obtained values. As we can see, the HF-RPA calculations successfully reproduce experimental values for the ISGMR in all four nuclei, however, the calculated values for the centroid energy of ISGDR systematically

exceeds the experimental values by 1.5-2.5 MeV. On the other hand the collective model based FLDM calculations with the collisional damping overestimates both $E0$ and $E1$ by 1.5-2.5 MeV in all four nuclei.

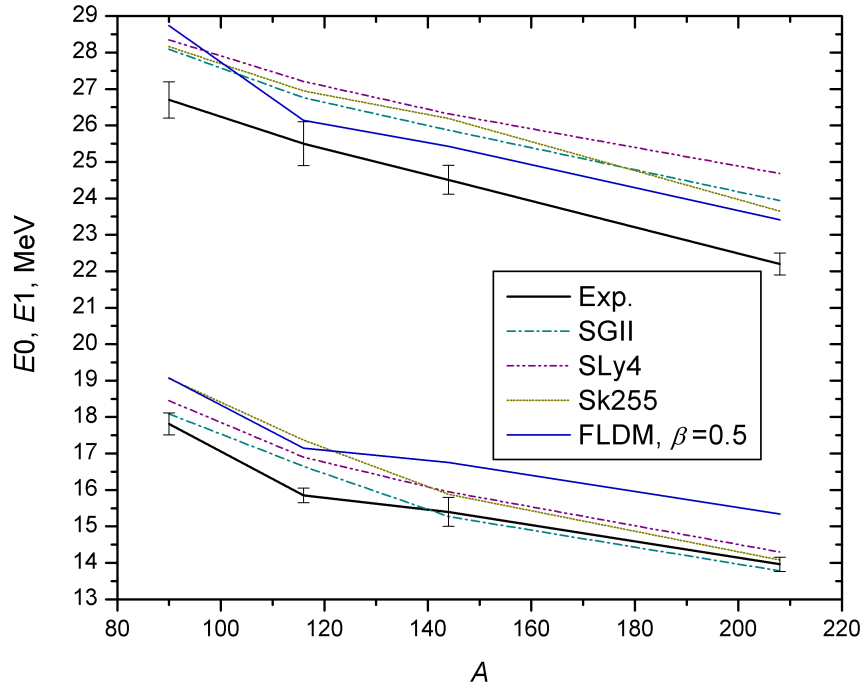


FIG. 6. Centroid energies $E0$ and $E1$ of the ISGMR and ISGDR excitations, respectively, obtained from the HF-RPA and the FLDM calculations. The experimental data [24,25] is presented by solid black line. We can see that the results of the microscopic (HF-RPA) as well as macroscopic (FLDM) calculations, systematically overestimate the centroid energy of the dipole excitation. The experimental values of the monopole energy are successfully reproduced by the HF-RPA calculations; however, the FLDM results show an overestimate on the order of 2.5 MeV, for $E0$ as well as $E1$.

4. Isoscalar Dipole Resonance Excitation from Cross Section Analysis

Parameters of the nucleon- α interaction (Eq. 6.1) for various Skyrme force parameterizations were obtained as result of the fit to the experimentally measured angular distributions of elastically scattered 240 MeV α -particles on ^{90}Zr , ^{116}Sn , ^{144}Sm and ^{208}Pb nuclei (see Refs. [24, 25]). These parameters are presented in Table VII. In Figure 7 we present a sample of elastic cross section calculated with the parameters obtained by such fit for the case of the SLy4 Skyrme force parameterization (solid line). Filled circles represent the experimentally measured elastic cross sections.

TABLE VII. Parameters of the density-dependent Gaussian form of the α -nucleon effective interactions for SL1, SkM*, SGII, SLy4 and Sk255 Skyrme-type interactions.

Nucleus	Interaction	α_V (fm ²)	β_V (fm ²)	V (MeV)	α_W (fm ²)	β_W (fm ²)	W (MeV)
^{90}Zr	SL1	3.70	-1.90	38.32	4.10	-1.90	15.63
	SkM*	3.70	-1.90	38.54	5.10	-1.90	12.56
	SGII	3.80	-1.90	38.61	4.70	-1.90	12.77
	SLy4	3.60	-1.90	41.06	4.60	-1.90	12.92
	Sk255	3.70	-1.90	39.66	4.60	-1.90	13.03
^{116}Sn	SL1	3.70	-1.90	42.51	5.10	-1.90	6.85
	SkM*	3.60	-1.90	43.33	5.10	-1.90	6.89
	SGII	3.30	-1.90	43.44	6.70	-1.90	6.87
	SLy4	3.10	-1.90	47.10	6.60	-1.90	6.98
	Sk255	3.20	-1.90	44.62	6.60	-1.90	6.90
^{144}Sm	SL1	3.60	-1.90	40.52	5.10	-1.90	10.65
	SkM*	3.6	-1.90	38.12	5.10	-1.90	10.72
	SGII	3.80	-1.90	37.89	5.10	-1.90	10.83
	SLy4	3.60	-1.90	40.36	5.10	-1.90	10.58
	Sk255	3.60	-1.90	40.32	5.10	-1.90	10.61
^{208}Pb	SL1	2.90	-1.90	53.0	6.10	-1.90	7.53
	SkM*	2.90	-1.90	49.86	6.90	-1.90	6.45
	SGII	3.20	-1.90	45.43	8.90	-1.90	3.71
	SLy4	2.90	-1.90	54.05	7.00	-1.90	5.98
	Sk255	2.90	-1.90	51.42	8.80	-1.90	3.70

The obtained parameters were used to calculate the transition potential (see Eq. 4.54) needed in the calculations of differential cross sections of inelastic reactions.

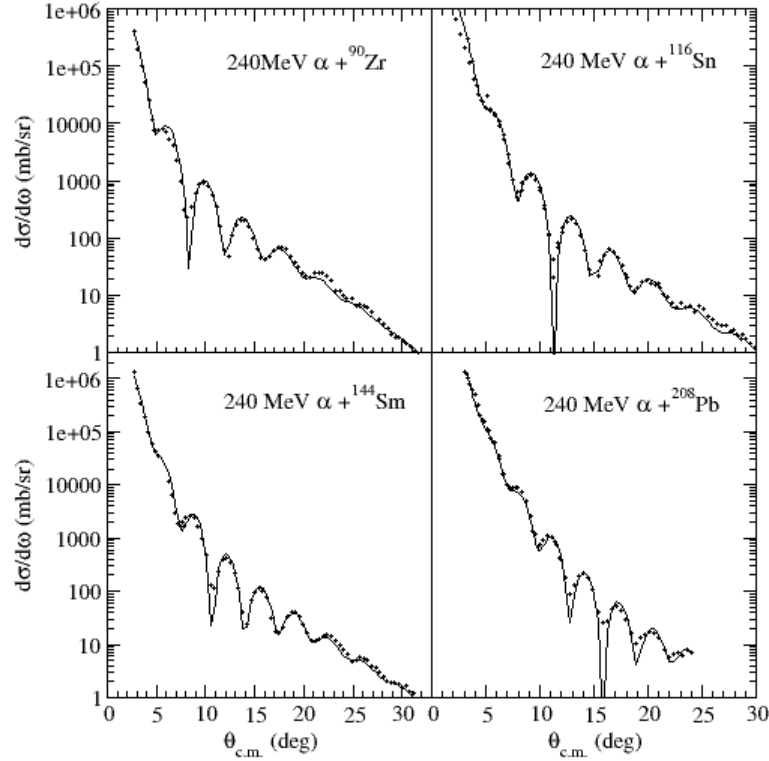


FIG. 7. Elastic scattering distributions for 240 MeV α -particles, obtained from the HF calculation for the ground state density using Sly4 interaction. Experimental data is presented by black dots. Solid lines present the best fit, obtained with the parameters given in Table VI.

In the procedure, we first use the HF-RPA method with the projected out SSM to obtain the strength distribution function (see Eqs. (3.24), (3.57)-(3.60) and (3.61)), and to calculate fraction of EWSR exhausted for each excitation energy bin (0.2 MeV). The solid line in the top panel of Figure 8 represents the results of such a calculation for ^{208}Pb nucleus completed using SL1 Skyrme interaction. Using this information we calculate transition densities for each excitation energy bin, normalized to the fraction of EWSR,

exhausted (see Eqs. (3.25) and (3.52)). By use of the microscopic shape of the transition density and the fraction of the EWSR exhausted at a given excitation energy we calculate the double-differential cross section and the angle of maximal cross section (presented in the middle panel of Fig. 8). In the experimental analysis it is customary to normalize the transition density to the 100% EWSR for each excitation energy region, and because our goal is the comparison of theoretical calculations with the experimentally obtained data, we renormalize microscopic transition density to the 100% EWSR exhausted for each excitation energy, and obtain a differential cross section at the angle of maximal cross section presented in the bottom panel of Figure 8.

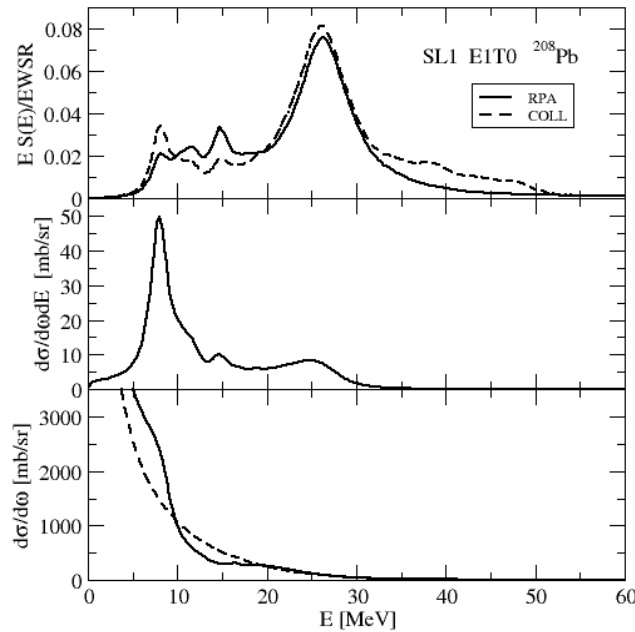


FIG. 8. Fractions of the EWSR of the ISGDR exhausted at a given excitation energy, calculated using the RPA with the SL1 Skyrme interaction (solid line) and the collective (dashed line) transition densities, are presented in the top panel. The middle panel presents the double-differential cross section calculated using the RPA transition density, obtained at the angle of maximal cross section. In the bottom panel we present the differential cross section. The solid line presents the result obtained using the RPA transition density renormalized to the 100%EWSR exhausted at a given excitation energy. The dashed line is obtained with the collective transition density.

In the bottom panel, the solid line presents the differential cross section at the angle of maximal cross-section that is obtained using the microscopic shape of the transition density renormalized to the 100% of the EWSR exhausted for each excitation energy bin. The dashed line presents the differential cross section at the angle of maximal cross section, obtained using the collective transition density (see Eq. (6.4)). Then, the dashed line in the top panel represents the fraction of the EWSR exhausted at a given excitation energy bin, as it would be calculated in the experimental analysis (with the collective shape of the transition density).

The analysis explained above has been completed for ^{90}Zr , ^{116}Sn , and ^{144}Sm , and the results for the %EWSR exhausted are presented in Figure 9 (for the SL1 interaction), in Figure 10 (for all nuclei of interest for the SkM*, SGII, Sly4 and Sk255 interactions).

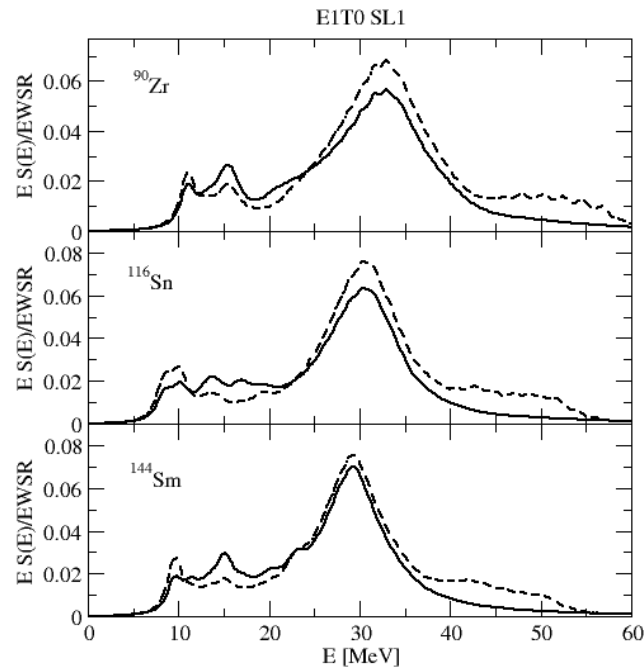


FIG. 9. Same as the top panel of Figure 8 with the SL1 interaction for ^{90}Zr , ^{116}Sn , and ^{144}Sm .

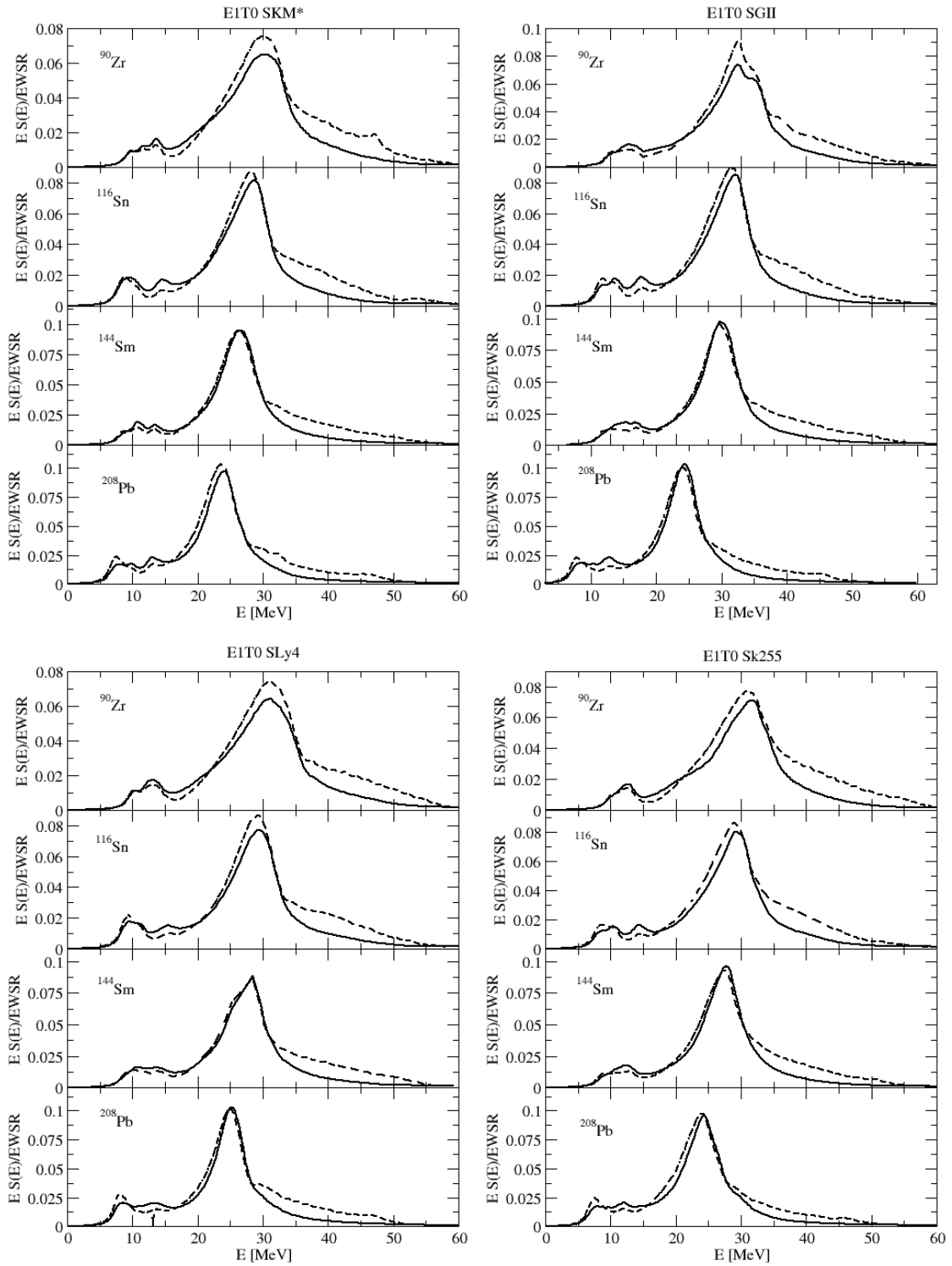


FIG. 10. Same as Figure 9 with the SKM* (top left), SGII (top right), SLy4 (bottom left) and Sk255 (bottom right) interactions for ^{90}Zr , ^{116}Sn , ^{144}Sm and ^{208}Pb nuclei.

As we can see the major finding of this calculation is that both the microscopic and the collective models predict the presence of the ISGDR strength outside of the experimentally explored region of 5-35 MeV. We also observe the trend of overestimation of the EWSR exhausted by the collective approximation of the transition density, which is widely used in the experimental studies.

To validate the results of our HF-RPA calculations we have performed the HF-RPA calculations with the fully self-consistent particle-hole interaction (see Refs. [69, 70]). The calculations were done with the SGII Skyrme interaction. The results of such calculations for nuclei of interest are presented in Table VIII.

TABLE VIII. Centroid energies of the ISGMR, $E0$, and the ISGDR, $E1$, obtained within fully self-consistent HF-RPA calculations [69,70] with the SGII interaction are presented for ^{90}Zr , ^{116}Sn , ^{144}Sm , and ^{208}Pb nuclei.

Nucleus	$E0$ (MeV)	$E1$ (MeV)
^{90}Zr	17.89	28.88
^{116}Sn	16.38	27.39
^{144}Sm	15.34	26.42
^{208}Pb	13.50	24.04

Comparison of the result of the fully self-consistent HF-RPA calculations, and of the HF-RPA calculations without the spin-orbit and Coulomb particle-hole interactions with the experimentally obtained values of the centroid energies of ISGMR and ISGDR, shows that both methods are quite successful in reproducing the energies of the breathing mode, $E0$, but overestimate the isoscalar dipole energies, $E1$, by 1-1.5 MeV for the fully self-consistent calculations and by 1.5-3.0 MeV for the calculations with approximated spin-orbit, momentum and Coulomb terms, . Hence, the ratios $E1/E0$ are

also overestimated with respect to experimental values. To address these issues we have turned to the Fermi liquid drop model with the collisional Fermi surface distortion.

B. Calculation of Centroid Energies E_0 and E_1 , Widths Γ_0 and Γ_1 , and Ratios E_1/E_0 within FLDM

To calculate the centroid energies of the isoscalar monopole and the isoscalar dipole resonance excitations, E_0 and E_1 , and their widths, and widths Γ_0 , and Γ_1 , respectively, we apply the Fermi liquid drop model with the effect of collisional damping, developed in Chapter V. The basic equation of motion for the bulk particle density variation in the nuclear interior, derived from the collisional Landau-Vlasov equation (5.63), under the assumption of the sharp density distribution (Eqs. (5.79), (5.80)), is presented in Eq. (5.65), with the bulk density variation defined by Eq. (5.48). The Fermi surface distortion is accounted for through the kinetic coefficients (Eqs. (5.66)) in the expressions for the sound velocity, c_0 , and the friction coefficient, γ , given by equations (5.68) and (5.69), respectively. The dispersion equation corresponding to the equation of motion is presented in Eq. (5.67).

To find the centroid energies E_0 , and E_1 , and the widths Γ_0 , and Γ_1 , of the ISGMR and ISGDR, respectively, we look for the lowest non-zero solutions of the secular equations describing the boundary conditions for the isoscalar monopole (Eq. (5.91)) and dipole (Eq. (5.87)) resonances, which satisfy the dispersion relation (5.67). According to equations (5.66), (5.68), and (5.69), the positions $E = \hbar \text{Re } \omega$, and the widths $\Gamma = \hbar \gamma q^2$ of the compression modes depend on the relaxation time, τ . Considering the nucleus to be cold, we take the relaxation time to be dependent on the collisional damping parameter, β , and the position of the resonance (Eq. (5.78)). Finding solutions for equations (5.91) and (5.87), augmented by the dispersion relation (5.67), gives us the dependence of the centroid energies of the isoscalar monopole and the isoscalar dipole excitations and their widths on the damping parameter β .

We carried out calculations using the following nuclear parameters: the nuclear surface tension was taken to be $\sigma=1.2\text{MeV}/\text{fm}^2$, the equilibrium nuclear radii, densities and Fermi energies for the nuclei of interest were determined from the experimentally measured rms-radii (see Ref. [65]) as

$$R_{eq} = \sqrt{\frac{5}{3} \langle r^2 \rangle_{\text{exp.}}} = r_0 A^{1/3}, \quad (6.5)$$

$$\rho_{eq} = \frac{3A}{4\pi R_{eq}^3}, \quad (6.6)$$

$$\varepsilon_F = (9\pi)^{2/3} \hbar^2 / 8m r_0^2. \quad (6.7)$$

The nucleus incompressibility K was determined from the experimental energy of the giant monopole resonance $E0_{\text{exp.}}$ and experimental rms-radii by using the scaling model definition. Namely,

$$K = \frac{m \langle r^2 \rangle_{\text{exp.}}}{\hbar^2} (E0_{\text{exp.}})^2. \quad (6.8)$$

Plots of the centroid energies of the ISGMR and ISGDR as a function of the damping parameter β for the nuclei of interest are presented in Figure 11. As we can see, for all four nuclei the centroid energies of both the ISGDR, $E1$, and the ISGMR, $E0$, are monotonic functions of β . We need to point out that the ISGDR energy $E1$ varies with β much faster than the ISGMR energy $E0$. Equations (5.66) are valid for any relaxation times and, thus, describe the rare and the frequent collisions limit, as well as the intermediate cases. In the rare collision regime ($\text{Re } \omega \tau \gg 1$, large β), the compression mode energies $E0$ and $E1$ are saturated at certain values, which correspond to the zero sound velocity $c_0 \xrightarrow{\omega \rightarrow \infty} = \sqrt{(K + (24/5)\varepsilon_F)/9m}$. In the frequent collision regime ($\text{Re } \omega \tau \ll 1$, small β), the contribution from the Fermi surface distortion in zero-sound velocity goes to zero, due to $\mu_F \xrightarrow{\omega_0 \tau \rightarrow 0} 0$, and both energies $E0$ and $E1$ reach the first sound limit of the liquid drop model (LDM) at $c_0 = c_1 = \sqrt{K/9m}$.

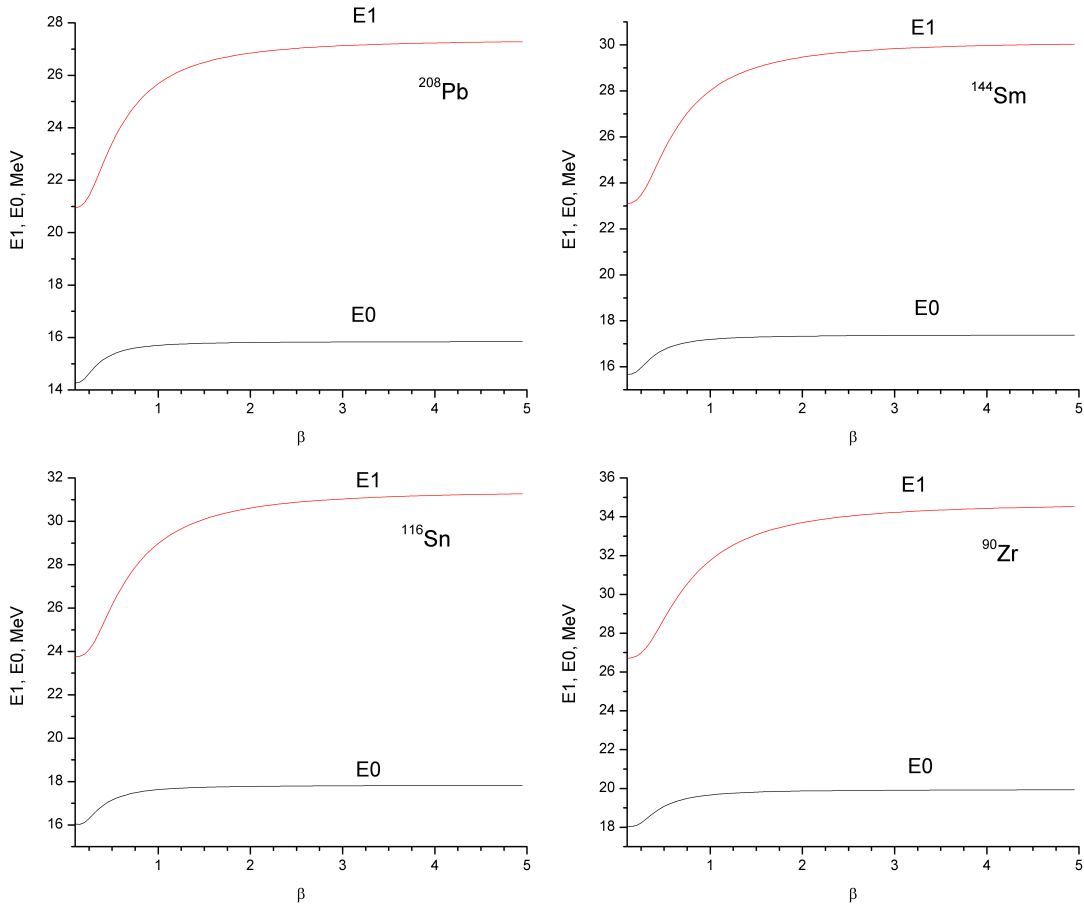


FIG. 11. Centroid energies of the ISGMR, E_0 , and the ISGDR, E_1 , in ^{90}Zr , ^{116}Sn , ^{144}Sm and ^{208}Pb nuclei presented as functions of the damping parameter β .

Our calculations also show the non-monotonic behavior of the widths Γ_0 and Γ_1 of the ISGMR and the ISGDR, respectively. This behavior is a consequence of the memory effect (ω -dependence) in the friction coefficient γ (see Eqs.(5.66) and (5.69)). In the rare collision regime the widths exhibit the quantum behavior, $\Gamma \propto 1/\tau$, while in the frequent collision regime we observe the hydrodynamic behavior, $\Gamma \propto \tau$. As it can be seen in Figure 12, the width of the ISGDR, Γ_1 , is significantly larger than width of the ISGMR, Γ_0 .

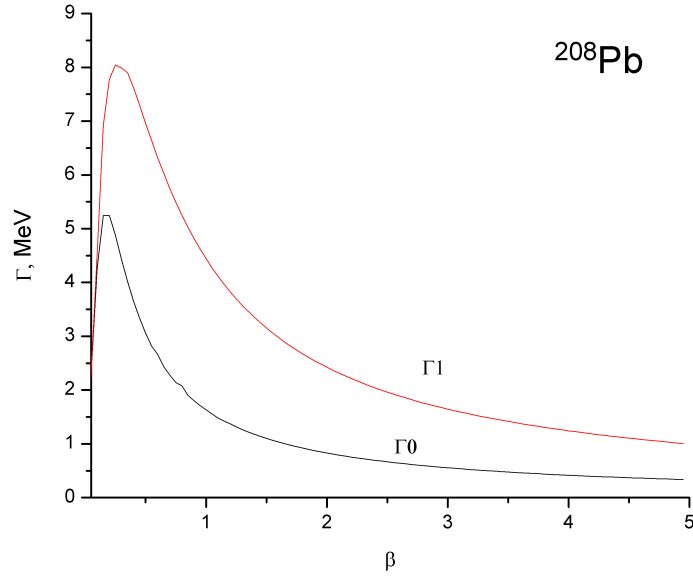


FIG. 12. Collisional widths Γ_0 and Γ_2 in ^{208}Pb of the ISGMR and ISGDR, respectively. A smooth non-monotonous dependence of the widths of collective excitation on the damping parameter β is observed

The relative location of the dipole and monopole energies for the four nuclei of interest ^{90}Zr , ^{116}Sn , ^{144}Sm , and ^{208}Pb is given by

$$(E1/E0)_{FLDM, \tau \rightarrow \infty} = 1.75 - 1.86, \quad (6.9)$$

$$(E1/E0)_{SC} = 1.76 - 1.80, \quad (6.10)$$

$$(E1/E0)_{RPA} = 1.62 - 1.76, \quad (6.11)$$

where $(E1/E0)_{FLDM, \tau \rightarrow \infty}$ was obtained in the zero-sound limit $\tau \rightarrow \infty$, and $(E1/E0)_{RPA}$ corresponds to the result of the microscopic HF-RPA calculations, presented in the previous sections of this chapter.

The ratio $(E1/E0)_{SC}$ is for the scaling model of Ref. [32], where

$$E0_{SC} = \hbar \sqrt{\frac{K}{m\langle r^2 \rangle}}, \quad \text{and} \quad E1_{SC} = \hbar \sqrt{\frac{7K + (27/25)\epsilon_F}{3m\langle r^2 \rangle}}. \quad (6.12)$$

The ratios of Eq. (6.3) exceed the LDM estimate $(E1/E0)_{LDM} = 1.43$ and the experimental data $(E1/E0)_{exp.} = 1.56 \pm 0.8$ of Ref. [24, 25]. The enhancement of the ratio $(E1/E0)_{FLDM, \tau \rightarrow \infty}$ with respect to the LDM estimate is due to the fact that the Fermi surface distortion effect on the monopole energy $E0$ is relatively small and $E0$ appears closer to the prediction of the classical LDM. On the other hand, due to the Fermi surface distortion, the FLDM centroid energy of the isoscalar dipole resonance $E1$ is significantly shifted up with respect to the LDM result.

The variation of the damping parameter β in equation (5.78) allows us to fit the ratio $(E1/E0)_{FLDM}$ to the experimental value, $(E1/E0)_{exp.}$. In Figure 13 we show the dependence of the energy ratio $E1/E0$ on the nuclear mass number A . Considering the dependence of the centroid energy ratio $(E1/E0)_{FLDM}$ on the damping parameter, β , we find a good agreement between the experimental centroid energy ratio $(E1/E0)_{exp.}$ and the results of the FLDM calculations for the value of the damping parameter, $\beta \approx 0.5$ (bright blue line in Fig. 13).

To compare the collisional widths of the isoscalar compression excitations with the experimental values reported in literature we calculate root-mean-square widths assuming a Gaussian form for the strength function and using the relation $\Gamma^2 = 4\sigma^2 \sqrt{2 \ln 2}$. In Figure 14 we have plotted the A -dependence of the collisional rms-widths for the ISGMR, σ_0 , and the ISGDR, σ_1 , (given by the dot lines) evaluated for the collisional damping parameter $\beta = 0.5$. The deviation of the FLDM collisional rms-widths σ from the reported experimental rms-width $\sigma_{exp.}$ (see Refs. [24, 25]), can be explained by an additional contribution to $\sigma_{exp.}$ due to the fragmentation width.

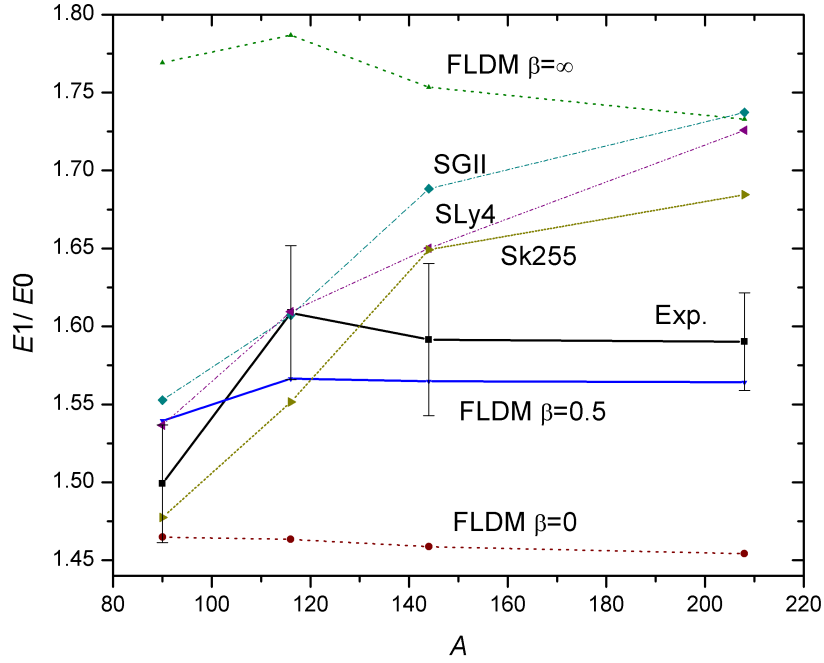


FIG. 13. Dependence of the energy ratio $E1/E0$ on the nuclear mass number A . The ratio $(E1/E0)_{FLDM}$ is obtained within the current model with the relaxation parameter (see Eq. 5.78) $\beta \rightarrow 0$ (dark red dashed line, LDM), $\beta \rightarrow \infty$ (dashed green line, zero sound regime), and $\beta = 0.5$ (solid blue line). The experimental ratios [24,25] for the nuclei of interest are presented by the solid black line. Also presented are ratios obtained as results of the HF-RPA calculations, performed with SGII (dash dot), SLy4 (dash dot dot), and Sk255 (short dot) Skyrme interactions.

We need to point out that the value of $\beta = 0.5$ is significantly smaller than the values of $\beta = 1.5 - 4.25$ obtained for nuclear matter [71-73]. Also, the fact that, for a finite nuclear system, the damping effects are enhanced in the surface region because of the diffuseness of the equilibrium phase-space distribution function in the collision integral [74], needs to be taken into consideration. Within the Fermi liquid drop model, this surface enhancement of the two-body relaxation can be phenomenologically imitated as an additional contribution to the collision integral and can lead to an effective decrease of the value of damping parameter with respect to the collisional damping parameter of the nuclear matter.

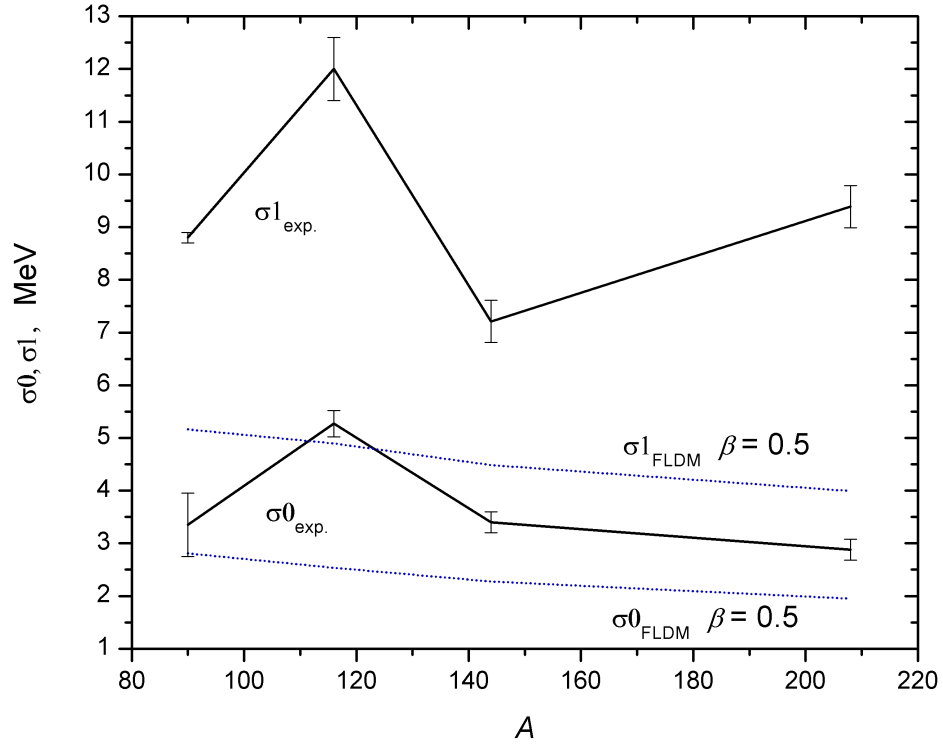


FIG. 14. Dependence of the ISGMR rms-width, σ_0 , and the ISGDR rms-width, σ_1 , on the nuclear mass number A . The FLDM result (dot-line) is obtained using the relaxation time of Eq. (5.78) with damping parameter $\beta = 0.5$. The experimental data is taken from Refs. [24,25].

CHAPTER VII

SUMMARY

In this dissertation we have presented a microscopic description of giant resonance excitations in several nuclei based on Hartree-Fock-RPA calculations performed with various Skyrme effective interaction parameterizations. Five of the existing parameterizations, namely SL1 [7], SkM* [5], SGII [33], Sly4 [37] and Sk255 [38], with the value of the nuclear matter incompressibility coefficient ranging from 215 MeV to 254 MeV were used in the analysis of collective excitations in ^{90}Zr , ^{116}Sn , ^{144}Sm and ^{208}Pb nuclei.

A theoretical description of the ground states of ^{90}Zr , ^{116}Sn , ^{144}Sm and ^{208}Pb nuclei was obtained within the Hartree-Fock method using all five Skyrme force parameterizations. Calculated values of the charge root-mean-square radii and binding energies are in satisfactory agreement with the experimental data.

The coordinate space formulation of the RPA Green's functions was used to obtain transition strength distributions for isoscalar monopole and isoscalar dipole excitations in ^{90}Zr , ^{116}Sn , ^{144}Sm and ^{208}Pb nuclei. The single-particle continuum was discretized and the width of excited single-particle states was approximated by introducing a Gaussian half-width into the free system Green's functions. The issue of the spurious state contribution at non-zero excitation energy in the isoscalar dipole strength distribution function due to the not fully self-consistent description of the particle-hole effective interaction within the RPA, has been addressed by the introduction of the projection operator,

$$\hat{f}_\eta = \sum_{i=1}^A f_\eta(\vec{r}_i) = \hat{f} - \eta \hat{f}_1.$$

The transition strength distribution functions, calculated with this correction, were used to determine the quantities of interest for the case of the isoscalar giant dipole resonance, such as average resonance energies, sum rules, and transition densities.

Fractions of the energy weighted sum rule exhausted within the experimentally accessible excitation energy region were calculated. Based on the results of calculations, it was concluded that practically the entire isoscalar monopole and isoscalar dipole energy weighted sum rule was located below the 35 MeV excitation energy in all nuclei considered. The theoretical results for the average (centroid) isoscalar monopole and isoscalar dipole resonance energies were compared to experimental values for ^{90}Zr , ^{116}Sn , ^{144}Sm and ^{208}Pb nuclei [24,25]. The HF-RPA average energies of the isoscalar monopole appeared to be in a good agreement with the experimental data for all Skyrme interactions used. However, for the interactions which give higher value for the nuclear matter incompressibility coefficient, namely, SL1 (230 MeV) and Sk255 (254 MeV), the average energies of the isoscalar monopole excitation were overestimated with respect to the experimental values by 0.8 MeV and 1.2 MeV (for SL1 and Sk255, respectively) in lighter nuclei. The HF-RPA results for the isoscalar dipole resonance provided information for both the low excitation energy component (at $1\hbar\omega$) and the high excitation energy component (at $3\hbar\omega$) of the resonance. The average energies of the high excitation energy component of the strength distribution appeared systematically higher than the experimentally observed values, by 1.5 to 3 MeV in all nuclei of interest. The average energies of the low excitation energy component of dipole resonance appeared systematically lower than experimental values by about 5 MeV in the case of ^{90}Zr and by about 3 MeV for ^{116}Sn , ^{144}Sm and ^{208}Pb nuclei. This might be an indication that a Skyrme type effective nucleon-nucleon interaction needs additional terms to describe the full complexity of the collective excitation in nuclei. It may also be necessary to consider higher order terms (such as two-particle-two-hole excitations of the ground state) in the theoretical calculations.

The differences of the DWBA descriptions of inelastic scattering reactions based on collective and microscopic transition densities were also investigated. The DWBA calculations were performed for 240 MeV α -particles scattering on ^{90}Zr , ^{116}Sn , ^{144}Sm and ^{208}Pb target nuclei. The optical potentials were obtained by folding the Hartree-Fock ground state density with a density-dependent Gaussian-shape α -nucleon interaction.

The parameters of the α -nucleon interaction were obtained by fitting experimentally measured elastic cross-sections for all nuclei of interest.

Transition potentials were calculated by folding the transition interaction expressed in terms of the α -nucleon effective interaction and its derivative with respect to the ground state density, with both microscopic (RPA) and collective model transition densities. Hartree-Fock ground state densities were used for calculations of the collective transition densities. Angular distributions of 240 MeV α -particles were obtained for the isoscalar dipole excitations of all of the target nuclei of interest. Analysis of the calculated inelastic cross sections under the assumption of the microscopic results as the experimental data, has shown that experimental analysis based on the DWBA reaction description and collective transition densities tend to overestimate the energy weighted sum rules for the isoscalar giant dipole resonance excitation. This conclusion might be important for interpretation of the experimental results. Particularly, in the case of isoscalar dipole resonance, obtaining 100% of the energy weighted sum rule within a certain excitation energy region does not assure that the entire energy weighted sum rule for the low excitation energy and the high excitation energy components of the isoscalar dipole resonance was found. That might indicate that the contribution to the transition strength at higher excitation energies has to be taken into consideration, which would raise the values of average resonance energies.

The inability of the HF-RPA description to correctly reproduce the average energies for the isoscalar giant dipole resonance was also observed. An alternative approach to studying properties of collective excitations, particularly, Fermi liquid drop model with the dynamical Fermi surface distortion was also investigated.

The relation of the Fermi liquid drop model and the time-dependent Hartree-Fock approximation was investigated within the Wigner distribution function formalism. A simple dispersion relation for the Fermi liquid with the dynamic (collisional) Fermi surface distortion was obtained from the linearized Landau-Vlasov kinetic equation. Appropriate boundary conditions for isoscalar monopole and isoscalar dipole excitations were drawn, and the centroid energies and the collisional widths of isoscalar monopole

and dipole excitations, as functions of the damping parameter β , were calculated. From the comparison of the theoretically calculated result (for the ratios of the centroid energies of the isoscalar dipole and the isoscalar monopole, $E1/E0$) to the experimental values of the ratios of isoscalar dipole to isoscalar monopole centroid energies, $E1/E0_{\text{exp}}$, the value of the damping parameter was deduced to be $\beta = 0.5$. Theoretical values of the root-mean-square widths of the isoscalar monopole and dipole excitations, corresponding to the mentioned value of the damping parameter, are lower than the experimentally observed root-mean-square widths for both the ISGMR and the ISGDR. The observed underestimation can be explained by the fact that only the collisional contribution to the widths was taken into account by the FLDM calculations. Also, more realistic approach to the description of the shape of the particle density on the nuclear surface might introduce additional contribution to the collisional width. It must be noted, that for the deduced value of the damping parameter the values of the calculated centroid energies were systematically higher than the experimental values for all nuclei of interest by 2.5 to 3 MeV and 3 to 4.5 MeV, for the isoscalar monopole and the isoscalar dipole resonances, respectively. Therefore, further investigation of this issue is necessary.

REFERENCES

- [1] T. H. R. Skyrme, *Phil. Mag.* **1**, 1043 (1956); T. H. R. Skyrme *Nucl. Phys.* **9**, 615 (1959).
- [2] J. S. Bell and T. H. R. Skyrme, *Phil. Mag.* **1**, 1055 (1956).
- [3] D. Vautherin and D. M. Brink, *Phys. Rev. C* **5**, 626 (1972).
- [4] J. W. Negele, *Phys. Rev. C* **1**, 1260 (1970).
- [5] J. Friedrich and P. -G. Reinhard, *Phys. Rev. C* **33**, 335 (1986).
- [6] M. Waroquier, J. Sau, and K. Heyde, *Phys. Rev. C* **19**, 1983 (1979).
- [7] K. -F. Liu, H. Luo, Z. Ma, Q. Shen, *Nucl. Phys.* **A534**, 1 (1991).
- [8] M. Beiner, H. Flocard, N. Van Giai, and P. Quentin, *Nucl. Phys.* **A238**, 29 (1975).
- [9] A. Kolomiets, O. Pochivalov, and S. Shlomo, *Phys Rev. C* **61**, 034312 (2000).
- [10] J. P. Blaizot, *Phys. Rep.* **64**, 171 (1980).
- [11] T. S. Dumitrescu and F. E. Serr, *Phys. Rev. C* **27**, 811 (1983).
- [12] H.P Morsch, M. Rogge, P. Turek, and C. Mayer-Boricke, *Phys. Rev. Lett.* **45**, 337 (1980).
- [13] C. Djalali, N. Marty, M. Morlet, and A. Willis, *Nucl. Phys.* **A380**, 42 (1982).
- [14] H. L. Clark, and Y. -W. Lui, and D. H. Youngblood, *Phys. Rev. C* **63**, 031301(R) (2001).
- [15] B. F. Davis, U. Garg, W. Reviol, M. N. Harakeh, A. Bacher, G. P. Berg, C. C. Foster, E. J. Stephenson, Y. Wang, J. Jänecke, K. Pham, D. Roberts, H. Akimune, M. Fujiwara, and J. Lisantti, *Phys. Rev. Lett.* **79**, 609 (1997).
- [16] I. Hamamoto, H. Sagawa, and X. Z. Zhang, *Phys. Rev. C* **57**, R1064 (1998).
- [17] S. Shlomo and A. I. Sanzhur, *Phys. Rev. C* **65**, 044310 (2002).
- [18] B. K. Agrawal, S. Shlomo, and A. I. Sanzhur, *Phys. Rev. C* **67**, 034314 (2003).
- [19] A. Kolomiets, O. Pochivalov and S. Shlomo, *Progress in Research* (Cyclotron Institute, Texas A&M University, Texas, 1999), p. III-1.
- [20] M. L. Gorelik, S. Shlomo and M. H. Urin, *Phys. Rev. C* **62**, 044301 (2000).

- [21] G. Colo, N. Van Giai, P. F. Bortington, and M. R. Quaglia, *Phys. Lett. B* **485**, 362 (2000).
- [22] D. Vretenar, A. Wandelt, and P. Ring, *Phys. Lett. B* **487**, 334 (2000).
- [23] J. Piekarewicz, *Phys. Rev. C* **62**, 051304(R) (2000).
- [24] D. H. Youngblood, H. L. Clark, and Y. -W. Lui, *Phys. Rev. C* **61**, 034315 (2004).
- [25] D. H. Youngblood, H. L. Clark, and Y. -W. Lui, *Phys. Rev. C* **61**, 054312 (2004).
- [26] M. Uchida, H. Sakaguchi, M. Itoh, M. Yosoi, T. Kawabata, Y. Yasuda, H. Takeda, T. Murakami, S. Terashima, S. Kishi, U. Garg, P. Boutachkov, M. Hedden, B. Kharraja, M. Koss, B. K. Nayak, S. Zhu, M. Fujiwara, H. Fujimura, H. P. Yoshida, K. Hara, H. Akimune, and M. N. Harakeh, *Phys. Rev. C* **69**, 051301 (2004).
- [27] D. J. Thouless, *Nucl. Phys.* **22**, 78 (1961).
- [28] G. F. Bertsch and S. F. Tsai, *Phys. Rep.* **18**, 125 (1975).
- [29] S. F. Tsai, *Phys. Rev. C* **17**, 1862 (1978).
- [30] S. Shlomo and G. F. Bertsch, *Nucl. Phys.* **A243**, 507 (1975).
- [31] A. M. Bernstein, in *Advances in Nuclear Physics*, edited by M. Baranger and E. Vogt (Plenum, New York, 1969), Vol. 3, p. 379.
- [32] S. Stringary, *Phys. Lett.* **108B**, 232 (1982).
- [33] N. Van Giai and H. Sagawa, *Nucl. Phys.* **A371**, 1 (1981).
- [34] H. L. Clark, Y. -W. Lui, D. H. Youngblood, K. Bachtr, U. Garg, M. N. Harakeh and N. Kalantar-Nayestanski, *Nucl. Phys.* **A649**, 57c (1999).
- [35] O. Bohigas, A. M. Lane, and J. Martorell, *Phys. Rep.* **51**, 267 (1979).
- [36] G. R. Satchler and W. G. Love, *Phys. Rep.* **55**, 183 (1979).
- [37] E. Chabanat, P. Bonche, P. Haensel, J. Meyer and R. Schaeffer, *Nucl. Phys.* **A635**, 231 (1998).
- [38] B. K. Agrawal, S. Shlomo and V. Kim Au, *Phys. Rev. C* **68**, 031304(R) (2003).
- [39] A. Bohr and B. Mottelson, *Nuclear Structure* (Benjamin, London, 1975), Vol. II, p. 399.
- [40] S. Shlomo, *Pramana-J.* **57**, 557 (2001).
- [41] G.F. Bertsch, *Suppl. Prog. Theor. Phys.* 74, 115 (1983).

- [42] E. P. Wigner, Phys. Rev. **104**, 749 (1932).
- [43] P. Ring and P. Schuk, *The Nuclear Many-Body Problem* (Springer-Verlag, New York 1980), p. 603.
- [44] V. M. Kolomietz and H. H. K. Tang, Phys. Scripta **24**, 915 (1981).
- [45] A. K. Kerman and S. E. Koonin, Ann. Phys. **100**, 332 (1976).
- [46] D. M. Brink, M. Di Toro, Nucl. Phys. **A372**, 151 (1981).
- [47] A. Vlasov, J. Phys. (USSR) **9**, 25 (1945).
- [48] C. Y. Wong and J. A. McDonald, Phys. Rev. C **16**, 1196 (1977).
- [49] C. Y. Wong, J. A. Maruhn, and T. A. Welton, Nucl. Phys. **A253**, 469 (1975).
- [50] G. F. Bertsch, edited by R. Balian, M. Rho, and G. Ripka, *Nuclear Physics with Heavy Ions and Mesons* (North-Holland, Amsterdam, 1978), Vol. 1, p. 207.
- [51] G. Bertsch, Nucl. Phys. **A249**, 253 (1975).
- [52] G. Holtzwarth and G. Eckart, Nucl. Phys. **A325**, 1 (1979).
- [53] G. Eckart, G. Holtzwarth, and J. P. Da Providencia, Nucl. Phys. **A364**, 1 (1981).
- [54] G. Holtzwarth and G. Eckart, Nucl. Phys. **A396**, 171c (1983).
- [55] V. M. Kolomietz, Sov. J. Nucl. Phys. **37**, 325 (1983).
- [56] D. J. Thouless, Nucl. Phys. **21**, 225 (1960).
- [57] L. D. Landau and E. M. Lifshitz, *Fluid Mechanics* (Pergamon, London, 1959), p. 47.
- [58] A. G. Magner, V. M. Kolomietz, H. Hofmann, and S. Shlomo, Phys. Rev. C **51**, 2457 (1995).
- [59] D. Kiderlen, V. M. Kolomietz, and S. Shlomo, Nucl. Phys. **A608**, 32 (1996).
- [60] V. M. Kolomietz and S. Shlomo, Phys. Rev. C **61**, 064302 (2000).
- [61] P. Ring and P. Schuk, *The Nuclear Many-Body Problem* (Springer-Verlag, New York 1980), p. 527.
- [62] K. F. Liu and G. E. Brown, Nucl. Phys. **A265**, 385 (1976).
- [63] M. Rhoades-Brown, M. H. Macfarlane, and Steven C. Pieper, Phys. Rev. C **21**, 2417 (1980); M. H. Macfarlane and S. C. Pieper, Argonne National Laboratory Report No. ANL-76-11, Rev. 1, 1978 (unpublished).

- [64] G. Audi and A. H. Wapstra, Nucl. Phys. **A565**, 1 (1993).
- [65] E. G. Nadjakov, K. P. Marinova, and Yu. P. Gangrsky, Atomic Data and Nuclear Data Tables **56**, 134, (1994).
- [66] D. H. Youngblood (private communications)
- [67] D. H. Youngblood, P. Boducki, J. D. Bronson, U Grag, Y. –W. Lui and C. M. Rozsa, Phys. Rev. C **23**, 1997 (1981).
- [68] P. Chomas, T. Suomijarvi, N. Van Giai, and J. Treiner, Phys. Lett. **B 281**, 6 (1992).
- [69] T. Sil, S. Shlomo, B. K. Agrawal and P. G. Reinhard, Phys. Rev. C **71**, 034316 (2006).
- [70] S. Shlomo, Tapas Sil, V. Kim Au and O. G. Pochivalov, Phys. Atom. Nucl. **69**, 1132 (2006).
- [71] H. S. Kohler, Nucl. Phys. **A378**, 159 (1982).
- [72] M. M. Abu-Samreh and H. S. Kohler, Nucl. Phys. **A552**, 101 (1984).
- [73] P. Danielewicz, Phys. Lett. **146B**, 168 (1984).
- [74] V. M. Kolomietz, S. V. Lukyanov, V. A. Plujko, and S. Shlomo, Phys. Rev. C **58**, 198 (1998).

APPENDIX A

SECOND QUANTIZATION

In this appendix we describe the second quantization (SQ) formalism. This formalism is an alternative formulation of the usual quantum mechanics, which has turned out to be very useful for handling the many-body problem. We are interested in the use of the SQ for fermions, and in the following we will give a short introduction and some important formulae.

We start with a complete orthogonal set of single-particle states $|\mu\rangle$, where μ stands for a set of quantum numbers, for example:

- (i) spatial coordinate \vec{r} , spin $\sigma \equiv \sigma_z$, and isospin $\tau \equiv \tau_z$ $|\vec{r}, \sigma, \tau\rangle$
- (ii) the quantum numbers of an oscillator basis $|nljm\rangle$

Orthogonality and completeness are expressed as

$$\langle \mu | \mu' \rangle = \delta_{\mu \mu'}, \quad \sum_{\mu} |\mu\rangle \langle \mu| = 1. \quad (\text{A.1})$$

(For continuous quantum numbers such as \vec{r} , the $\delta_{\mu \mu'}$ will mean $\delta(\vec{r} - \vec{r}')$ and the sum

\sum_{μ} will be replaced by $\int d\vec{r}$.)

The coordinate representation of the state $|\mu\rangle$ is given by

$$\varphi_{\mu}(1) = \varphi_{\mu}(\vec{r}_1, \sigma_1, \tau_1) = \langle \vec{r}_1, \sigma_1, \tau_1 | \mu \rangle. \quad (\text{A.2})$$

Starting with this set of single-particle states, we can construct a complete orthogonal set of totally antisymmetric A -body wave functions as:

$$\begin{aligned} \Phi_{\mu_1 \dots \mu_A}(1, \dots, A) &= \frac{1}{\sqrt{A!}} \sum_P \text{sign}(P) P \{ \varphi_{\mu_1}(1) \dots \varphi_{\mu_A}(A) \} \equiv \\ &= \frac{1}{\sqrt{A!}} \det \{ \mu_1 \dots \mu_A \}. \end{aligned} \quad (\text{A.3})$$

In this equation, $(1)\cdots(A)$ are particle indices. We can also characterize the wave function $\Phi_{\mu_1\cdots\mu_A}$ by the “occupation numbers”, $\{n_\mu\}$, which for a system of fermions indicate whether a particular number μ is contained in the A numbers $\{\mu_1\cdots\mu_A\}$.

Obviously we have

$$\sum_{\mu} n_{\mu} = A. \quad (\text{A.4})$$

We now can construct a Hilbert space, which contains a vacuum (no particle) $|0\rangle$, all the one-particle states, all the antisymmetrized two-particle states, and so on...

$$\mathcal{H} = \{\mathcal{H}_0, \mathcal{H}_1, \mathcal{H}_2, \dots\}.$$

The wave functions $\Phi_{\mu_1\cdots\mu_A} = \Phi_{\{n_\mu\}}$ correspond to basis states $|n_1, n_2, \dots\rangle$ in this Hilbert space, which characterized by the occupation numbers n_μ (occupation numbers representation), such that

$$\Phi_{\{n_\mu\}}(1, \dots, A) = \langle 1, \dots, A | n_1, n_2, \dots \rangle. \quad (\text{A.6})$$

These states are orthonormalized

$$\langle n_1, n_2, \dots, n_\mu, \dots | n'_1, n'_2, \dots, n'_\mu, \dots \rangle = \delta_{n_1 n'_1} \delta_{n_2 n'_2} \dots \delta_{n_\mu n'_\mu} \dots \quad (\text{A.7})$$

We now will address ourselves to a fermion system. Since n_μ can only have values 0 and 1, we may define the action of the *annihilation operator* \hat{a}_μ as

$$\hat{a}_\mu |n_1, \dots, n_\mu = 1, \dots\rangle = |n_1, \dots, n_\mu = 0, \dots\rangle, \quad \hat{a}_\mu |n_1, \dots, n_\mu = 0, \dots\rangle = 0, \quad (\text{A.8})$$

from which, by taking a complex conjugate, we get the *creation operator*, \hat{a}_μ^+ , as

$$\hat{a}_\mu^+ |n_1, \dots, n_\mu = 0, \dots\rangle = |n_1, \dots, n_\mu = 1, \dots\rangle, \quad \hat{a}_\mu^+ |n_1, \dots, n_\mu = 1, \dots\rangle = 0. \quad (\text{A.9})$$

From definitions (A.8) and (A.9) we gain the fact that

$$\left(\hat{a}_\mu \hat{a}_\nu^+ + \hat{a}_\nu^+ \hat{a}_\mu \right) |n_1, \dots, n_\mu, \dots, n_\nu, \dots\rangle = \begin{cases} 0, & \text{for } \mu \neq \nu, \\ |n_1, \dots, n_\mu, \dots\rangle, & \text{for } \mu = \nu, \end{cases} \quad (\text{A.10})$$

and, hence, get the anti-commutation relations,

$$[\hat{a}_\mu, \hat{a}_\nu^+]_{\pm} \equiv \{\hat{a}_\mu, \hat{a}_\nu^+\} \equiv \hat{a}_\mu \hat{a}_\nu^+ + \hat{a}_\nu^+ \hat{a}_\mu = \delta_{\mu\nu}. \quad (\text{A.11})$$

In the same way, one can show that

$$[\hat{a}_\mu, \hat{a}_\nu]_{\pm} = [\hat{a}_\mu^+, \hat{a}_\nu^+]_{\pm} = 0. \quad (\text{A.12})$$

The state with the occupation numbers $|0,0,0,\dots\rangle = |0\rangle$ is the *vacuum*. We thus have

$$\hat{a}_\mu |0\rangle = 0, \quad \text{for all } \mu, \text{ hence,}$$

$$|n_1, \dots, n_\nu, \dots\rangle = \prod_{\mu} (\hat{a}_\mu^+)^{n_\mu} |0\rangle = \hat{a}_{\nu_1}^+ \dots \hat{a}_{\nu_A}^+ |0\rangle. \quad (\text{A.14})$$

1. Field operators in the coordinate space

Using the single-particle wave functions $\varphi_\mu(\vec{r}_1, \sigma_1, \tau_1)$ in the Eq. (A.2) we can define creation and annihilation operators $\hat{a}^+(\vec{r}, \sigma, \tau)$, $\hat{a}(\vec{r}, \sigma, \tau)$, which depend on the coordinates \vec{r} , σ , and τ :

$$a(\vec{r}, \sigma, \tau) = \sum_{\mu} \varphi_{\mu}(\vec{r}, \sigma, \tau) \hat{a}_{\mu}; \quad a^+(\vec{r}, \sigma, \tau) = \sum_{\mu} \varphi_{\mu}(\vec{r}, \sigma, \tau) \hat{a}_{\mu}^+. \quad (\text{A.15})$$

With Eq. (A.1) we can invert this relation,

$$\hat{a}_{\mu} = \sum_{\sigma, \tau} \int d\vec{r} \varphi_{\mu}^*(\vec{r}, \sigma, \tau) a(\vec{r}, \sigma, \tau), \quad \hat{a}_{\mu}^+ = \sum_{\sigma, \tau} \int d\vec{r} \varphi_{\mu}(\vec{r}, \sigma, \tau) a^+(\vec{r}, \sigma, \tau), \quad (\text{A.16})$$

and gain anticommutators

$$\begin{aligned} [a(\vec{r}, \sigma, \tau), a^+(\vec{r}', \sigma', \tau')]_{\pm} = \\ \sum_{\mu, \nu} \varphi_{\mu}(\vec{r}, \sigma, \tau) \varphi_{\nu}^*(\vec{r}', \sigma', \tau') [\hat{a}_{\mu}, \hat{a}_{\nu}^+]_{\pm} = \delta_{\sigma\sigma'} \delta_{\tau\tau'} \delta(\vec{r} - \vec{r}'), \end{aligned} \quad (\text{A.17})$$

$$[a(\vec{r}, \sigma, \tau), a(\vec{r}', \sigma', \tau')]_{\pm} = [a^+(\vec{r}, \sigma, \tau), a^+(\vec{r}', \sigma', \tau')]_{\pm} = 0. \quad (\text{A.18})$$

We can express the many-body wave function in Eq. (A.3) by

$$\Phi_{\mu_1 \dots \mu_A}(\mathbf{l}, \dots, A) = \Phi_{\{\nu_{\mu}\}}(\mathbf{l}, \dots, A) = \frac{1}{\sqrt{A!}} \langle 0 | a(A) \dots a(1) | n_1, n_2, \dots, n_A \rangle, \quad (\text{A.19})$$

and

$$|n_1, n_2, \dots, n_A\rangle = \int d1 \dots dA \frac{1}{\sqrt{A!}} \Phi_{\{n_\mu\}}(1, \dots, A) a^+(1) \dots a^+(A) |0\rangle. \quad (\text{A.20})$$

2. Representation of operators

Starting from a vacuum $|0\rangle$ we have expressed all states of the many-body system by creation and annihilation operators \hat{a}_μ^+ , \hat{a}_μ . In the following, the same will be done for operators. We have to distinguish between one- and two-body operators.

A *one-body operator* of an A -particle system, is given by the sum of A operators \hat{f}_i which act on the coordinate of particle i :

$$\hat{F} = \sum_{i=1}^A \hat{f}_i. \quad (\text{A.21})$$

Its matrix elements in the $|\mu\rangle$ representation are

$$f_{\mu\nu} = \langle \mu | \hat{f} | \nu \rangle, \quad (\text{A.22})$$

that is,

$$\hat{f}_i \varphi_\mu(i) = \sum_\nu f_{\nu\mu} \varphi_\nu(i). \quad (\text{A.23})$$

The representation of \hat{F} in the operators \hat{a}_μ^+ , \hat{a}_μ is given by

$$\hat{F} = \sum_{\mu, \nu} f_{\mu\nu} \hat{a}_\mu^+ \hat{a}_\nu. \quad (\text{A.24})$$

To show this, we need to prove that

$$\sum_i \hat{f}_i \Phi(1, \dots, A) = \langle 1, \dots, A | \sum_{\mu, \mu'} f_{\mu\mu'} \hat{a}_\mu^+ \hat{a}_{\mu'} | \Phi \rangle. \quad (\text{A.25})$$

On the l. h. s., from Eqs. (A.19), (A.16), and (A.23) we have

$$\begin{aligned} & \sum_i \hat{f}_i \langle 0 | a(A) \dots a(i) \dots a(1) | n_1, \dots, n_i, \dots, n_A \rangle = \\ & \sum_i \sum_{\mu_1 \dots \mu_A} \hat{f}_i \varphi_{\mu_A}(A) \dots \varphi_{\mu_i}(i) \dots \varphi_{\mu_1}(1) \langle 0 | \hat{a}_{\mu_A} \dots \hat{a}_{\mu_1} | \Phi \rangle = \\ & \sum_i \sum_{\mu} \sum_{\mu_1 \dots \mu_A} f_{\mu\mu_i} \varphi_{\mu_A}(A) \dots \varphi_{\mu_i}(i) \dots \varphi_{\mu_1}(1) \langle 0 | \hat{a}_{\mu_A} \dots \hat{a}_{\mu_1} | \Phi \rangle. \end{aligned}$$

This is identical to the r. h. s.:

$$\begin{aligned} & \sum_{\mu\mu'} \sum_{\mu_1 \dots \mu_A} f_{\mu\mu'} \varphi_{\mu_A}(A) \dots \varphi_{\mu_i}(i) \dots \varphi_{\mu_1}(1) \langle 0 | \hat{a}_{\mu_A} \dots \hat{a}_{\mu_i} \hat{a}_{\mu'}^+ \hat{a}_{\mu'} | \Phi \rangle = \\ & \sum_i \sum_{\mu} \sum_{\mu_1 \dots \mu_A} f_{\mu_i \mu} \varphi_{\mu_A}(A) \dots \varphi_{\mu_i}(i) \dots \varphi_{\mu_1}(1) \langle 0 | \hat{a}_{\mu_A} \dots \hat{a}_{\mu_i} \dots \hat{a}_{\mu_1} | \Phi \rangle. \end{aligned}$$

In the most general case \hat{f}_i will be an integral operator (a “nonlocal” one-particle operator):

$$\hat{f}\varphi(\vec{r}, \sigma, \tau) = \sum_{\sigma', \tau'} \int d\vec{r}' f_{\sigma\sigma', \tau\tau'}(\vec{r}, \vec{r}') \varphi(\vec{r}', \sigma', \tau'). \quad (\text{A.26})$$

A *two-particle operator* as, for example, a two-body interaction, is given by a sum of operators v_{ij} which acts on the coordinates of the particles i and j

$$\hat{V} = \sum_{i < j=1}^A \hat{v}_{ij} \equiv \frac{1}{2} \sum_{i \neq j}^A \hat{v}_{ij}. \quad (\text{A.27})$$

In complete analogy to Eq. (A.24), we can show that \hat{V} can be written as

$$\hat{V} = \frac{1}{2} \sum_{\mu\nu, \mu'\nu'} v_{\mu\nu\mu'\nu'} \hat{a}_{\mu}^+ \hat{a}_{\nu}^+ \hat{a}_{\nu'} \hat{a}_{\mu'} = \frac{1}{4} \sum_{\mu\nu, \mu'\nu'} (v_{\mu\nu\mu'\nu'} - v_{\mu\nu\nu'\mu'}) \hat{a}_{\mu}^+ \hat{a}_{\nu}^+ \hat{a}_{\nu'} \hat{a}_{\mu'}, \quad (\text{A.28})$$

where

$$v_{\mu\nu\mu'\nu'} - v_{\mu\nu\nu'\mu'} = \bar{v}_{\mu\nu\mu'\nu'} \quad (\text{A.29})$$

is the fully antisymmetrized matrix element of the interaction.

In the most general case, v_{ij} will be an integral operator in two variables, with matrix elements given as:

$$v_{\mu\nu\mu'\nu'} = \langle \mu\nu | \hat{v} | \mu'\nu' \rangle = \int d1 d2 d3 d4 \varphi_{\mu}^*(1) \varphi_{\nu}^*(2) v(1,2,3,4) \varphi_{\mu'}(3) \varphi_{\nu'}(4). \quad (\text{A.30})$$

APPENDIX B

ENERGY DENSITY CONTRIBUTIONS FROM DENSITY DEPENDENT AND
TENSOR TERMS OF THE EXTENDED SKYRME FORCE

In this appendix, the total energy density of the Skyrme effective interaction is found for closed-shell axially symmetric nuclei.

$$\begin{aligned} \langle \Phi | V_{Skyrme} | \Phi \rangle &= \int d\vec{r} H_{Skyrme}(\vec{r}) \\ H_{Skyrme}(\vec{r}) &= H_C(\vec{r}) + H_{S.O.}(\vec{r}) + H_{D.D.}(\vec{r}) + H_T(\vec{r}). \end{aligned} \quad (\text{B.1})$$

The central and the spin-orbit term contributions to the energy density are well known from literature (see Ref. [3]):

$$\begin{aligned} H_C(r) &= \frac{1}{2} t_0 \left(1 + \frac{1}{2} x_0 \right) \rho^2(\vec{r}) - \frac{1}{2} t_0 \left(\frac{1}{2} + x_0 \right) [\rho_p^2 + \rho_n^2] \\ &+ \frac{1}{4} \left[t_1 \left(1 + \frac{1}{2} x_1 \right) + t_2 \left(1 + \frac{1}{2} x_2 \right) \right] \rho(\vec{r}) \tau(\vec{r}) \\ &- \frac{1}{4} \left[t_1 \left(\frac{1}{2} + x_1 \right) - t_2 \left(\frac{1}{2} + x_2 \right) \right] [\rho_p(\vec{r}) \tau_p(\vec{r}) + \rho_n(\vec{r}) \tau_n(\vec{r})] \\ &- \frac{1}{16} \left[3t_1 \left(1 + \frac{1}{2} x_1 \right) - t_2 \left(1 + \frac{1}{2} x_2 \right) \right] \rho(\vec{r}) \nabla^2 \rho(\vec{r}) \\ &+ \frac{1}{16} \left[3t_1 \left(\frac{1}{2} + x_1 \right) + t_2 \left(\frac{1}{2} + x_2 \right) \right] [\rho_p(\vec{r}) \nabla^2 \rho_p(\vec{r}) + \rho_n(\vec{r}) \nabla^2 \rho_n(\vec{r})] \\ &+ \frac{1}{16} [t_1 - t_2] (\vec{J}_p^2(\vec{r}) + \vec{J}_n^2(\vec{r})) - \frac{1}{16} [t_1 x_1 + t_2 x_2] \vec{J}^2(\vec{r}) \end{aligned} \quad ; \quad (\text{B.2})$$

$$H_{S.O.}(\vec{r}) = -\frac{1}{2} W_0 [\rho(\vec{r}) \vec{\nabla} \vec{J}(\vec{r}) + \rho_p(\vec{r}) \vec{\nabla} \vec{J}_p(\vec{r}) + \rho_n(\vec{r}) \vec{\nabla} \vec{J}_n(\vec{r})], \quad (\text{B.3})$$

This is done through calculations of matrix elements of these components for the Slater determinant wave function Φ given by Eq. (2.13). For a two-body interaction

$\frac{1}{2} \sum_{ij} V_{ij}$ such a matrix element is given by:

$$\frac{1}{2}\langle\Phi|\sum_{ij}V_{ij}|\Phi\rangle=\frac{1}{2}\sum_{ij}\langle ij|V_{12}(1-P_{12}^rP_{12}^\sigma P_{12}^T)|ij\rangle, \quad (\text{B.4})$$

while for three-body interaction $\frac{1}{6}\sum_{ijk}V_{ijk}$ the matrix element becomes:

$$\begin{aligned} \frac{1}{6}\langle\Phi|\sum_{ijk}V_{ijk}|\Phi\rangle &= \frac{1}{6}\sum_{ijk}\langle ijk|V_{123}(1-P_{12}^rP_{12}^\sigma P_{12}^T - P_{23}^rP_{23}^\sigma P_{23}^T \\ &\quad - P_{13}^rP_{13}^\sigma P_{13}^T + P_{13}^rP_{13}^\sigma P_{13}^T P_{23}^rP_{23}^\sigma P_{23}^T \\ &\quad + P_{23}^rP_{23}^\sigma P_{23}^T P_{13}^rP_{13}^\sigma P_{13}^T)|ijk\rangle, \end{aligned} \quad (\text{B.5})$$

where $|ij\rangle$ and $|ijk\rangle$ are products of single particle wave functions $\varphi_i(\vec{r}_1)$, $\varphi_j(\vec{r}_2)$, and $\varphi_k(\vec{r}_3)$, and P^r , P^σ , and P^T are exchange operators for special, spin, and isospin coordinates, respectively. The explicit form of the spin exchange operator is:

$$P_{nm}^\sigma = \frac{1}{2}(1 + \vec{\sigma}_n \cdot \vec{\sigma}_m), \quad (\text{B.6})$$

where $\vec{\sigma}_n$ and $\vec{\sigma}_m$ are spin operator acting on the single-particle wave functions depending coordinates \vec{r}_n and \vec{r}_m , respectively, which, in spin coordinate representation, are the Pauli matrices. We assume that there is no charge mixing as a result of isospin coordinate exchange, and, thus, the isospin exchange operator is given by:

$$P_{nm}^T = \delta_{\tau_n \tau_m}, \quad (\text{B.7})$$

where τ_n and τ_m are marking the isospin coordinates ($\tau = +\frac{1}{2}$ for protons and $\tau = -\frac{1}{2}$ for neutrons).

The results of calculations are expressed in terms of nucleon densities $\rho_\tau(\vec{r})$, $\rho(\vec{r})$, kinetic energy densities $\tau_\tau(\vec{r})$, $\tau(\vec{r})$, and spin current densities $\vec{J}_\tau(\vec{r})$, $\vec{J}(\vec{r})$, where index τ denotes the isospin. These densities are defined in terms of single-nucleon wave functions:

$$\rho_\tau(\vec{r}) = \sum_{i=1}^A \sum_{\sigma} \varphi_i^*(\vec{r}, \sigma, \tau) \varphi_i(\vec{r}, \sigma, \tau), \quad \rho(\vec{r}) = \sum_{\tau} \rho_\tau(\vec{r}); \quad (\text{B.8})$$

$$\tau_\tau(\vec{r}) = \sum_{i=1}^A \sum_{\sigma} |\vec{\nabla} \varphi_i(\vec{r}, \sigma, \tau)|^2, \quad \tau(\vec{r}) = \sum_{\tau} \tau_\tau(\vec{r}); \quad (\text{B.9})$$

$$\vec{J}_\tau(\vec{r}) = -i \sum_{i=1}^A \sum_{\sigma, \sigma'} \varphi_i^*(\vec{r}, \sigma, \tau) [\vec{\nabla} \varphi_i(\vec{r}, \sigma', \tau) \times \langle \sigma | \vec{\sigma} | \sigma' \rangle], \quad \vec{J}(\vec{r}) = \sum_{\tau} \vec{J}_\tau(\vec{r}). \quad (\text{B.10})$$

Before evaluating matrix elements (B.4) and (B.5) for the density dependent and tensor terms of the Skyrme interaction, it is useful to introduce several identities, which involve single-nucleon wave functions and will be used in all derivations below.

Under the assumption of time reversal invariance, if state i is occupied, then the time reversed state \tilde{i} is also occupied. For spinor particles, the wave function $\varphi_{\tilde{i}}(\vec{r}, \sigma, \tau)$ of state \tilde{i} can be obtained from wave function $\varphi_i(\vec{r}, \sigma, \tau)$ as:

$$\varphi_{\tilde{i}}(\vec{r}, \sigma, \tau) = \hat{\Theta} \varphi_i(\vec{r}, \sigma, \tau) = -2\sigma \varphi_i^*(\vec{r}, -\sigma, \tau), \quad \sigma = \pm \frac{1}{2}. \quad (\text{B.11})$$

Therefore, from Eq. (B.7) and (B.10) it follows that

$$\sum_i \varphi_i^*(\vec{r}, \sigma_1, \tau) \varphi_i(\vec{r}, \sigma_2, \tau) = \frac{1}{2} \delta_{\sigma_1 \sigma_2} \rho_\tau(\vec{r}). \quad (\text{B.12})$$

From expression (B.11) and from the explicit form of the Pauli matrices, the following identity can be deduced:

$$\sum_{i, \sigma_1, \sigma_2} \varphi_i^*(\vec{r}, \sigma_1, \tau) \langle \sigma_1 | \vec{\sigma} | \sigma_2 \rangle \varphi_i(\vec{r}, \sigma_2, \tau) = 0,$$

or in the spinor form:

$$\sum_i \varphi_i^*(\vec{r}) \vec{\sigma} \varphi_i(\vec{r}) = 0. \quad (\text{B.13})$$

The condition of the time reversal invariance, together with Eqs. (B.8), (B.9), and (B.13), provide us with the following results:

$$\sum_{i, \sigma} \varphi_i^*(\vec{r}, \sigma, \tau) \vec{\nabla} \varphi_i(\vec{r}, \sigma, \tau) = \frac{1}{2} \vec{\nabla} \rho_\tau(\vec{r}), \quad (\text{B.14})$$

$$\sum_{i, \sigma} \varphi_i^*(\vec{r}, \sigma, \tau) \nabla^2 \varphi_i(\vec{r}, \sigma, \tau) = \frac{1}{2} \nabla^2 \rho_\tau(\vec{r}) - \tau_\tau(\vec{r}). \quad (\text{B.15})$$

Finally, using the identity

$$\begin{aligned} (\vec{\nabla}_1 \cdot \vec{\nabla}_2) (\vec{\sigma}_1 \cdot \vec{\sigma}_2) &= \frac{1}{3} (\vec{\nabla}_1 \cdot \vec{\sigma}_1) (\vec{\nabla}_2 \cdot \vec{\sigma}_2) + \frac{1}{2} (\vec{\nabla}_1 \times \vec{\sigma}_1) (\vec{\nabla}_2 \times \vec{\sigma}_2) \\ &\quad + (\vec{\nabla}_1 \otimes \vec{\sigma}_1)^{(2)} (\vec{\nabla}_2 \otimes \vec{\sigma}_2)^{(2)}, \end{aligned} \quad (\text{B.16})$$

where indices 1 and 2 by operators $\vec{\nabla}$ and $\vec{\sigma}$ indicate that these operators act on functions of coordinates \vec{r}_1 and \vec{r}_2 respectively, we evaluate in terms of the spin currents, the expression:

$$\sum_{i,j} \varphi_i^*(\vec{r}_1, \vec{\tau}_1) \varphi_j^*(\vec{r}_2, \vec{\tau}_2) (\vec{\nabla}_1 \vec{\nabla}_2) (\vec{\sigma}_1 \vec{\sigma}_2) \varphi_i(\vec{r}_1, \vec{\tau}_1) \varphi_{ji}(\vec{r}_2, \vec{\tau}_2), \quad (\text{B.17})$$

where the third term is a product of two second-rank tensors. Under the assumption of the axial symmetry together with the time reversal invariance, and upon insertion of Eq. (B.14) into (B.17), the only non-vanishing term is the term containing $(\vec{\nabla}_1 \times \vec{\sigma}_1) (\vec{\nabla}_2 \times \vec{\sigma}_2)$. Therefore, according to definition (B.10), we obtain:

$$\sum_{i,j} \varphi_i^*(\vec{r}_1, \vec{\tau}_1) \varphi_j^*(\vec{r}_2, \vec{\tau}_2) (\vec{\nabla}_1 \vec{\nabla}_2) (\vec{\sigma}_1 \vec{\sigma}_2) \varphi_i(\vec{r}_1, \vec{\tau}_1) \varphi_{ji}(\vec{r}_2, \vec{\tau}_2) = -\frac{1}{2} \vec{J}_{\tau_1}(\vec{r}_1) \vec{J}_{\tau_3}(\vec{r}_2). \quad (\text{B.18})$$

Now we can express the contributions to the energy density from density dependent and tensor terms of the Skyrme interaction in terms of nucleon, kinetic energy, and spin current densities defined in Eqs. (B.8)–(B.10).

$$1. \text{ Density dependent term: } V_{ij} = \frac{1}{6} t_3 (1 + x_3 P_{ij}^\sigma) \rho^\alpha \left(\frac{\vec{r}_i + \vec{r}_j}{2} \right) \delta(r_i - r_j)$$

Following Eq. (B.4) with the spin and isospin exchange operators defined by the Eqs. (B.6) and (B.7), taking into account presence of a δ -function that renders $P_{12}^r = 1$, and eliminating terms that vanish because of Eq. (B.10), one obtains:

$$V_{D,D}^{(1)} = \frac{1}{2} \langle \Phi | \sum_{ij} \frac{1}{6} t_3 (1 + x_3 P_{ij}^\sigma) \rho^\alpha \left(\frac{\vec{r}_i + \vec{r}_j}{2} \right) \delta(\vec{r}_i - \vec{r}_j) | \Phi \rangle =$$

$$\frac{1}{12} t_3 \sum_{ij} \langle ij | \rho^\alpha \left(\frac{\vec{r}_i + \vec{r}_j}{2} \right) \delta(\vec{r}_i - \vec{r}_j) \left[1 - \frac{1}{2} \delta_{\tau_i \tau_j} + x_3 \left(\frac{1}{2} - \delta_{\tau_i \tau_j} \right) \right] | ij \rangle.$$

Integrating over one of the special variables and using Eq. (B.8) yields:

$$V_{D,D}^{(1)} = \frac{t_3}{2} \int d\vec{r} \left[\rho^\alpha(\vec{r}) \left(\rho^2(\vec{r}) (1 + \frac{1}{2} x_3) - \sum_{\tau} \rho_{\tau}^2(\vec{r}) (x_3 + \frac{1}{2}) \right) \right].$$

Hence, the contribution to the energy density from this term is:

$$H_{D,D}^{(1)} = \frac{t_3}{2} \left[\rho^{\alpha+2}(\vec{r}) (1 + \frac{1}{2} x_3) - \rho^\alpha(\vec{r}) (\rho_p^2(\vec{r}) + \rho_n^2(\vec{r})) (x_3 + \frac{1}{2}) \right]. \quad (\text{B.19})$$

2. Density dependent term:

$$V_{ijk} = \frac{1}{2} t_{13} (1 + x_{13} P_{ij}^\sigma) \left[\bar{k}_{ij}^2 \delta(\vec{r}_i - \vec{r}_j) \delta(\vec{r}_j - \vec{r}_k) + \delta(\vec{r}_i - \vec{r}_j) \delta(\vec{r}_j - \vec{r}_k) \bar{k}_{ij}^2 \right].$$

To calculate matrix elements of the first and second terms we use Eq. (B.5). Using the properties of integration of the δ -functions one obtains:

$$\begin{aligned} V_{D.D.}^{(2)} &= \frac{1}{12} \langle \Phi | \sum_{ijk} t_{13} (1 + x_{13} P_{ij}^\sigma) \left[\bar{k}_{ij}^2 \delta(\vec{r}_i - \vec{r}_j) \delta(\vec{r}_j - \vec{r}_k) + \delta(\vec{r}_i - \vec{r}_j) \delta(\vec{r}_j - \vec{r}_k) \bar{k}_{ij}^2 \right] | \Phi \rangle = \\ &= \frac{t_{13}}{6} \sum_{ijk} \langle ijk | (1 - 2P_{jk}^\sigma P_{jk}^T) (1 + x_{13} P_{ij}^\sigma) \delta(\vec{r}_i - \vec{r}_j) \delta(\vec{r}_j - \vec{r}_k) \bar{k}_{ij}^2 (1 - P_{ij}^r P_{ij}^\sigma P_{ij}^T) | ijk \rangle. \end{aligned}$$

We can again substitute $P_{ij}^r = 1$. Using Eqs. (B.6) and (B.7) for spin and isospin exchange operators, the explicit form of \bar{k}_{ij}^2 ($\bar{k}_{ij}^2 = -\frac{1}{4}(\nabla_i^2 - 2\vec{\nabla}_i \vec{\nabla}_j + \nabla_j^2)$), and omitting the terms which vanish because of Eq. (B.13), one can rewrite the expression above in the following form:

$$\begin{aligned} V_{D.D.}^{(2)} &= -\frac{t_{13}}{24} \sum_{ijk} \langle ijk | \delta(\vec{r}_i - \vec{r}_j) \delta(\vec{r}_j - \vec{r}_k) \left\{ \left[\nabla_i^2 - 2\vec{\nabla}_i \vec{\nabla}_j + \nabla_j^2 \right] \right. \\ &\quad \left. \left[\left(1 + \frac{1}{2} x_{13} \right) (1 - \delta_{\tau_j \tau_k}) - \left(x_{13} + \frac{1}{2} \right) \delta_{\tau_i \tau_j} (1 - \delta_{\tau_j \tau_k}) \right] \right. \\ &\quad \left. - (\vec{\nabla}_i \vec{\nabla}_j) (\vec{\sigma}_i \vec{\sigma}_j) \left[x_{13} (1 - \delta_{\tau_j \tau_k}) - \delta_{\tau_i \tau_j} (1 - \delta_{\tau_j \tau_k}) \right] \right\} | ijk \rangle. \end{aligned}$$

Integrating over any two special coordinates and using Eqs. (B.14), (B.15), and (B.18), we obtain:

$$\begin{aligned} V_{D.D.}^{(2)} &= -\frac{t_{13}}{24} \int d\vec{r} \left[\left(1 + \frac{1}{2} x_{13} \right) \left(\rho^2 \nabla^2 \rho - 2\rho^2 \tau - \frac{1}{2} \rho (\vec{\nabla} \rho)^2 \right. \right. \\ &\quad \left. \left. - \sum_{\tau} \left\{ \frac{1}{2} \rho_{\tau}^2 \nabla^2 \rho - \rho_{\tau}^2 \tau + \frac{1}{2} \rho \rho_{\tau} \nabla^2 \rho_{\tau} - \rho \rho_{\tau} \tau_{\tau} - \frac{1}{2} \rho_{\tau} \vec{\nabla} \rho_{\tau} \vec{\nabla} \rho \right\} \right) \right. \\ &\quad \left. - \left(x_{13} + \frac{1}{2} \right) \sum_{\tau} \left\{ \rho \rho_{\tau} \nabla^2 \rho_{\tau} - 2\rho \rho_{\tau} \tau_{\tau} - \frac{1}{2} \rho (\vec{\nabla} \rho_{\tau})^2 - \rho_{\tau}^2 \nabla^2 \rho_{\tau} + 2\rho_{\tau}^2 \tau_{\tau} + \frac{1}{2} \rho_{\tau} (\vec{\nabla} \rho_{\tau})^2 \right\} \right] \end{aligned}$$

$$-\frac{1}{2}x_{13}\left(\sum_{\tau}\rho_{\tau}\bar{J}\bar{J}_{\tau}-\rho J^2\right)+\sum_{\tau}\frac{1}{2}\left\{\rho_{\tau}J_{\tau}^2-\rho J_{\tau}^2\right\}.$$

Using identities:

$$(\bar{\nabla}\rho_{\tau})^2=\frac{1}{2}\nabla^2\rho_{\tau}^2-\rho_{\tau}\nabla^2\rho_{\tau}, \quad (\text{B.20})$$

$$\bar{\nabla}\rho_{\tau}\bar{\nabla}\rho=\frac{1}{2}\left[\nabla^2(\rho\rho_{\tau})-\rho_{\tau}\nabla^2\rho-\rho\nabla^2\rho_{\tau}\right], \quad (\text{B.21})$$

integrating by parts and performing some algebra, one obtains:

$$\begin{aligned} V_{D.D.}^{(2)} = & -\frac{t_{13}}{24}\int d\vec{r}\left[\frac{1}{8}(5+4x_{13})(\rho_p^2(\vec{r})\nabla^2\rho_n(\vec{r})+\rho_n^2(\vec{r})\nabla^2\rho_p(\vec{r}))\right. \\ & +\frac{1}{4}(5-2x_{13})\rho_p(\vec{r})\rho_n(\vec{r})\nabla^2\rho(\vec{r})-\left(1+\frac{1}{2}x_{13}\right)(\rho_p^2(\vec{r})\tau_n(\vec{r})+\rho_n^2(\vec{r})\tau_p(\vec{r})) \\ & -\left(2-\frac{1}{2}x_{13}\right)\rho_p(\vec{r})\rho_n(\vec{r})\tau(\vec{r})+\frac{1}{2}x_{13}(\rho_p(\vec{r})\bar{J}_n(\vec{r})+\rho_n(\vec{r})\bar{J}_p(\vec{r}))\bar{J}(\vec{r}) \\ & \left. -\frac{1}{2}(\rho_p(\vec{r})\bar{J}_n^2(\vec{r})+\rho_n(\vec{r})\bar{J}_p^2(\vec{r}))\right]. \end{aligned}$$

Therefore, contribution to the energy density is:

$$\begin{aligned} H_{D.D.}^{(2)} = & -\frac{t_{13}}{24}\left[\frac{1}{8}(5+4x_{13})(\rho_p^2(\vec{r})\nabla^2\rho_n(\vec{r})+\rho_n^2(\vec{r})\nabla^2\rho_p(\vec{r}))\right. \\ & +\frac{1}{4}(5-2x_{13})\rho_p(\vec{r})\rho_n(\vec{r})\nabla^2\rho(\vec{r})-\left(1+\frac{1}{2}x_{13}\right)(\rho_p^2(\vec{r})\tau_n(\vec{r})+\rho_n^2(\vec{r})\tau_p(\vec{r})) \\ & -\left(2-\frac{1}{2}x_{13}\right)\rho_p(\vec{r})\rho_n(\vec{r})\tau(\vec{r})+\frac{1}{2}x_{13}(\rho_p(\vec{r})\bar{J}_n(\vec{r})+\rho_n(\vec{r})\bar{J}_p(\vec{r}))\bar{J}(\vec{r}) \\ & \left. -\frac{1}{2}(\rho_p(\vec{r})\bar{J}_n^2(\vec{r})+\rho_n(\vec{r})\bar{J}_p^2(\vec{r}))\right] \quad (\text{B.22}) \end{aligned}$$

$$3. \text{ Density dependent term: } V_{ijk} = t_{23}(1+x_{23}P_{ij}^{\sigma})\left[\bar{k}_{ij}\delta(\vec{r}_i-\vec{r}_j)\delta(\vec{r}_j-\vec{r}_k)\bar{k}_{ij}\right]$$

Equation (B.5) for the matrix element of this term reduces to

$$\begin{aligned}
V_{D.D.}^{(3)} &= \frac{1}{6} \langle \Phi | \sum_{ijk} t_{23} (1 + x_{23} P_{ij}^\sigma) [\bar{k}_{ij} \delta(\bar{r}_i - \bar{r}_j) \delta(\bar{r}_j - \bar{r}_k) \bar{k}_{ij}] | \Phi \rangle = \\
&= \frac{t_{23}}{6} \sum_{ijk} \langle ijk | (\bar{k}_{ij} - 2\bar{k}_{ik} P_{jk}^\sigma P_{jk}^T) (1 + x_{23} P_{ij}^\sigma) \delta(\bar{r}_i - \bar{r}_j) \delta(\bar{r}_j - \bar{r}_k) \times \\
&\quad \bar{k}_{ij} (1 - P_{ij}^r P_{ij}^\sigma P_{ij}^T) | ijk \rangle.
\end{aligned}$$

For this term we use $P_{ij}^r = -1$. Using the definitions of $\bar{k}_{nm} = \frac{\bar{v}_n - \bar{v}_m}{2i}$, and $\bar{k}_{nm} = -\frac{\bar{v}_n - \bar{v}_m}{2i}$ with Eqs. (B.6), (B.7), and (B.13), the above expression can be rewritten in the following form:

$$\begin{aligned}
V_{D.D.}^{(3)} &= \frac{t_{23}}{24} \sum_{ijk} \langle ijk | \left(1 + \frac{1}{2} x_{23} + \delta_{\tau_i \tau_j} (x_{23} + \frac{1}{2}) \right) \left[(2 - \delta_{\tau_j \tau_k}) \bar{\nabla}_i \delta(\bar{r}_i - \bar{r}_j) \delta(\bar{r}_j - \bar{r}_k) \bar{\nabla}_i \right. \\
&\quad - (2 - \delta_{\tau_j \tau_k}) \bar{\nabla}_i \delta(\bar{r}_i - \bar{r}_j) \delta(\bar{r}_j - \bar{r}_k) \bar{\nabla}_j + \delta_{\tau_j \tau_k} \bar{\nabla}_k \delta(\bar{r}_i - \bar{r}_j) \delta(\bar{r}_j - \bar{r}_k) \bar{\nabla}_i \\
&\quad \left. - \delta_{\tau_j \tau_k} \bar{\nabla}_k \delta(\bar{r}_i - \bar{r}_j) \delta(\bar{r}_j - \bar{r}_k) \bar{\nabla}_j \right] + (x_{23} + \delta_{\tau_i \tau_j}) \delta(\bar{r}_i - \bar{r}_j) \delta(\bar{r}_j - \bar{r}_k) \cdot \\
&\quad \left[\left(1 - \frac{1}{2} \delta_{\tau_j \tau_k} \right) (\bar{\nabla}_i \bar{\nabla}_j) (\bar{\sigma}_i \bar{\sigma}_j) - \frac{1}{2} \delta_{\tau_j \tau_k} (\bar{\nabla}_i \bar{\nabla}_k) (\bar{\sigma}_i \bar{\sigma}_k) + \frac{1}{2} \delta_{\tau_j \tau_k} (\bar{\nabla}_j \bar{\nabla}_k) (\bar{\sigma}_j \bar{\sigma}_k) \right] \\
&\quad + \delta_{\tau_j \tau_k} (1 + \delta_{\tau_i \tau_j} x_{23}) \delta(\bar{r}_i - \bar{r}_j) \delta(\bar{r}_j - \bar{r}_k) (\bar{\nabla}_j \bar{\nabla}_k) (\bar{\sigma}_j \bar{\sigma}_k) | ijk \rangle.
\end{aligned}$$

To obtain terms containing $(\bar{\nabla}_n \bar{\nabla}_m) (\bar{\sigma}_n \bar{\sigma}_m)$ we integrate by parts, and use Eq. (B.13) and the property of a δ -functions: $\bar{\nabla}_n \delta(\bar{r}_n - \bar{r}_m) = -\bar{\nabla}_m \delta(\bar{r}_n - \bar{r}_m)$. Utilizing Eqs. (B.8)-(B.12), after integration over two arbitrary special coordinates we obtain:

$$\begin{aligned}
V_{D.D.}^{(3)} &= \frac{t_{23}}{24} \int d\bar{r} \left[\left(1 + \frac{1}{2} x_{23} \right) \left(2\rho^2 \tau - \frac{1}{2} \rho (\bar{\nabla} \rho)^2 - \sum_{\tau} \left\{ \rho_{\tau}^2 \tau - \frac{1}{2} \rho_{\tau} \bar{\nabla} \rho_{\tau} \bar{\nabla} \rho + \frac{1}{4} \rho (\bar{\nabla} \rho_{\tau})^2 \right\} \right) \right. \\
&\quad + \left(x_{23} + \frac{1}{2} \right) \sum_{\tau} \left\{ 2\rho \rho_{\tau} \tau - \frac{1}{2} \rho (\bar{\nabla} \rho_{\tau})^2 - \rho_{\tau}^2 \tau + \frac{1}{4} \rho_{\tau} (\bar{\nabla} \rho_{\tau})^2 \right\} + \frac{1}{2} \sum_{\tau} \left\{ \frac{1}{2} \rho_{\tau} J_{\tau}^2 - 2\rho J_{\tau}^2 \right\} \\
&\quad \left. - \frac{1}{2} x_{23} \left(\rho J^2 - \sum_{\tau} \left\{ \rho_{\tau} \bar{J} \bar{J}_{\tau} - \frac{1}{2} \rho J_{\tau}^2 - \rho_{\tau} J_{\tau}^2 \right\} \right) \right].
\end{aligned}$$

After collecting similar terms (having utilized Eqs. (B.20) and (B.21)) we arrive at:

$$\begin{aligned}
H_{D.D.}^{(3)} = & \frac{t_{23}}{24} \left[\frac{3}{16} (1 + x_{23}) (\rho_p^2(\vec{r}) \nabla^2 \rho_p(\vec{r}) + \rho_n^2(\vec{r}) \nabla^2 \rho_n(\vec{r})) \right. \\
& - \frac{1}{16} (4 + 5x_{23}) (\rho_p^2(\vec{r}) \nabla^2 \rho_n(\vec{r}) + \rho_n^2(\vec{r}) \nabla^2 \rho_p(\vec{r})) + \frac{1}{8} (8 + 7x_{23}) \rho_p(\vec{r}) \rho_n(\vec{r}) \nabla^2 \rho(\vec{r}) \\
& + \frac{3}{2} (1 + x_{23}) (\rho_p^2(\vec{r}) \tau_p(\vec{r}) + \rho_n^2(\vec{r}) \tau_n(\vec{r})) + \frac{1}{2} (2 + x_{23}) (\rho_p^2(\vec{r}) \tau_n(\vec{r}) + \rho_n^2(\vec{r}) \tau_p(\vec{r})) \\
& + (5 + 4x_{23}) \rho_p(\vec{r}) \rho_n(\vec{r}) \tau(\vec{r}) - \frac{3}{4} (1 + x_{23}) (\rho_p(\vec{r}) J_p^2(\vec{r}) + \rho_n(\vec{r}) J_n^2(\vec{r})) \\
& \left. - \frac{1}{4} (4 + 3x_{23}) (\rho_p(\vec{r}) J_n^2(\vec{r}) + \rho_n(\vec{r}) J_p^2(\vec{r})) - \frac{1}{2} x_{23} \rho(\vec{r}) \vec{J}_p(\vec{r}) \vec{J}_n(\vec{r}) \right]. \quad (\text{B.23})
\end{aligned}$$

4. Tensor force term: $V_{ij} = \frac{1}{2} T \delta(\vec{r}_i - \vec{r}_j) \left[(\vec{\sigma}_i \vec{k}_{ij}) (\vec{\sigma}_j \vec{k}_{ij}) - \frac{1}{3} (\vec{\sigma}_i \vec{\sigma}_j) k_{ij}^2 + c.c. \right] (\vec{\tau}_i \vec{\tau}_j)$.

According to Eq. (B.4), the matrix element of this term has the form:

$$\begin{aligned}
V_T^{(1)} = & \frac{1}{2} \langle \Phi | \sum_{ij} V_{ij} | \Phi \rangle = \\
& \frac{T}{2} \sum_{ij} \langle ij | \delta(\vec{r}_i - \vec{r}_j) \left[(\vec{\sigma}_i \vec{k}_{ij}) (\vec{\sigma}_j \vec{k}_{ij}) - \frac{1}{3} (\vec{\sigma}_i \vec{\sigma}_j) k_{ij}^2 \right] (\vec{\tau}_i \vec{\tau}_j) (1 - P_{ij}^r P_{ij}^\sigma P_{ij}^T) | ij \rangle,
\end{aligned}$$

where we have accounted for the fact that adding the complex conjugate term doubles matrix element of the direct term, $\frac{1}{2} T \left[(\vec{\sigma}_i \vec{k}_{ij}) (\vec{\sigma}_j \vec{k}_{ij}) - \frac{1}{3} (\vec{\sigma}_i \vec{\sigma}_j) k_{ij}^2 \right] (\vec{\tau}_i \vec{\tau}_j)$. In the above expression we can use $P_{ij}^r = 1$. Moreover, considering the fact, that a tensor interaction gives a non-zero contribution only when it acts on a spin triplet state, we can substitute $P_{ij}^\sigma = 1$ as well. Considering the formal definition of the isospin exchange operator $P_{nm}^T = \frac{1}{2} (1 + \vec{\tau}_n \vec{\tau}_m)$, we obtain:

$$\vec{\tau}_n \vec{\tau}_m = 2P_{nm}^T - 1.$$

Using the explicit form of \vec{k}_{nm} , Eqs. (B.8) and (B.24), and keeping only the terms which do not vanish due to Eq. (B.13) and due to the axial symmetry, we obtain:

$$V_T^{(1)} = \frac{3}{8} T \sum_{ij} \langle ij | \delta(\vec{r}_i - \vec{r}_j) \left[(\vec{\sigma}_i \vec{\nabla}_j) (\vec{\sigma}_j \vec{\nabla}_i) - \frac{2}{3} (\vec{\sigma}_i \vec{\sigma}_j) (\vec{\nabla}_i \vec{\nabla}_j) \right] (\delta_{\tau_i \tau_j} - 1) | ij \rangle.$$

Using the identity:

$$(\bar{A}\bar{B})(\bar{C}\bar{D}) = (\bar{A}\bar{C})(\bar{B}\bar{D}) + (\bar{C} \times \bar{B})(\bar{D} \times \bar{A}), \quad (\text{B.25})$$

we rewrite term $(\bar{\sigma}_i \bar{\nabla}_j)(\bar{\sigma}_j \bar{\nabla}_i)$ as:

$$(\bar{\sigma}_i \bar{\nabla}_j)(\bar{\sigma}_j \bar{\nabla}_i) = (\bar{\nabla}_i \bar{\nabla}_j)(\bar{\sigma}_i \bar{\sigma}_j) - (\bar{\nabla}_i \times \bar{\sigma}_i)(\bar{\nabla}_j \times \bar{\sigma}_j).$$

Now, by making use of Eqs. (B.11) and (B.18) we obtain:

$$V_T^{(1)} = -\frac{5}{8}T \int d\bar{r} \bar{J}_p(\bar{r}) \bar{J}_n(\bar{r}).$$

Therefore, the contribution to the energy density from this term is:

$$H_T^{(1)} = -\frac{5}{8}T \bar{J}_p(\bar{r}) \bar{J}_n(\bar{r}). \quad (\text{B.26})$$

5. Tensor force term:

$$V_{ij} = \frac{1}{2}U [(\bar{\sigma}_i \bar{k}_{ij})\delta(\bar{r}_i - \bar{r}_j)(\bar{\sigma}_j \bar{k}_{ij}) - \frac{1}{3}(\bar{\sigma}_i \bar{\sigma}_j) \bar{k}_{ij} \delta(\bar{r}_i - \bar{r}_j) \bar{k}_{ij}] (\bar{\tau}_i \bar{\tau}_j).$$

According to the Eq. (B.4), the matrix element of this term is:

$$V_T^{(2)} = \frac{U}{2} \sum_{ij} \langle ij | [(\bar{\sigma}_i \bar{k}_{ij})\delta(\bar{r}_i - \bar{r}_j)(\bar{\sigma}_j \bar{k}_{ij}) - \frac{1}{3}(\bar{\sigma}_i \bar{\sigma}_j) \bar{k}_{ij} \delta(\bar{r}_i - \bar{r}_j) \bar{k}_{ij}] (\bar{\tau}_i \bar{\tau}_j) (1 - P_{ij}^r P_{ij}^\sigma P_{ij}^T) | ij \rangle.$$

In this case we are allowed to use $P_{ij}^r = -1$, $P_{ij}^\sigma = 1$. Following the same line of inquiry as for the previous term yields:

$$V_T^{(2)} = \frac{U}{8} \sum_{ij} \langle ij | \delta(\bar{r}_i - \bar{r}_j) [(\bar{\sigma}_i \bar{\nabla}_j)(\bar{\sigma}_j \bar{\nabla}_i) - \frac{2}{3}(\bar{\nabla}_i \bar{\nabla}_j)(\bar{\sigma}_i \bar{\sigma}_j)] (\delta_{\tau_i \tau_j} + 1) | ij \rangle.$$

Integrating the expression above over any of two coordinates gives:

$$V_T^{(2)} = \frac{5}{48}U \int d\bar{r} [J^2(\bar{r}) + J_p^2(\bar{r}) + J_n^2(\bar{r})].$$

Therefore, the contribution to the energy density from the second term of the tensor-interaction is:

$$H_T^{(2)}(\bar{r}) = \frac{5}{48}U [J^2(\bar{r}) + J_p^2(\bar{r}) + J_n^2(\bar{r})]. \quad (\text{B.27})$$

Combining Eqs. (B.19), (B.22), and (B.23), we get the contribution to the energy density for density dependent terms:

$$\begin{aligned}
H_{D.D.}(\vec{r}) &= H_{D.D.}^{(1)} + H_{D.D.}^{(2)} + H_{D.D.}^{(3)} = \\
&\frac{1}{12}t_3 \left[\rho^{\alpha+2}(\vec{r}) \left(1 + \frac{1}{2}x_3 \right) - \rho^\alpha(\vec{r}) (\rho_p^2(\vec{r}) + \rho_n^2(\vec{r})) \left(x_3 + \frac{1}{2} \right) \right] \\
&- \frac{1}{192} \left[\frac{1}{2}t_{23}(4+5x_{23}) + t_{13}(5+4x_{13}) \right] (\rho_p^2(\vec{r})\nabla^2\rho_n(\vec{r}) + \rho_n^2(\vec{r})\nabla^2\rho_p(\vec{r})) \\
&+ \frac{1}{128}t_{23}(1+x_{23})(\rho_p^2(\vec{r})\nabla^2\rho_p(\vec{r}) + \rho_n^2(\vec{r})\nabla^2\rho_n(\vec{r})) \\
&+ \frac{1}{96} \left[\frac{1}{2}t_{23}(8+7x_{23}) - t_{13}(5-2x_{13}) \right] \rho_p(\vec{r})\rho_n(\vec{r})\nabla^2\rho(\vec{r}) \\
&+ \frac{1}{48} [t_{23}(2+x_{23}) + t_{13}(2+x_{13})] (\rho_p^2(\vec{r})\tau_n(\vec{r}) + \rho_n^2(\vec{r})\tau_p(\vec{r})) \\
&+ \frac{1}{16}t_{23}(1+x_{23})(\rho_p^2(\vec{r})\tau_p(\vec{r}) + \rho_n^2(\vec{r})\tau_n(\vec{r})) \\
&+ \frac{1}{24} \left[t_{23}(5+4x_{23}) + \frac{1}{2}t_{13}(4-x_{13}) \right] \rho_p(\vec{r})\rho_n(\vec{r})\tau(\vec{r}) \\
&- \frac{1}{48} \left[\frac{1}{2}t_{23}(4+3x_{23}) + t_{13}(x_{13}-1) \right] (\rho_p(\vec{r})J_n^2(\vec{r}) + \rho_n(\vec{r})J_p^2(\vec{r})) \\
&- \frac{1}{32}t_{23}(1+x_{23})(\rho_p(\vec{r})J_p^2(\vec{r}) + \rho_n(\vec{r})J_n^2(\vec{r})) \\
&- \frac{1}{48} [t_{23}x_{23} + t_{13}x_{13}] \rho(\vec{r})\vec{J}_p(\vec{r})\vec{J}_n(\vec{r}).
\end{aligned}$$

By combining Eqs. (B.26) and (B.27), one obtains the contribution to the energy density from tensor-interaction terms:

$$H_T(\vec{r}) = H_T^{(1)}(\vec{r}) + H_T^{(2)}(\vec{r}) = \frac{5}{8} \left[\frac{1}{3}U - T \right] \vec{J}_p(\vec{r})\vec{J}_n(\vec{r}) + \frac{5}{24}U [J_p^2(\vec{r}) + J_n^2(\vec{r})]. \quad (\text{B.29})$$

6. Local energy density of the extended Skyrme nucleon-nucleon interaction.

Sum of the central, spin-orbit, density dependent and tensor terms of the energy density provides an expression:

$$\begin{aligned}
H_{Skyrme}(\vec{r}) = & \frac{1}{2}t_0\left(1 + \frac{1}{2}x_0\right)\rho^2(\vec{r}) - \frac{1}{2}t_0\left(\frac{1}{2} + x_0\right)\left[\rho_p^2(\vec{r}) + \rho_n^2(\vec{r})\right] \\
& + \frac{1}{4}\left[t_1\left(1 + \frac{1}{2}x_1\right) + t_2\left(1 + \frac{1}{2}x_2\right)\right]\rho(\vec{r})\tau(\vec{r}) \\
& + \frac{1}{12}t_3\left[\rho^{\alpha+2}(\vec{r})\left(1 + \frac{1}{2}x_3\right) - \rho^\alpha(\vec{r})(\rho_p^2(\vec{r}) + \rho_n^2(\vec{r}))\left(x_3 + \frac{1}{2}\right)\right] \\
& + \frac{1}{24}\left[t_{23}(5 + 4x_{23}) + \frac{1}{2}t_{13}(4 - x_{13})\right]\rho_p(\vec{r})\rho_n(\vec{r})\tau(\vec{r}) \\
& - \frac{1}{4}\left[t_1\left(\frac{1}{2} + x_1\right) - t_2\left(\frac{1}{2} + x_2\right)\right](\rho_p(\vec{r})\tau_p(\vec{r}) + \rho_n(\vec{r})\tau_n(\vec{r})) \\
& + \frac{1}{16}t_{23}(1 + x_{23})(\rho_p^2(\vec{r})\tau_p(\vec{r}) + \rho_n^2(\vec{r})\tau_n(\vec{r})) \\
& + \frac{1}{48}\left[t_{23}(2 + x_{23}) + t_{13}(2 + x_{13})\right](\rho_p^2(\vec{r})\tau_n(\vec{r}) + \rho_n^2(\vec{r})\tau_p(\vec{r})) \\
& - \frac{1}{16}\left[3t_1\left(1 + \frac{1}{2}x_1\right) - t_2\left(1 + \frac{1}{2}x_2\right)\right]\rho(\vec{r})\bar{\nabla}^2\rho(\vec{r}) \\
& - \frac{1}{96}\left[t_{13}(5 - 2x_{13}) - \frac{1}{2}t_{23}(8 + 7x_{23})\right]\rho_p(\vec{r})\rho_n(\vec{r})\bar{\nabla}^2\rho(\vec{r}) \\
& + \frac{1}{16}\left[3t_1\left(\frac{1}{2} + x_1\right) + t_2\left(\frac{1}{2} + x_2\right)\right](\rho_p(\vec{r})\bar{\nabla}^2\rho_p(\vec{r}) + \rho_n(\vec{r})\bar{\nabla}^2\rho_n(\vec{r})) \\
& + \frac{1}{128}t_{23}(1 + x_{23})(\rho_p^2(\vec{r})\bar{\nabla}^2\rho_p(\vec{r}) + \rho_n^2(\vec{r})\bar{\nabla}^2\rho_n(\vec{r})) \\
& - \frac{1}{192}\left[t_{13}(5 + 4x_{13}) + \frac{1}{2}t_{23}(4 + 5x_{23})\right](\rho_p^2(\vec{r})\bar{\nabla}^2\rho_n(\vec{r}) + \rho_n^2(\vec{r})\bar{\nabla}^2\rho_p(\vec{r}))
\end{aligned}$$

$$\begin{aligned}
& + \frac{1}{16} \left[t_1(1-x_1) - t_2(1+x_2) + \frac{10}{3}U \right] (\vec{J}_p^2(\vec{r}) + \vec{J}_n^2(\vec{r})) \\
& - \frac{1}{32} t_{23}(1+x_{23}) (\rho_p(\vec{r})\vec{J}_p^2(\vec{r}) + \rho_n(\vec{r})\vec{J}_n^2(\vec{r})) \\
& - \frac{1}{48} \left[t_{13}(x_{13}-1) + \frac{1}{2}t_{23}(4+3x_{23}) \right] (\rho_p(\vec{r})\vec{J}_n^2(\vec{r}) + \rho_n(\vec{r})\vec{J}_p^2(\vec{r})) \quad .(B.30) \\
& - \frac{1}{8} \left[t_1x_1 + t_2x_2 + 5T - \frac{5}{3}U \right] \vec{J}_p(\vec{r})\vec{J}_n(\vec{r}) - \frac{1}{48} [t_{13}x_{13} + t_{23}x_{23}] \rho(\vec{r})\vec{J}_p(\vec{r})\vec{J}_n(\vec{r}) \\
& - \frac{1}{2} W_0 [\rho(\vec{r})\vec{\nabla}\vec{J}(\vec{r}) + \rho_p(\vec{r})\vec{\nabla}\vec{J}_p(\vec{r}) + \rho_n(\vec{r})\vec{\nabla}\vec{J}_n(\vec{r})]
\end{aligned}$$

Using the definition of the particle kinetic energy density (B.9), the total local energy density can be written as:

$$H = \frac{\tau_p^2}{2m_p} + \frac{\tau_n^2}{2m_n} + H_{Skyrme} + H_{Coulomb}, \quad (B.31)$$

where $H_{Coulomb}$ is the Coulomb energy density contribution, containing both direct and exchange terms:

$$H_{Coulomb} = \frac{e^2}{2} \left[\rho_{ch.}(r) \int d\vec{r}' \frac{\rho_{ch.}(\vec{r}')}{|\vec{r}-\vec{r}'|} - \int d\vec{r}' \frac{|\rho_{ch.}(\vec{r}, \vec{r}')|^2}{|\vec{r}-\vec{r}'|} \right]. \quad (B.32)$$

VITA

Oleksiy Grigorievich Pochivalov was born in Moscow, Russian Federation in 1975. He attended High School No.140 of the Gorkiy district in Tashkent, Uzbekistan before being admitted to the Physics Department of Kiev State University, Kiev, Ukraine in 1992. He graduated from Kiev State University in 1997, with a B.S. degree in nuclear and particle physics, and after passing the entrance examination, started his graduate study at the Kiev Institute for Nuclear Research. In 1998 he was accepted to the Graduate Program at Texas A&M University. In 1999 he had temporarily left the program due to family matters. In 2001 he was re-accepted to the Graduate Program at Texas A&M University, and came to College Station to pursue his Ph. D. in physics. He can be reached at the Department of Geology and Geophysics, Texas A&M University Mail Stop 3115, College Station, TX 77843-3115.